FINAL REPORT

Energy Performance Monitoring and Optimization System for DoD Campuses

ESTCP Project EW-201142

FEBRUARY 2014

Veronica Adetola
Trevor Bailey
Sorin Bengea
Keunmo Kang
Francesco Leonardi
Pengfei Li
Teems Lovett
Stevo Mijanovic
Soumik Sarkar
United Technologies Research Center

Francesco Borrelli
Anthony Kelman
Sergey Vichik
University of California, Berkeley

ESTCP

REPORT DOCUMENTATION PAGE

Form Approved
OMB No. 0704-0188

1. REPORT DATE *(DD-MM-YYYY)*	**2. REPORT TYPE**	**3. DATES COVERED** *(From - To)*
02-25-2014	FINAL	MAY 2011 – MAR 2013

4. TITLE AND SUBTITLE
ENERGY PERFORMANCE MONITORING AND OPTIMIZATION

5a. CONTRACT NUMBER
W912HQ-11-C-0016

5b. GRANT NUMBER

5c. PROGRAM ELEMENT NUMBER

6. AUTHOR(S)
Veronica Adetola, Trevor Bailey, Sorin Bengea, Francesco Borrelli, Keunmo Kang, Anthony Kelman, Francesco Leonardi, Pengfei Li, Teems Lovett, Stevo Mijanovic, Soumik Sarkar, Sergey Vichik

5d. PROJECT NUMBER
EW-201142

5e. TASK NUMBER

5f. WORK UNIT NUMBER

7. PERFORMING ORGANIZATION NAME(S) AND ADDRESS(ES)
Trevor Bailey,
United Technologies Research Center
411 Silver Lane, MS 129-78
East Hartford, CT, 06108
Peter Behrens
Great Lakes Naval Facility &Eng CMD
525 Bronson Street BLDG 112
Great Lakes IL 60088

8. PERFORMING ORGANIZATION REPORT NUMBER

9. SPONSORING / MONITORING AGENCY NAME(S) AND ADDRESS(ES)
ENVIRONMENTAL SECURITY TECHNOLOGY CERTIFICATION PROGRAM
ENERGY AND WATER

10. SPONSOR/MONITOR'S ACRONYM(S)
ESTCP EW

11. SPONSOR/MONITOR'S REPORT NUMBER(S)

12. DISTRIBUTION / AVAILABILITY STATEMENT
Approved for public release; distribution is unlimited

13. SUPPLEMENTARY NOTES

14. ABSTRACT
A campus-scale building Energy Performance Monitoring and Optimization (EPMO) system prototype was designed, developed, implemented, and demonstrated. The EPMO system technology utilized robust algorithms for dynamic optimization of control schedules and analytical tools for diagnostics of building and district heating systems. The technology was implemented at the Naval Station Great Lakes in Illinois and demonstrated its robustness and scalability by reducing energy consumption by more than 20% and diagnosing faults with 85% probability of success averaged over multiple demonstration windows during the 2012-2013 heating season. The campus-scale EPMO system was implemented as a stand-alone software environment, comprising of control and diagnostic algorithms and performance visualization tools that interfaced directly with the Naval Station Great Lakes Building Management System. The key enabling technologies that were matured and demonstrated are: 1) Reduced-order dynamic models for the campus cooling plant, building and HVAC systems; 2) Optimal control algorithms for the district heating system integrated with on-line fault accommodation to dynamically update control inputs; and 3) Tools for on line energy performance visualization and automated detection, isolation and prioritization of faults that impact performance adversely.

15. SUBJECT TERMS
Heating, Ventilation, and Air Conditioning; Optimal Control; Diagnostics; Fault-accommodating control; Measurement-based performance assessment

16. SECURITY CLASSIFICATION OF:			**17. LIMITATION OF ABSTRACT**	**18. NUMBER OF PAGES**	**19a. NAME OF RESPONSIBLE PERSON**
					Trevor Bailey
a. REPORT	**b. ABSTRACT**	**c. THIS PAGE**	SAR	119	**19b. TELEPHONE NUMBER** *(include area code)*
SAR	SAR	SAR			+1 860-610-1554

Contents

LIST OF FIGURES AND TABLES

ACRONYMS

AC: Alternating Current

AHU: Air Handling Unit

ANSI: American National Standards Institute

ASHRAE: American Society of Heating, Refrigerating, and Air-Conditioning Engineers

BACnet: Building Automation and Control Networks

BLOM: Berkeley Library for Optimization Modeling

BMS: Building Management System

CAT: Category

CFM: Cubic Feet per Minute

CFR: Code of Federal Regulations

CHW: Chilled Water

CO_2: Carbon Dioxide

CPR: Cardiopulmonary Resuscitation

CT: Current Transducer

CUSUM: Cumulative Summation

DB: Database

DC: Direct Current

DD: Data Diagnostic

DDC: Direct Digital Control

DoD: Department of Defense

EEMCS: Extended Energy Management and Control System

EHS: Environment, Health, and Safety

EIS: Energy Information Systems

EMCS: Energy Management and Control System

ESTCP: Environmental Security Technology Certification Program

FCU: Fan-Coil Unit

FDD: Fault Detection and Diagnosis

GB: Gigabyte

GFCI: Ground Fault Circuit Interrupter

GHz: Gigahertz

GPM: Gallon per Minute

HASP: Health and Safety Plan

HVAC: Heating, Ventilation and Air Conditioning

HW: Hot Water

IBPSA: International Building Performance Simulation Association

ICC: International Code Council

IPMVP: International Performance and Measurement Verification Protocol

ISDN: Integrated Services Digital Network

ISM: Integrated Safety Management

ISO: International Standards Organization

LOTO: LockOut/TagOut

MPC: Model Predictive Control

NAVFAC: Naval Facilities Engineering Command

NFPA: National Fire Protection Association

NIOSH: National Institute for Occupational Safety and Health

PACRAT: Performance and Continuous Re-Commissioning Analysis Tool

PC: Personal Computer

PI: Principal Investigator

POC: Point of Contact

PPE: Personal Protective Equipment

RH: Relative Humidity

SIR: Savings to Investment Ratio

SJHAWA: Subcontractor Job Hazards Analysis and Work Authorization

SPF: Spruce Pine Fir

SQL: Structured Query Language

UFGS: Unified Facilities Guide Specifications

UPS: Uninterruptible Power Supply

U.S.: United States

USACERL: United States of America Construction Engineering Research Laboratory

UTRC: United Technologies Research Center

V: Volts

VA: Veterans Affairs

VAV: Variable Air Volume

VFD: Variable Frequency Drive

ACKNOWLEDGMENTS

This work was performed under the project EW2011-42 administered by ESTCP (Environmental Security Technology Certification Program) technology program of the Department of Defense. We would also like to thank ESTCP Director, Dr. Jeffrey Marqusee and the Program Manager, Dr. James Galvin and the Energy Manager at Naval Station Great Lakes, Mr. Peter Behrens, for their support.

EXECUTIVE SUMMARY

The United Technologies Research Center (UTRC), with sponsorship from the Department of Defense Environmental Security Technology Certification Program (ESTCP) for Energy and Water, conducted a demonstration of the Energy Performance and Monitoring Optimization (EPMO) system prototype used to improve the energy efficiency of both heating and cooling systems. The EPMO system was implemented in this demonstration project as an extension of the existing Building Management Systems (BMS) for optimization of control schedules, energy performance visualization and system diagnostics for building and district heating systems. The system was demonstrated in two buildings at Navy Recruit Training Center in Great Lakes, Illinois, during the 2012-2013 heating season for three Air Handling Units (AHUs) and 54 terminal units.

The EPMO system integrates optimal control algorithms with system performance monitoring, diagnostic and visualization tools. The control algorithms use weather forecast data, zone sensor data, meter data and information from the AHUs and terminal units to generate optimal control schedules. For example, an optimal control schedule can control the discharge air temperature values to minimize energy consumption while meeting comfort constraints. The EPMO diagnostics tool uses the sensor and meter data to detect and isolate equipment faults, such as stuck dampers or valves, to prioritize the fault correction based on energy impact. The EPMO visualization tool continuously displays the diagnostics information to facilitate understanding the equipment fault impacts on energy consumption.

The main technical objectives of the demonstration for energy savings and system robustness were met. Based on the performance data recorded during the demonstration period, it was estimated that, on average, the EPMO system exceeded the energy consumption reduction target of 20% and improved occupant thermal comfort by reducing the number of instances outside of the temperature comfort band by 75%. The scalability of the EPMO system was confirmed through the use of an automated method for control schedule optimization, which requires minimal customization for each new system compared to the effort required to retune baseline system control schedules. The robustness of the EPMO system was confirmed by the system correctly diagnosing equipment faults for heat exchanger dampers and valves 84% of the time.

The economic objectives of the demonstration were also met with a Simple Payback of 3.5 years and Savings-to-Investment Ratio of 2 for the EPMO system for the demonstration site buildings. The EPMO system performance was estimated using the sensor and meter data recorded during 26 demonstrations days conducted during the period from November 2012 to March 2013 for three AHUs and 54 terminal units. These economic impacts depend on several variables (equipment age, building type, etc.) and may be different for other sites. A unique feature of the EPMO system is its adaptability that can lead to reduced operational costs by automatically re-optimizing the control schedules to accommodate equipment faults that are detected in real-time.

The scalability and energy savings potential demonstrated in this effort proved to be a successful demonstration that has led to continued efforts and investments from UTRC targeted at maturing the EPMO system components, including automation to operate without expert supervision. Encouraged by the results and potential of advanced diagnostics and controls technologies implementation in the building HVAC application space, UTRC in cooperation with UTC

Climate, Controls, and Security business unit is continuing the development and maturation of these technologies with the objective of commercializing them in the near future. The EPMO diagnostics technology has continued to be matured on a several full-scale building HVAC systems. The EPMO optimal control system technology was further matured and implemented in the Energy Efficient Buildings Hub, in Philadelphia, Pennsylvania. In addition, UTRC has also been developing and demonstrating adaptive optimization-based building HVAC control algorithm with the objective of maximizing energy savings and comfort control with less reliance on a-priori developed building and HVAC equipment models.

1.0 INTRODUCTION

1.1 BACKGROUND

The DoD is the largest single user of energy in the United States, representing 0.8% of the total US energy consumed and 78% of the energy consumed by the Federal government [1]. Approximately 25% of the DoD energy use is consumed by its buildings and facilities. The DoD currently has 316,238 buildings across 5,429 sites and in 2006 its facility energy bill was over $3.5 Billion [2]. The Office of the Secretary of Defense (OSD) published an energy policy to 'ensure that the DoD infrastructure is secure, safe, reliable and efficient' [3], and subsequent energy policy is being guided by the Energy Policy Act of 2005, Executive Order 13423, and the Energy Independence and Security Act of 2007 to ensure a 30% energy reduction by 2015. Due to the large energy footprint of DoD facilities, increasing building energy efficiency offers the largest opportunity for reducing DoD energy consumption. Building HVAC systems consume greater than 30% of a building's energy consumption[1] and ensuring sustained, operational efficiencies of building HVAC systems is the focus of this proposal.

Buildings are subject to significant uncertainties and changes during their lifecycle, including weather cycles, changes in facility usage and occupancy, and equipment (including actuators and sensors) degradation. Consequently, building systems, equipment and controls optimized, designed, and configured initially cannot be expected to maintain optimal energy performance during the course of the facility operation which spans several years or even decades. In the case of district heating system that serve a campus of buildings, the hot water flow rates and temperatures are configured to be either fixed or selected based on local feedback measurements at an individual building (e.g., outside air temperature). The actual loads seen by the district heating system that reflect the variation across the campus building loads, uncertainty in environmental conditions and operational states (normal or faulty) are not utilized to optimize operation schedules for energy performance.

Advances in computationally efficient physics-based models that allow application of optimal control methods for large scale systems and enterprise-scale web-enabled networked control systems present new cost-effective opportunities for improving the energy performance of existing facilities. Recent studies of University campus cooling systems conducted by the proposal team have shown the potential for 5-10% gains in system energy efficiency when utilizing real-time and forecasted knowledge of the plant loads and environmental disturbances (on a daily basis) in a LEED Gold certified central chilled water plant [29]. This study served to demonstrate as a proof-of-concept the benefits of predictive model-based control algorithms and systems that recognize and use the dynamic patterns in the cooling plant demand. However, full-scale implementation of the advanced control policies surfaced three major challenges and deficiencies:

(i) the energy performance benefits are strong functions of the seasonal variations in the outdoor conditions and facility usage that occur over longer time scales;

(ii) the achievable energy performance is limited by equipment operation and actuator constraints (arising from changed equipment or sensor performance or faults); and

[1]Energy savings are based on 3.8 billion kWh per year of electricity consumed by DOD facilities in 2006 [1].

(iii) facility operators typically monitor specific equipment or sensor conditions for faults but are not able to discern system-level energy performance degradation or its causes.

It is now well recognized that while typical retrofit measures involving the upgrade, modification or tuning of heating and cooling plants systems and their controls can provide 10-20% reduction in energy consumption, the benefits quickly erode due to changes in the facility use or seasonal adjustments[2], thus requiring frequent re-commissioning. Furthermore, there can be discrepancies between the building control sequences actually implemented and those that were intended during design. An ongoing study being performed with ESTCP support in a LEED Gold DoD facility (SI-0929) revealed significantly higher outside air intake into the air handling units (50% of total supply air flow in comparison to the 30% intended during design stage) resulting from improperly configured outside air damper and improper fan speed tracking. The heating season energy consumption impact of such operational faults was estimated to be nearly 40%. While the individual components and sensors were all operating correctly, the faulty operation and its energy performance impact was not visible to the operator using a state-of-the-art building automation system.

The demonstration of an optimally configured building control system with integrated real-time performance monitoring and diagnostics at the scale of a campus of buildings was proposed for this effort. Such an energy performance monitoring and optimization (EPMO) system can ensure the sustained operation of facility energy conservation measures across a broader stock, and also deliver a platform where new opportunities for energy performance improvements can be identified and justified on an ongoing basis. The key technical challenges in accomplishing repeatable and robust solutions to the above problem with economically attractive payback are:

(i) obtaining models of the heating plant, buildings and control systems that can be assembled rapidly and deployed easily in commercially available building management system platforms;
(ii) achieving energy consumption reduction through advanced controls when the loads and demand are highly uncertain and actuators are constrained; and
(iii) having techniques for energy performance visualization and diagnostics to automatically detect and isolate faults that are responsible for system-level performance degradation.

The United Technologies Research Center (UTRC), in partnership with the University of California, Berkeley and Naval Station Great Lakes proposed to demonstrate a campus-scale EPMO system prototype that utilizes advanced algorithms for real-time optimization of control schedules and analytical tools for energy performance visualization and diagnostics. The demonstration focused on a district heating system connected to buildings 7113 and 7114 at the Naval Station campus.

Expected Benefits: It is expected that the broad deployment of an EPMO system for district heating[3] systems at DoD facilities will deliver and sustain 20% energy savings achieving greater

[2] Piette/Mills/LBNL Study on Performance Degradation & Commissioning
[3] It is expected that the EPMO system can reduce energy consumption for cooling system. The level of energy savings has to be evaluated through similar demonstrations.

than 0.75 billion kWh per year or $75M per year[4] with a tangible reduction of 450,000 metric ton of CO2 per year[5]. The energy reduction is achieved by providing HVAC set points that would optimize system level performance and applying energy performance monitoring and diagnostics that enable facility engineers to more proactively identify and correct poor system performance. For the selected demonstration site, the demonstrated simple payback is less than 5 years.

1.2 OBJECTIVE OF THE DEMONSTRATION

The objective of this project was to develop a standalone software environment for demonstrating a multi-building campus EPMO system for district heating system that can achieve 20% energy savings. The demonstration was carried out at the Naval Station Great Lakes in Illinois for the Bachelor Enlisted Quarters campus buildings 7113 and 7114. The demonstration activities were redirected from the chiller plant that serves the two buildings, as originally planned, to the heating plant, as a result of a mitigation plan generated after one chiller started to malfunction at the beginning of the 2012 cooling season. The EPMO system can be implemented for both chiller and heating plants.

The campus EPMO system, illustrated in Figure 1.1 consists of integrated technologies for dynamic central plant, building and HVAC modeling, model-based optimal predictive control, and energy performance visualization and diagnostics. The EPMO system was implemented as a software environment that extends the capabilities of the current existing Building Management System. For the Naval Station Great Lakes demonstration, this system interfaced directly with the Siemens Building Management System and resided on an independent computer.

[4] Energy savings are based on: 1) 0.06 quads BTU chilled water sent out from district cooling systems in the DOD facility; 2) 1 kW/ton efficiency for chilled water plant; 3) Average 10 cents per kWh.
[5] CO_2 emission reduction based on U.S. average of 1329 lb of CO_2/MWh of electricity generated (0.60 metric ton CO_2/MWh). http://www.epa.gov/cleanenergy/energy-resources/refs.html.

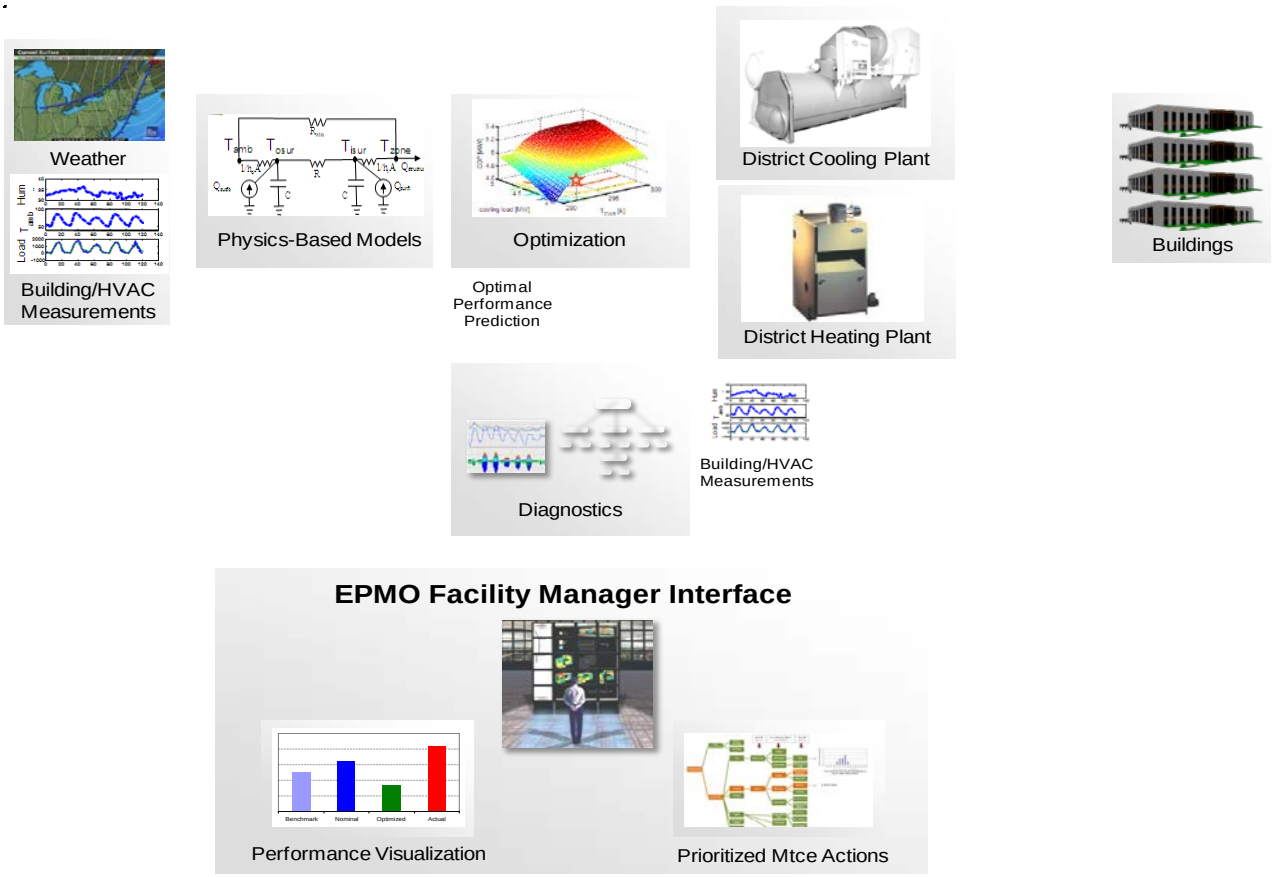

Figure 1.1 Campus Energy Performance Monitoring and Optimization (EPMO) System

The specific technical objectives, as detailed in Section 5.1, were: (i) to demonstrate 20% energy savings and enhanced campus system operational effectiveness as a result of the performance optimization algorithms within the proposed EPMO system and tools for ongoing energy performance visualization and diagnoses to sustain energy efficient facility performance; and (ii) to demonstrate EPMO system robustness and scalability for broader DoD deployment.

The technologies demonstrated address the challenges noted above, and include: 1) Reduced-order dynamic models for the campus cooling plant, building and HVAC systems; 2) Optimal control algorithms for the district cooling system integrated with online parameter estimation to dynamically update control inputs; and 3) Tools for online energy performance visualization and automated detection, isolation and prioritization of faults that impact performance.

1.3 DRIVERS

Executive Order 13423 [7] and the Energy Independence and Security Act of 2007 (Title IV Subtitle C) require that U.S. federal agencies improve energy efficiency and reduce greenhouse gas emissions by 30% by 2015 relative to a 2003 baseline.

2.0 TECHNOLOGY DESCRIPTION

2.1 TECHNOLOGY OVERVIEW

The campus-scale EPMO system was implemented as a stand-alone software environment, comprising of control and diagnostic algorithms and performance visualization tools that were interfaced directly with the Naval Station Great Lakes Building Management System (BMS) for buildings 7113 and 7114. The novelty of the proposed effort consisted in the delivery of a single platform and operator environment that integrates optimal control algorithms that use real-time data and predictive physics-based models with performance monitoring and diagnostic tools that measure actual heating plant and building energy performance.

1) Control-Oriented Building-System Performance and Zone-Temperature Models. Dynamic thermal simulation takes simulates how the two buildings interact with the internal and external disturbances. Reduced-order models for HVAC systems and buildings are based on thermodynamics, thermo-fluid law, and heat transfer analysis and are the main tools for generating predictions, diagnostics and control inputs for optimizing the plant operation and building energy utilization performance. The following specific models were developed:

- HVAC system
  - Supply and return fans power consumption
  - Mixed air temperature (return from the building zones and outdoor air)
  - Heating coils thermal power consumption
  - Total supply flow rate
  - Return temperature
- Zone VAV units
  - Thermal power consumption for reheat coils
- Zones
  - Temperature dynamic models for each zone as function of weather temperature forecast and zone thermal inertia

Each of the enumerated models was calibrated and validated using measurement data from functional tests and the BMS database. Specific tests were designed for each component by controlling in a coordinated way combinations of actuators (dampers, valves) and set points (flows, discharge temperatures) for AHUs and VAVs. The generated functional test data was combined with historical data and used to estimate performance parameters for the models. A segment of the data was used for estimation, and a different segment was used to validate the models, and thus to ensure that the models have adequate predictive capabilities. The specific models and their statistical performance are described in more details in Appendices B.1 and B.2.

2) Model-Based Optimal Predictive Control. A module was developed to generate real-time optimal set points for the site building HVAC systems using algorithms that search for the most energy efficient sequences subject to system constraints (building comfort, component performance) and disturbances (weather) by using the control-oriented building-system performance and zone-temperature models. The proposed model-based optimal control formulation integrated in the same framework: HVAC system performance models, zone temperature dynamic models, operational and thermal comfort constraints, and plant efficiency

in the same framework [30-33]. In this framework, 4-hour horizon forecasted loads and ambient conditions are used to compute the next set points values that meet the overall system objectives and individual component constraints. The process repeats at 15 minute time intervals and consists of calculating the performance impact of set points and of their efficient selection until an optimal set is reached. This repeated calculation of optimal set points ensures solution robustness and its optimal features by using the most recent measurements, load and ambient forecasts. The main computations performed at every time step are illustrated in Figure 2.1.

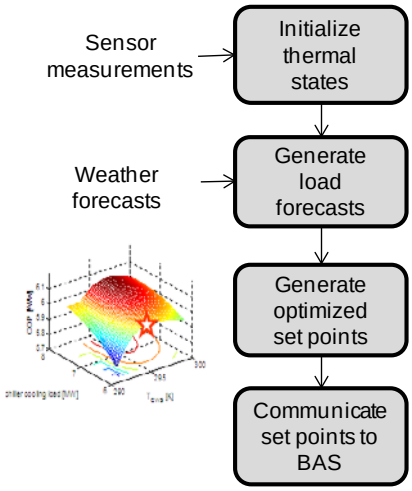

Figure 2.1. Main steps in computing the optimal set point values at 15 min time intervals

3) Model Library and Language for Optimization Problem Formulation. A software package that automates the formulation of the Model Predictive Control (MPC) problem for building HVAC systems was developed and employed as part of the project. This tool considerably reduces the effort needed to design the MPC algorithm, therefore reducing the payback time, and enhances the scalability of the approach. Specifically, the optimization modeling language uses the models described above in conjunction with information such as: thermal comfort constraints, equipment constraints, energy performance objectives. All the information is automatically integrated into an overall optimization problem that is exported to a solver (IPOPT was selected for this project). The workflow is illustrated in Figure 2.2 and its efficiency was demonstrated in particular when the algorithm was implemented on multiple AHUs. Simple modifications were made to each AHU model and the BLOM tool was used to rapidly generate all the problem formulations.

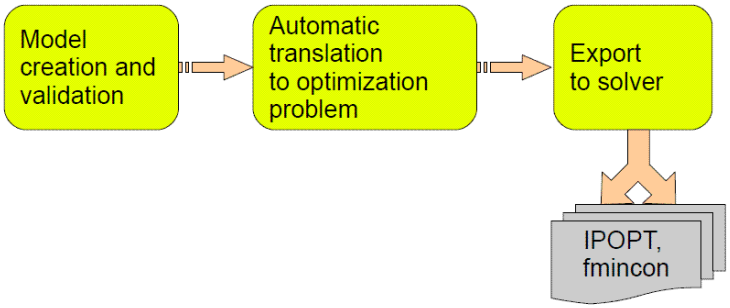

Figure 2.2. Typical workflow with BLOM

4) Diagnostics. The Diagnostics module was developed and implemented to: 1) identify and isolate faulty components or ill-configured control schedules that are responsible for the system performance deviation and degradation; and 2) make visible and prioritize the maintenance or facility operation tuning needs by quantifying the energy performance and economic losses occurring. A data-driven based diagnostics approach was used to monitor HVAC system performance. The data was represented in a hierarchical structure of energy usage and individual subsystem delivered functions. Data that was made available within the EPMO system for the building HVAC systems included: 1) BMS operational data (hot water temperatures, hot water flow rate, heating plant pump speed, and AHU fan speed, etc.); 2) HVAC equipment energy usage (AHU, and VAV); 3) weather forecast (outside air temperature and humidity); and 4) estimated and derived parameters (internal loads, unmeasured temperatures etc.) from physics-based models described above. The Diagnostic algorithms were implemented and executed during multiple time periods when actuator faults were injected by overriding the controller values, without communicating the override values to the algorithm. Faults at VAV and AHU level were injected, but it was it was determined based on measurements that the AHU faults had a significantly larger energy impact and the effort focused on these faults, in particular on damper and heating coil valve faults (stuck at various positions). The Diagnostic algorithm is described more details in Appendix B.3.

5) Fault-Accommodating Control. Model Predictive Control and Diagnostics algorithms have been integrated to generate a fault-accommodating feature of the EPMO system. The optimal control algorithm adapts on-line to the faulty system by using new constraints values when they are detected by the FDD algorithm. Two demonstrations have been conducted where faults have been injected by overriding the BMS commands for AHU dampers and heating coil valve without communicating these overrides to the EPMO system. The FDD algorithm detects the faults, diagnoses them, and communicates the new, stuck actuator positions to the control algorithm. The control algorithm uses the new constrained ranges of the actuators and accommodates to these faults by generating the optimal set points within the new constraints.

6) Data Management Software. A software tool chain was customized to allow seamless communication of Control and Diagnostics algorithms with the site BAS. The data management software comprises of a set of drivers and incorporates a database where historical BMS data was recorded for allowing both off-line and on-line access. The Control and Diagnostics algorithm receive sensor data from the BMS and communicate optimal set point values to the BMS in real-time via this software. Additional features were implemented to ensure a reliable operation of the entire software tool chain. These features monitor the status of the applications and in the rare occurrences when it fails the site BMS retakes control of the building HVAC system. The software tool chain and the mentioned failsafe features are further detailed in Appendix B.6.

2.2 ADVANTAGES AND LIMITATIONS OF THE TECHNOLOGY

The broad application of building energy management systems that apply advanced methods for HVAC operational controls and energy diagnostics to DoD's facilities is key for achieving the DoD's energy reduction targets. The energy reduction is achieved by providing HVAC set points that would optimize system level performance and applying energy performance monitoring and

diagnostics that enable facility engineers to more proactively identify and correct poor system performance. A 40% HVAC system energy reduction achieved through the application of the proposed technologies would offer greater than $150M per year savings potential across all existing DoD facilities with district heating systems[6].

The developed EPMO system differs from existing advanced building energy management systems in the following ways:

- Integrating HVAC equipment set point optimization and fault detection and diagnostics algorithms for determining the most efficient set point values when HVAC equipment malfunctions while maintaining thermal comfort whenever possible. It is a first-of-a-kind system that integrates these fault-accommodating technologies, and when faults are too severe the algorithm minimizes the impact on thermal comfort.
- Having a set point optimization algorithm (Model Predictive Control) based on optimization algorithms that uses weather forecasts, HVAC equipment models, and zone temperature models for minimizing energy consumption while meeting thermal comfort.
- By employing a model-based approach (for heat exchangers, temperature dynamics, power consumption) to reduce the manual tuning required for most of the currently implemented advanced building management systems.

The developed and demonstrated EPMO technology was matured to Technology Readiness Level 6 and several aspects need to be further investigated:

- The trade-off between instrumentation cost and the energy consumption levels for various types of buildings is not completely known. The number of sensors installed as part of the demonstration of the EPMO system was small based on the fact that the AHUs in the two demonstration buildings were similar. The project replicated some of the models developed for one AHU. This resulted in decreased instrumentation cost, but increased the uncertainty in the energy consumption.
- The EPMO technology requires expert assistance and could not be transferred to the site Facilities. The EPMO system was demonstrated for several days at a time but there were occasions when the optimization algorithms generated warnings that could only be analyzed by an expert. The complete list of warnings is not completely known for all the scenarios (weather, load, equipment health status) that might be encountered. More demonstration data is needed to determine all scenarios that can occur.
- The implementation cost was reduced compared to previous demonstrations due to the employment of software tools that automate part of the design (this was facilitated by the BLOM tool described Section 2.1). This cost can be further reduced by automating even larger parts of the EPMO system.
- The limits of robustness of the EPMO system have only been partially tested. Due to the complexity of the system, the system was tested during a limited time period when specific faults were injected (by overriding specific HVAC set points as described in other sections). At the completion of the demonstration there is limited data to determine what the performance degradation limits are for various faults.

[6] Energy savings are based on: 1) 0.06 quads BTU chilled water sent out from district cooling systems in the DOD facility; 2) 1 kW/ton efficiency for chilled water plant; 3) Average 10 cents per kWh.

3.0 FACILITY/SITE DESCRIPTION

3.1 FACILITY/SITE LOCATION AND OPERATIONS

The selected demonstration campus consisted of Buildings 7113 and 7114 at Naval Training Center, Great lakes, IL. Building 7113 is a 149,875 ft^2 recruit barracks and is a long rectangular building, consisting of a large block of berthing compartments, heads (bathrooms), laundry rooms, classrooms, a quarterdeck with a two-story atrium and office spaces, and a large cafeteria/galley. Buildings 7113 and 7114 were functionally similar (i.e. include barracks, classroom, and cafeteria etc.) and share common central steam-to-hot-water heat-transfer plant.

Figure 3.1 shows the location of Buildings 7113 and 7114 schematically within a map illustrating a part of the Navy Great Lakes campus.

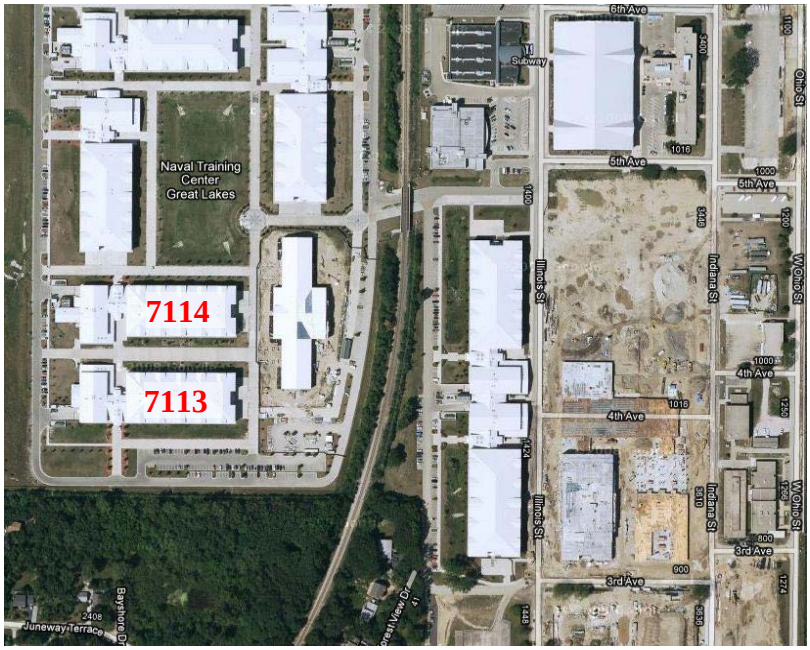

Figure 3.1. Location of Buildings 7113 and 7114

3.2 FACILITY/SITE CONDITIONS

When Buildings 7113 and 7114 are occupied by recruits, the buildings are occupied 24 hours a day for seven days a week. Recruits spend about 85% of their time in the barracks. They leave the barracks for drills and marches and during personal time on Sunday and holidays. The HVAC equipment in Building 7113 is located in five (5) mechanical rooms and attic space. Building 7114 shares the absorption chillers, cooling tower, heating hot water heat exchangers, chilled water pumping system, heating hot water pumping system, and the condenser water pumping system with building 7113. The following equipment is used in Building 7113:

- First Floor Mechanical Room
    - One (1) Air Handling Unit
    - One (1) Condensate Pump and Receiver

    - Two (2) Exhaust Fans
    - One (1) Return Fan
- Attic Mechanical Rooms
    - Two (2) Air Handling Units
    - Two (2) Toilet Exhaust Fans
    - Two (2) Coil Run Around Heat Recovery Systems
    - Two (2) Mechanical Room Ventilation Exhaust Fans
- Attic Space
    - Two (2) Return Air Fans
    - Two (2) General Exhaust Fans
    - Four (4) Attic Exhaust Fans
- Second Floor Mechanical Room 2063
    - One (1) Air Handling Unit
    - One (1) Air Conditioning Unit
    - One (1) Return Fan
- Second Floor Mechanical Room 2068
    - One (1) Air Handling Unit
    - One (1) Return Fan
- Outdoor
    - Seven (7) Roof Exhaust Fans For Dining/Galley
    - One (1) Air Cooled Condensing Unit for the refrigerators/freezers
- Miscellaneous
    - Eighteen (18) Drying Room Cabinet Unit Heaters
    - Five (5) Hot Water Unit Heaters
    - Three (3) Electric Unit Heaters
    - One (1) Vestibule Cabinet Unit Heater
    - One (1) Vestibule Radiator
    - One (1) Trash Room Exhaust Fan
    - One (1) Trash Compactor Room Exhaust Fan

The HVAC equipment in Building 7114 is located in six (6) mechanical rooms and attic space. The following equipment is used in Building 7114:

- First Floor Mechanical Room

    - Two (2) Trane Absorption Chillers
    - Three (3) Primary Chilled Water Pumps
    - Three (3) Condenser Water Pumps
    - One (1) Condensate Pump and Receiver
    - Two (2) Exhaust Fans
- Mezzanine Mechanical Room
    - One (1) Air Handling Unit
    - Two (2) Heating Hot Water Heat Exchangers
    - Three (3) Secondary Chilled Water Pumps
    - Three (3) Heating Hot Water Pumps
    - One (1) Return Fan
    - One (1) Exhaust Fan
- Attic Mechanical Rooms
    - Two (2) Air Handling Units
    - Two (2) Toilet Exhaust Fans
    - Two (2) Coil Run Around Heat Recovery Systems
    - Two (2) Mechanical Room Ventilation Exhaust Fans
- Attic Space
    - Two (2) Return Air Fans
    - Two (2) General Exhaust Fans
    - Four (4) Attic Exhaust Fans
- Second Floor Mechanical Room 2063
    - One (1) Air Handling Unit
    - One (1) Air Conditioning Unit
    - One (1) Return Fan
- Second Floor Mechanical Room 2068
    - One (1) Air Handling Unit
    - One (1) Return Fan
- Outdoor
    - One (1) Cooling Tower
    - Seven (7) Roof Exhaust Fans For Dining/Galley
    - One (1) Air Cooled Condensing Unit for the refrigerators/freezers

- Miscellaneous
    - Eighteen (18) Drying Room Cabinet Unit Heaters
    - Five (5) Hot Water Unit Heaters
    - Six (6) Electric Unit Heaters
    - One (1) Vestibule Cabinet Unit Heater
    - One (1) Vestibule Radiator
    - One (1) Trash Room Exhaust Fan
    - One (1) Trash Compactor Room Exhaust Fan

A distributed DDC control system, APOGEE™ Insight by Siemens Building Technologies is installed in Buildings 7113/7114. This system monitors all major lighting and environmental systems. Building electric and water meters will also be read by the DDC system. Operator workstations provide graphics with real-time status for all DDC input and output connections.

The heat water flow generated steam-to-hot-water heating plant is distributed between the 5 AHUs of each of the two buildings as follows:

- AHUs 1 and 2, which serves the sleeping compartments, consume 18.5% of the total capacity each
- AHU 3, which serves the classrooms, consumes 3% of the total capacity
- AHU 4, which serves the galley and dining areas, consumes about 9.5% of the total capacity
- AHU 5, which serves the quarterdeck area, consumes 0.5% of the total capacity.

Figure 3.2 illustrates the screenshot from the site BMS and highlights AHUs 1 and 2 from both buildings that were used for demonstration. Figure 3.3 illustrates the riser diagram for one AHU, and includes AHU 1 components, all the served supply and return VAVs on all three floors.

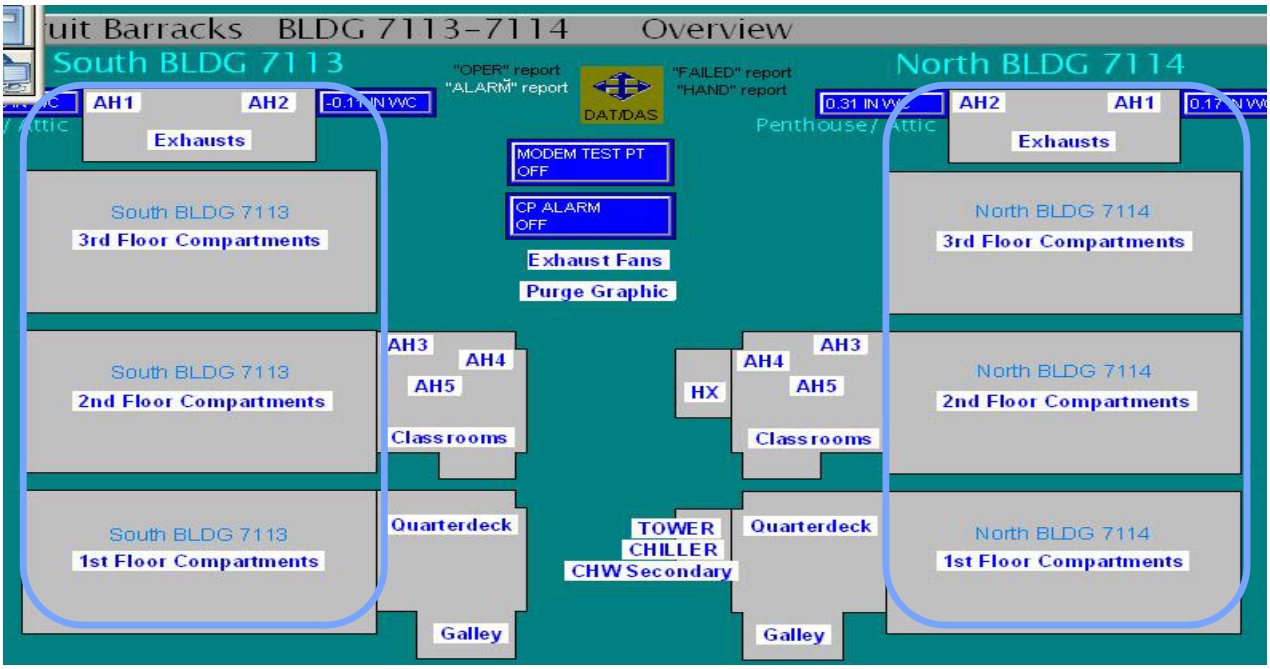

Figure 3.2. BMS screenshot that shows the AHUs used for demonstration in both buildings

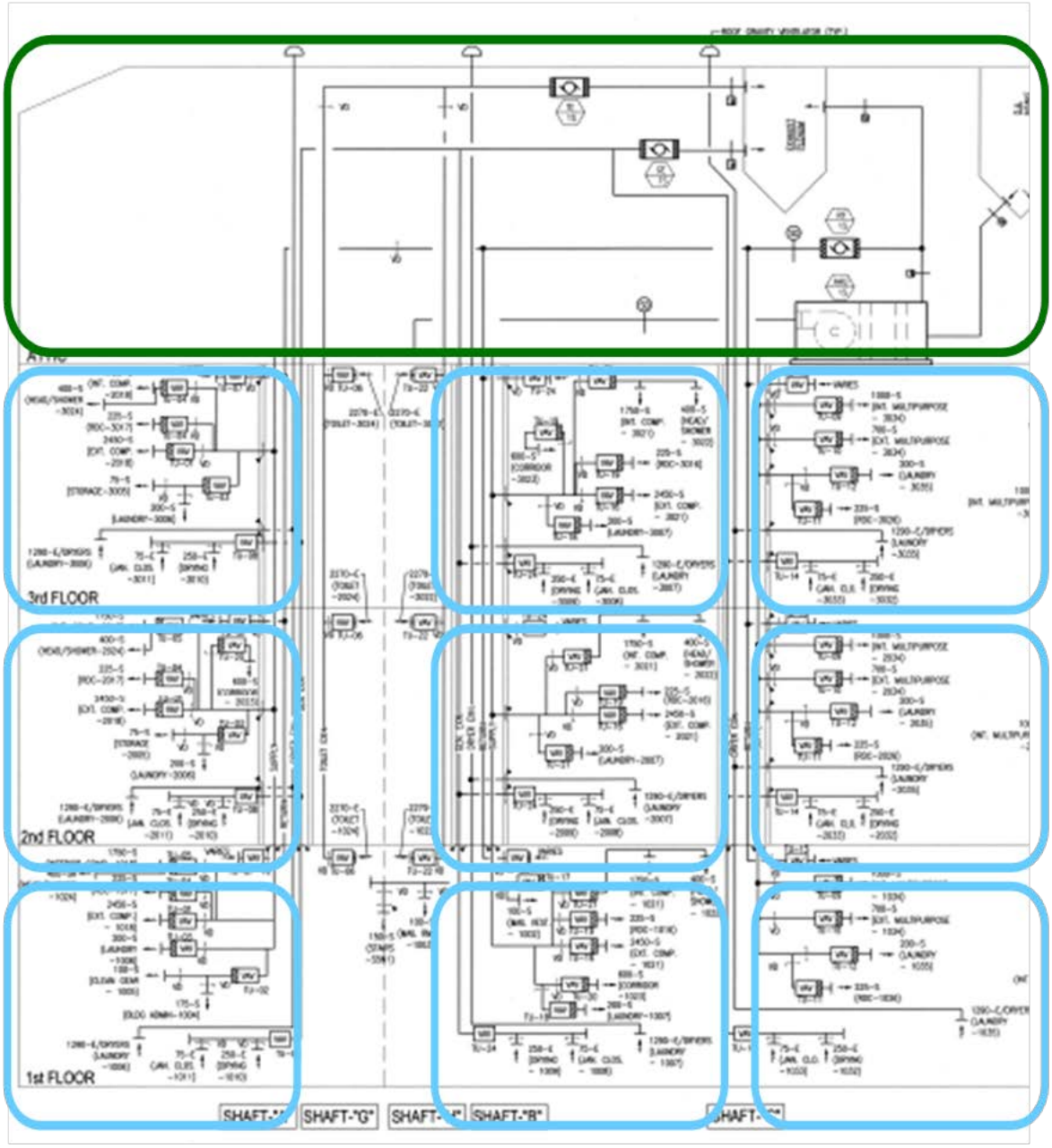

Figure 3.3 Riser diagram for one of the AHUs used for demonstrations of the EPMO system

In Figure 3.3, the main AHU components are illustrated in green box; the 9 compartments served by this AHU and the associated VAVs are grouped in the blue boxes. The EPMO system was implemented for three AHUs serving in total 54 VAV units, therefore controlling about 55% of the two-building site. The three AHUs are: AHU 1 and 2 in Building 7114, and AHU 1 in Building 7113. It was determined that AHU 2 in Building 7114 had some issues with a critical temperature sensor and the project team decided to not include AHU 2 in the demonstration and use it as a baseline, for energy performance comparison purposes (for which the temperature was estimated based on other sensor data)

3.3 SITE-RELATED PERMITS AND REGULATIONS

The site specific permits relate to any hot work (i.e., cutting, welding) required for building instrumentation installation (i.e., water flow meters). In addition, electrical Lock-Out-Tag-Out procedures will be used by our subcontractors for installing electrical power instrumentation. No other permits or regulations are applicable other than complying with EM385-1-1 (safety issues) [20].

4.0 TEST DESIGN

4.1 CONCEPTUAL TEST DESIGN

The project consisted of three demonstrations conducted for several days from November 2012 to March 2013. The total test duration was 26 days for all three AHUs (two in Building 7114 and one in Building 7113) and 54 terminal units. The number of demonstrations were constrained by the physical access to the site; a remote connection to the site BMS would facilitate more demonstrations. During the EPMO testing period the system executed the following tasks:

- Optimal Control: The EPMO system uses real-time data from HVAC, heating plant, and building sensors to determine the optimal set points that could reject the building loads with minimum energy consumption while maintaining occupant comfort.
- Fault Detection and Diagnostics: The EPMO system used BMS real-time data to first detect and then diagnosed HVAC equipment faults. The faults were associated with HVAC actuators (dampers and valves at terminal unit and AHU levels) and were detected based on the discrepancies between model-based predictions and sensor measurements.
- Fault-Accommodation: Upon diagnosing HVAC system faults, the EPMO system adapted the set point values to compensate for the faults while maintaining the occupant thermal comfort with minimum energy possible energy consumption.

The sequential operation of the EPMO technologies and baseline strategies (illustrated in Figures 4.1 and detailed further in Section 4.4) over a heating season 2012-2013 ensures that the performance improvement estimates are consistent and representative for a wider range of operating conditions (ambient, loads). Baseline strategy is represented by the set point logic implemented in the building BMS.

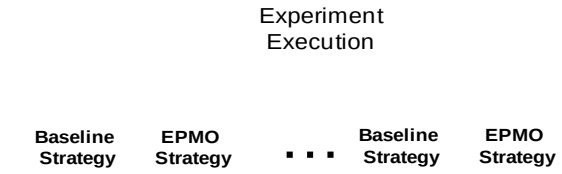

Figure 4.1 Staggered test schedule executed from Nov. 2012 – March 2013

4.2 BASELINE CHARACTERIZATION

The baseline system performance was characterized only for days with the same ambient temperature pattern as the days in which the EPMO system was implemented. The healthy baseline system performance was estimated using the metrics described in Table 5.1 based on the measurements recorded during normal operation of the HVAC system as explained in Section 5.1. The intent was to use operational data collected during various combinations of load and ambient conditions that could help characterize the variability of the Table 5.1 metrics.

The faulty baseline system HVAC system performance was estimated using data recorded while the baseline set-point schedule was implemented with controlled faults. The performance estimate of the faulty HVAC system presented challenges due to the randomness inherent in the HVAC component malfunction occurrences. The additional challenge was to replicate the same fault for the EPMO system in order to estimate performance improvements in similar operational conditions. To increase the confidence in the EPMO system improvement estimates, the tests implemented specific faults that were realized by restricting actuator ranges (valves, and dampers) and therefore mimicking the observed and detected naturally-occurring faults. During the demonstration period these artificial faults were implemented both for the baseline system and for the EPMO system. The characterization of the baseline performance took into account the impact of these malfunctions.

Due to the challenges in replicating similar faults for the baseline and EPMO schedules the baseline characterization had the following limitations:

- Only the impact of *controlled*[7] faults was investigated.
- The controlled fault set was a subset of naturally occurring malfunctions.
- EPMO system performance is subject to large (and only partly known) uncertainty when the load and ambient conditions vary significantly between the baseline and EPMO policy implementation periods.

4.3 DESIGN AND LAYOUT OF TECHNOLOGY COMPONENTS

Instrumentation and Monitoring Building 7113/7114

The required measurement points and measurement accuracy were taken from the *Specifications Guide for Performance Monitoring Systems* (http://cbs.lbl.gov/performance-monitoring/specifications/).

The additional hardware and software necessary to implement the EPMO system in Buildings 7113 and 7114 are listed in Table 4.1. All of the building performance monitoring points that were used by the EPMO system are listed in Table 4.2. Approximately 2665 points were mapped from Siemens BMS system to the EPMO system. The cost estimates for these monitoring points are provided in Section 6.

Table 4.1. Additional system tool components for Buildings 7113 and 7114

Component	Quantity	Note
PC	1	Window XP, 2.5GHz processor speed, 1 GB memory, 250 GB hard drive, UPS is recommended.
Siemens BACnet Server	1	Established the communication capability between the Siemens APOGEE™ system and the EPMO system (data acquisition).

[7] *Artificial* or *controlled* faults: the HVAC test conditions where actuator ranges (valves, fans, dampers) are intentionally restricted, via set point control, to specific and limited operational ranges with the purpose of replicating faults observed during normal HVAC system operation.

Table 4.2. Performance monitoring points list for Buildings 7113 and 7114

Point needed	Status		Note
	New	Existing	
Building pressure		X	
Plug load power		X	Installed in two compartments
Absorption chilled steam condensate flow meter			
CHW primary pump power		X	One time power measurement
CHW secondary pump power		X	Utilize the VFD power measurement.
CHW supply temp		X	
CHW return temp		X	
CHW flow meter		X	
HW pump power		X	Utilize the VFD power measurement.
HW supply temp		X	
HW return temp		X	
HW flow meter		X	
AHU supply fan power		X	Utilize the VFD power measurement.
AHU return fan power		X	Utilize the VFD power measurement
Zone temperatures		X	
Zone relative humidity (RH)		X	
VAV box damper position		X	
VAV box air flow		X	
VAV box-reheat coil valve		X	
AHU supply air temperature		X	
AHU mixed air temperature		X	Average sensors were installed for AHU 1
AHU return air temperature		X	
AHU static pressure		X	
AHU air flow		X	

AHU heating coil		X	
AHU cooling coil		X	
AHU economizer damper position		X	
AHU fan pressure rise	X		
VAV airside pressure drop		X	
Secondary pump pressure rise	X		
Secondary pump flow rate	X		
Absorption chiller steam inlet temperature	X		
Absorption chiller steam outlet temperature	X		
Absorption chiller steam inlet pressure	X		
Absorption chiller steam outlet pressure	X		
Cooling tower water flow rate	X		
Cooling tower air outlet temperature	X		
Cooling tower fan power		X	
Cooling tower outlet humidity or wet bulb	X		
Cooling tower pump power	X		Constant speed pump
Steam inlet temperature for the steam-to-hot water heat exchangers	X		
Steam outlet temperature for the steam-to-hot water heat exchangers	X		
Steam inlet pressure for the steam-to-hot water heat exchangers	X		
VAV damper position feedback		X	
AHU damper position feedback		X	
Valve position sensors	X		Encoders or limit switches to verify valve positions. They may be placed on the valves for the cooling tower, chiller, AHU, and/or VAV
Btu meters on AHUs	X		Installed for both heating and cooling deck for AHU 1

Performance Monitoring System PC Server

The overall system schematic diagram is shown in Figure 4.2. The PC server that executed the EPMO system was located in the same building location as the PC running the Siemens EMCS. The Siemens BACnet interface was a gateway between the Siemens server and the EPMO system. The gateway enabled two-way communication of relevant real time building and heating plant measurements between the Siemens server and the EPMO data exchange system through an individual Ethernet connection separated from the Navy's Intranet network.

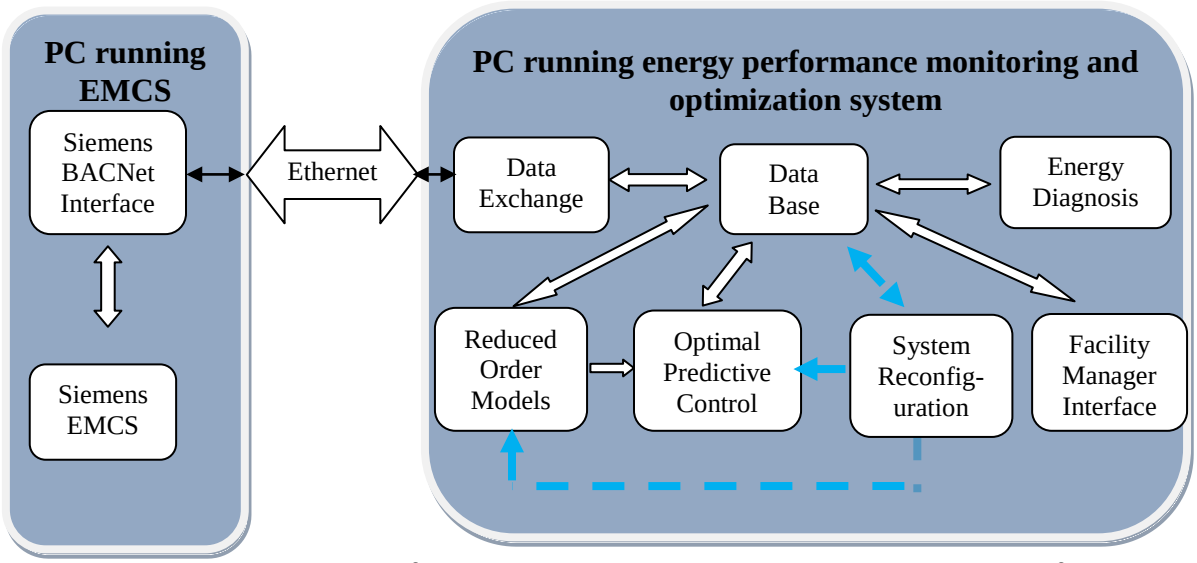

Figure 4.2. Schematic diagram of the EPMO system main components and its interface with the EMCS

Within the EPMO system there are several modules necessary to achieve the proposed system functional requirements. The exchange module will transfer the received data to the Data Base module which will store data into the database. The calibrated Reduced Order Model (ROM) module that represents the design/optimal building performance will receive the relevant data (e.g., weather data, estimated loads) used by the simulation and execute the reference ROM model at each sampling interval. The ROM simulated results will then be passed back to the Data Base module where the results will be stored in the database. The optimal predictive control module will use the ROM and sensors measurements to calculate optimal set-points for the district steam-to-hot water heat-exchangers plant. The set-points will satisfy the imposed systems constraints and minimize energy cost. The module operates on-line and communicates with the Siemens server through the data exchange and the Data Base module. The optimal performance prediction will also be sent to the Siemens server through the facility manager. The Energy Diagnostic tool will communicate directly with the database to retrieve a data history (building measurements, building reference model predictions and actuator inputs generated by the optimal predictive control). The Energy Diagnostic tool will apply data mining and anomaly detection methods to identify building faults.

The database stores all the relevant building performance data, ROM simulation results and the Energy Diagnostic tool results (faults and recommendations) every hour. The database can be any Structured Query Language (SQL) database (e.g., MySQL, PostgreSQL).

The system reconfiguration module will be activated when a significant and correctable fault is detected. The module (in conjunction with the ROM and the optimal predictive control modules) will be used to predict operational improvements and energy savings that could be achieved when the supervisory control is re-configured to compensate for the fault. The module will include tools for functional testing to isolate faults and tools for modifying the internal model or the constraints used in the optimal predictive control module. The decision to implement the proposed corrective action(s) automatically or manually will be coordinated with the facility manager.

The facility manager interface module will be the user front-end interface to demonstrate the results as well as to display the building performance data. The building data includes system and equipment performance, controller status and fault status. The module will be an interactive, visual interface platform that allows the facility team to access the impact of an isolated fault and make informed operational decisions.

4.4 OPERATIONAL TESTING

The challenge in estimating the performance improvements of the EPMO system stemmed from the randomness of HVAC system faults. Although the staggered schedule operation discussed in Section 5.1 ensured consistency and robustness of performance estimates for healthy systems, the occurrence of different faults while the two systems are operating increases the uncertainty of the performance estimates. To reduce this uncertainty, controlled faults were emulated by means of restricting actuator operational range whenever possible and representative. We distinguished three operational testing scenarios. The characterization of the baseline and estimates of the performance improvements is explained below for each individual test types.

- Test Type 1: In this case, the HVAC system was controlled with both the baseline and EPMO policies, and its operation was not affected by controlled faults. The policy measurements from both experiments were used directly to compute the energy-related metrics described in Table 5.1 and to estimate the performance of the optimal set point calculation algorithm for a healthy system.

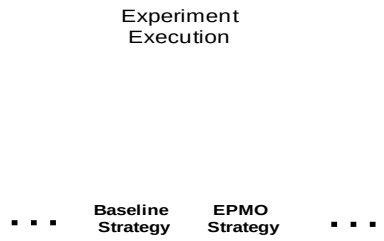

Figure 4.3. Illustration of testing scenario for the healthy system

- Test Type 2: In this case, the same controlled faults were injected in the system to test the performance and robustness of the EPMO system. These faults consisted of restrictions to specific ranges of AHU and VAV damper and valve positions. The implementation of these faults was accomplished by constraining the range of mentioned actuators through appropriate set points communicated to EMCS. The same controlled faults were implemented for both strategies and in this case measurements were used directly to estimate energy efficiency improvements. The faults associated with the VAVs, such as constrained ranges for dampers and re-heat coil valves were deemed to have small impact on energy performance. Therefore they were tested only for a few hours.

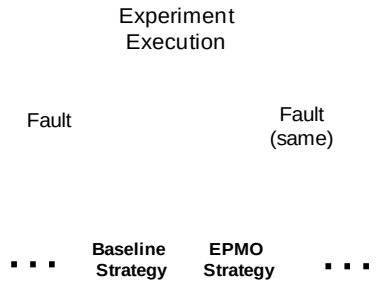

Figure 4.4. Illustration of testing scenario for the faulty system

The tests described above were implemented as part of the EPMO system demonstration between November 2013 and March 2013 as illustrated in Table 4.3. In total, the EPMO system was demonstrated for 26 days (all test days combined for all AHUs).

Table 4.3. Tests executed for the three AHUs during the demonstration period November 2012-March 2013

	B7114 AHU1	B7114 AHU2	B7113 AHU1
Oct.	Functional tests		
Nov.	Functional tests & MPC Demonstrations	Functional tests & MPC demonstrations	Functional tests & MPC demonstrations
Dec.	MPC demonstrations & Fault diagnostics (VAV)	MPC demonstrations	MPC demonstrations
Feb.	Functional tests for Fault Accommodating Control (AHU)	MPC demonstrations	Fault Insertion
Mar.	MPC demonstrations	MPC demonstrations	MPC demonstrations

4.5 SAMPLING PROTOCOL

The existing Siemens APOGEE™ EMCS collects all the building performance data, including the additional measurement data proposed by this project. The data communication within the APOGEE™ is accomplished by a Siemens proprietary protocol. In order to acquire the relevant data for this demonstration project, an APOGEE™ BACnet interface was installed. This

BACnet interface allowed the existing Siemens EMCS to exchange data with the external data acquisition system through the BACnet protocol. The existing data scan intervals used in the Siemens APOGEE™ EMCS (seconds) were matched by the Data Acquisition module within the EPMO system to ensure the collection of sufficient data to represent the real-world building operating conditions.

BACnet is a communications protocol for building automation and control networks. It is an ASHRAE, ANSI, and ISO standard protocol. BACnet was designed to allow communication of building automation and control systems for applications such as heating, ventilating, and air-conditioning control, lighting control, access control, and fire detection systems and their associated equipment. The BACnet protocol provides mechanisms for computerized building automation devices to exchange information, regardless of the particular building service they perform.

The Data Acquisition module in EPMO system served to acquire the relevant building performance data from the Siemens BACnet interface. The communication was established through an Ethernet connection. Data quality control information was provided in Section 5.6.2. Section 5.3.2 presents some information about the data sampling and the relevant building performance sampling points to be collected are presented in Table 4.2 in Section 5.3.1.

4.6 EQUIPMENT CALIBRATION AND DATA QUALITY ISSUES

Calibration of Equipment

All the equipment components specified in Section 4.3 were calibrated by the manufacturer, before the installation was commissioned.

During the building performance monitoring period, sensor data was used to computes various statistics to ensure computed values are within acceptable ranges. Specifically, data for each measured point was used to compute the minimum value, maximum value, mean (average) and standard deviation. These are computed periodically for various lengths of time and the values are compared with reference values obtained from accuracy analysis (using spiked values or duplicates when appropriate). If the computed values are outside of the reference range, then the data is flagged and further analyzed to identify and (and possibly discard) any false data points. In one of these cases it was determined that one VAV had a damper malfunction; in another case it was determined that one of the AHU controller generated inadequate set point values, and the control software was re-loaded. All measurement points were directly from existing BMS, the controller vendors (e.g., Siemens at Great Lakes) monitored these points based on control industry standards and protocols to make sure that all the measurements were in the acceptable accuracy band.

Calibration of Reference Model

The ROM model represented the desired performance of the building envelope, HVAC, lighting and control systems. Metering data for building electricity and hot water usage, and sub-metering data for HVAC equipment (e.g., AHUs, heating hot water heat exchangers, pumps) were used to calibrate and validate the ROM model. Real-time weather forecast data was separately entered into the algorithm, due to lack of availability of an Ethernet connection at the site. During the

calibration process, some inputs, such as internal gains (loads), were calibrated as accurately as possible.

Quality Assurance Sampling

Data quality was very important for the performance of the EPMO system. The sampling frequency had effects on the types of faults that the system could detect. Higher frequency sampling was limited by the bandwidth capability of the communication network with the BMS. Since the goal was to communicate set points and detect the energy consumption related faults, a five-minute sample frequency was used for most monitoring data. Scripts were used to automatically remove the duplicated data and spiked samples from raw data, synchronize data, and output clean, conditioned data for an analysis within the EPMO system. This process served as a final check before the data is used for diagnostics.

The reality of instrumentation-related research is that missing data is possible even though the instrumentation and monitor systems are designed and commissioned to be reliable. Statistic methods such as extrapolation, interpolation and trend analysis, augmented by domain expertise, were applied to fill the missing data.

Accuracy is the closeness of agreement between the result of a measurement and a true value of the measurement [23]. Since the true value cannot be determined exactly, the measured or calculated value of highest available accuracy is typically taken to be the true value. This was addressed in two ways as described below:

- Spiked samples – Spiked samples are defined as measurements that are taken for certain points and then compared against expected values obtained in "laboratory setting". Spiked samples are used to measure accuracy. For the sensors used in building systems such as temperatures sensor and flow sensors, it is difficult to have this spiked sample testing after these sensors are in place. However, these sensors were tested and calibrated before the installation. For example, temperatures sensors are usually calibrated in the lab for certain points such as 32°F / 0°C (ice-water mixture) and 212°F / 100°C (water boiling point).
- Blanks samples - Blank samples are clean samples, produced in the field, used to detect analytical problems during the whole process. In the proposed system, blanks samples were created when the building was in normal operation in order to establish and calibrate a baseline model.

Data Analysis

Quality of the data acquired from the BMS was crucial for the success of this project and data quality review was an integral aspect of the proposed approach. Robust data quality evaluation includes testing for precision, accuracy, representativeness (including sampling rate and latency issues) and completeness of the data.

Data precision [23] is the closeness of agreement between indications obtained by replicate measurements on the same or similar objects under specified conditions. Precision is used to define measurement repeatability and measurement reproducibility. Repeatability is the variability of a measurement due to keeping all controllable and uncontrollable factors constant. It is typically measured by taking data very close together in time, under as close to the same

conditions as possible in a laboratory setting. Reproducibility is the variability due to specific controllable or uncontrollable factors by observing measurements at various system configurations. Typical statistical techniques used to accomplish this are analysis of variance and analysis of covariance methods. We use the specification sheets provided by sensor manufacturers as a guideline but in cases where sensors did not perform as expected, further analysis was performed and root causes investigated with the installer's assistance.

5.0 PERFORMANCE ASSESSMENT

5.1 SUMMARY OF PERFORMANCE OBJECTIVES AND OUTCOMES

The EPMO system results are shown in Table 5.1 and discussed in details in the next section.

Table 5.1. EPMO system performance table

Performance Objective	Metric	Data Requirements	Success Criteria[8]	Measured Performance
Quantitative Performance Objectives				
Reduce Campus Energy Consumption (Energy) & Greenhouse Gas Emissions (CO2)	Building total electric consumption (kWh/ft^2-yr), and peak demand (kW) Steam consumption for heating plant operation (therm/ ft^2-yr) and peak demand Building total equivalent CO_2 emissions (kg)	Metering data for building electric and heating plant steam usage Building simulation data for equivalent CO_2 emissions	>20% reduction in building total energy consumption (over baseline) >15% reduction in building peak demand energy (over baseline) >20% reduction in building total equivalent CO_2 emissions (over baseline)	>40% reduction in building total energy consumption (over baseline) >10% reduction in building peak demand energy (over baseline) >40% reduction in building total equivalent CO_2 emissions (over baseline)
Reduce HVAC Equipment Specific Energy Consumption (Energy)	Specific energy consumption for each individual component Steam-to-hot-water heat-transfer plant (BTU/ton) AHU (kW/ton) Fan (kW/CFM) Pump (kW/gpm)	Sub-metering data for all HVAC equipment to compute energy and mass flows through each unit	>10% reduction in HVAC equipment energy consumption (over baseline)	Objective not met: Insufficient meters[9] to estimate specific energy consumption
Reduce Building Loads (Energy)	Lighting loads (kWh) Plug loads (kWh)	Sub-metering data for lighting and plug loads	5-10% reduction in lighting and plug loads (over baseline)	Objective not met: The lighting and plug loads were not addressed in the selected demonstration buildings[10]

[8] Success criteria related to building and HVAC equipment energy consumption was assessed using both model-based simulations and actual energy measurements. Note: only those recommended energy fault corrective actions and HVAC operation strategies that are implemented by DOD facilities during the execution of this project will be assessed using actual energy measurements.

[9] All relevant meters were installed for chillers. When the chillers started to malfunction in 2011, the team changed focus, with approval from ESTCP, to heating plants. However, a significant part of the instrumentation budget was spent on chiller meters.

[10] At the time when these performance metrics were proposed, the team selected different buildings at the Navy campus for which reduction in lighting and plug loads presented a larger potential. In buildings 7113 and 7114 were the demonstrations were conducted, lighting and plug loads are significantly smaller compared with thermal loads.

Performance Objective	Metric	Data Requirements	Success Criteria[11]	Measured Performance
Quantitative Performance Objectives				
Maintain/Improve temperature regulation[12]	Average zonal temperature deviation [deg C] (from set points) during periods of occupancy when systems (heating plant, AHUs, VAVs) operate without faults	Zone temperature measurements and set-points during no-fault system operation	Metric with optimized control policy <= Metric with baseline control policy	Discomfort reduced by 75%.[13]
Energy Performance Monitoring and Optimization System Robustness	Percentage of faults classified correctly[14]	Building energy fault identified/classified by Energy Performance Monitoring and Optimization System	85% of faults identified are classified correctly (during the demonstration period)	84% of the faults were classified correctly (during the demonstration period)
Energy Performance Monitoring and Optimization (EPMO) System Payback[15]	Simple payback time, SIR (Savings-to-Investment Ratio), NPV (Net Present Value)	Cost to install and implement EPMO system Savings from using EPMO system	Simple payback time is less than 5 years[16] SIR is greater than 1.25 NPV is greater than 0	Simple payback is 3.56 years SIR = 2.06 NPV = $86,168
Qualitative Performance Objectives				
Ease of Use	Ability of an energy manager and/or facility team skilled in the area of building energy modeling and control to use the technology	Feedback from the energy manager and/or facility team on usability of the technology and time required to learn and use	With some training, An energy manager and/or facility team skilled in HVAC able to use the Energy Performance Monitoring and Optimization System to identify and correct poor HVAC system performance	Objective not met: EPMO system was matured to TRL level 6 in this demonstration. At this level expert supervision is required.
Prioritization of Energy Faults and Corresponding HVAC System	Ability to detect, classify and prioritize building faults Ability to prioritize the alternative energy	Building measured data Building simulation data	Energy manager and/or facility team able to prioritize building faults and corresponding energy- efficient HVAC	Objective partly met: A visualization tool was installed as part of another similar effort. The

[11] Success criteria related to building and HVAC equipment energy consumption will be assessed using both model-based simulations and actual energy measurements. Note: only those recommended energy fault corrective actions and HVAC operation strategies that are implemented by DOD facilities during the execution of this project will be assessed using actual energy measurements.
[12] For system with no faults
[13] The metric selected for discomfort is the total time when any of the zone temperatures exceeds the comfort band (during heating season this is 68^0F-76^0F)
[14] Faults which can be verified using functional tests
[15] This payback success criterion is only applied to the case when the only retrofits considered are those that do not involve major equipment retrofits
[16] DoD Energy Managers Handbook http://www.wbdg.org/ccb/DOD/DOD4/dodemhb.pdf

Operation Strategies	efficient HVAC system operation strategies		system operating strategies by comparing simulated or measured building performance for various faults or operating strategies.	team did not receive feedback from Facilities.

5.2 PERFORMANCE ESTIMATION METHOD

The quantitative metric values of Table 5.1 were estimated based on comparisons between the performance of baseline HVAC control logic implemented in the building BMS and that of the EMPO system. HVAC system performance is affected by several sources of uncertainty that results in large performance variations even for the same control schedule during the same season. These uncertainties impact the EPMO system performance estimates:

- **Leakages:** in supply and return duct; infiltration and exfiltration from the building
- **Incompletely known baseline control sequences:** it was observed during the EPMO system demonstration that the BMS control sequences were not entirely consistent with the sequence of operations
- **Equipment health status:** several faults were diagnosed and repaired by the building HVAC technicians for the equipment with more instrumentation; it is possible that several other pieces of equipment were affected by similar faults but these could not be diagnosed due to insufficient instrumentation
- **Varying thermal loads:** the building is subjected to several load types that cannot be fully determined: occupants; solar radiation; building insulation quality; open windows.

The performance estimate was based on comparing energy and peak power consumption, and thermal comfort between days when the EPMO system was demonstrated and historical performance of the HVAC system on days with similar ambient temperature. The estimation method is summarized below.

The performance estimation method consists of several steps which are detailed below for one AHU and for one single test period:

- For each day when the EPMO system was implemented, multiple historical days with similar temperature values were identified when the baseline schedule was executed (in general we selected three historical days with the closest temperature profile). An example is provided in Table 5.2.1 where the MPC and the corresponding baseline days are described. Figure 5.2.1 illustrating the temperature time series data corresponding to these days. It is observed that the MPC day temperature is in general lower than the Baseline day temperatures which is likely to result in conservative (lower) energy savings estimates (during heating season). In Figure 5.2.1, the number of selected samples coincides with the samples when the EPMO system was executed.

Table 5.2.1 Case study: date and time of selected MPC and baseline days

Scenarios	Date	Time
MPC Day	Feb. 13, 2013	0AM to 24PM (24 hours)
Baseline Day 1	Dec. 11, 2011	0AM to 24PM (24 hours)
Baseline Day 2	Dec. 26, 2011	0AM to 24PM (24 hours)
Baseline Day 3	Jan. 8, 2013	0AM to 24PM (24 hours)

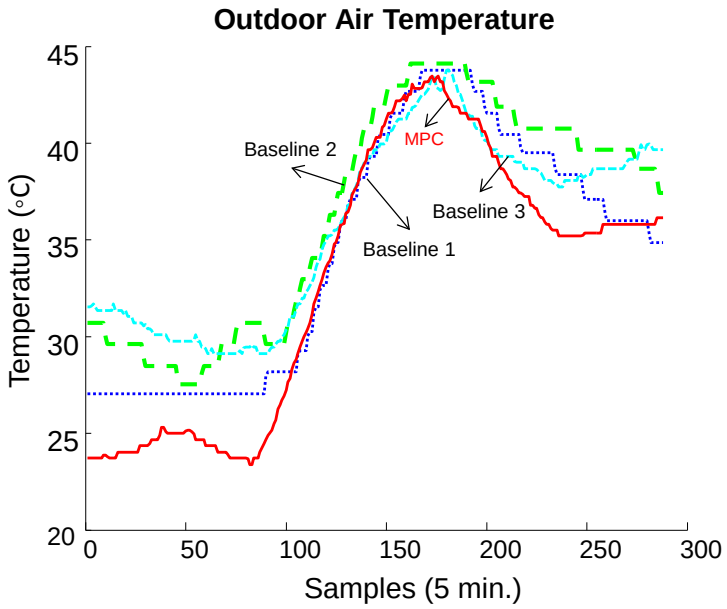

Figure 5.2.1 Ambient temperatures for EPMO (red) and BMS systems (blue, cyan, and green).

Figure 5.2.2 shows the comparisons of power consumption of AHU heating coil, fan, and VAV reheat coils, respectively. As can be observed, MPC consumed more heating power (heating coil + reheat coils) during the samples [0 to 50] and [225 to 288]. This was due to the heating-set-point increases (step-change) in the morning (~3:45AM) and evening (~6:50PM) period. The MPC algorithm was able to adapt itself to these set point changes and thus consumed more energy to maintain the comfort during these periods.

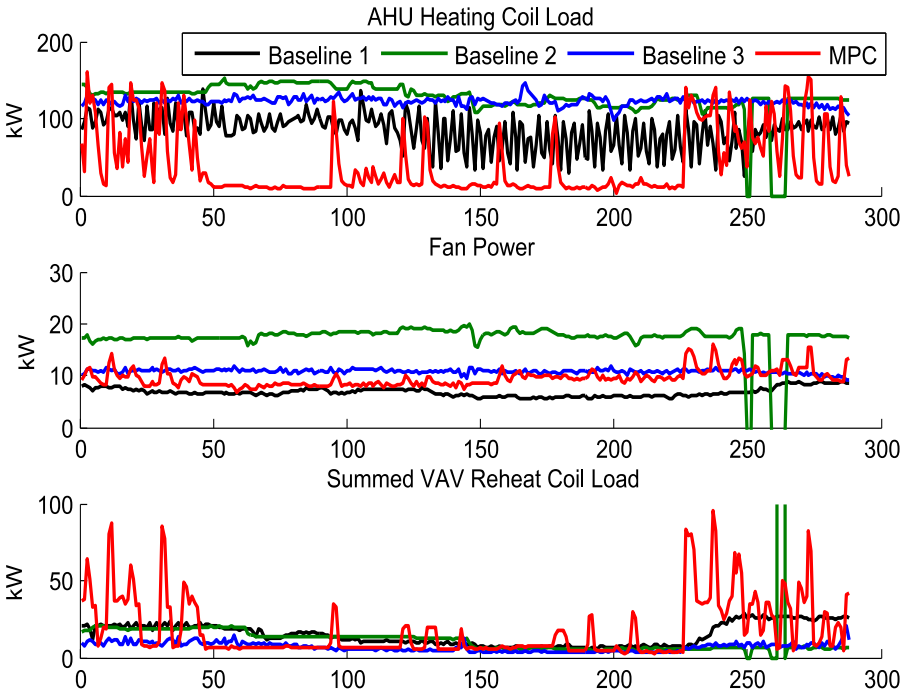

Figure 5.2.2 Comparison of power consumption components (heating coil, fan, and reheat coils)

Figure 5.2.3 shows the comparisons of energy consumption breakdown between the baseline control and the MPC. The system with the proposed MPC strategy has demonstrated more than 40% average energy consumption reductions. It can be further observed that most energy reductions come from the heating coil at the AHU level.

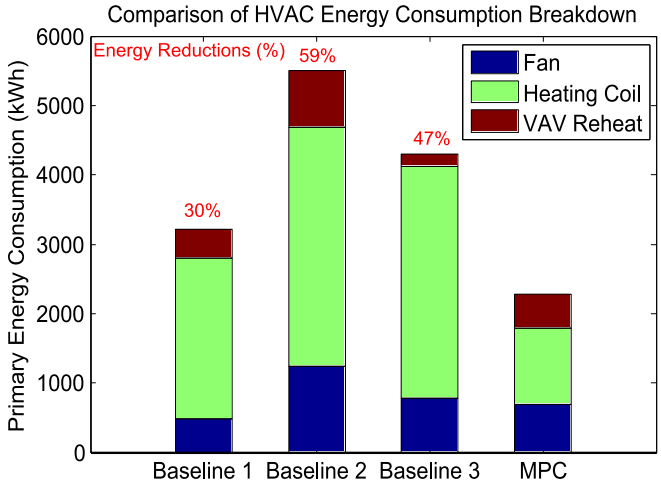

Figure 5.2.3 Comparison of energy consumption components (heating coil, fan, and reheat coils)

- Performance estimates where generated for each demonstration day by comparing energy consumption and thermal comfort for the same days as those selected at the previous step. For each AHU_i, the relative performance comparison was computed using the following formulae

$$Performance\_Relative_{AHU_i,DemoDay_j} = Average_{HistoricalDay_k}\left[1 - \frac{MPC\_Performance_{AHU_i,DemoDay_j}}{Baseline\_Performance_{AHU_i,BaselineDay_k}}\right]$$

where the average is calculated over the baseline days $BaselineDay_k$ with the same ambient temperature pattern as the demonstration day $DemoDay_j$. The performance values correspond to energy consumption (electric and thermal), peak power, and occupant's thermal discomfort (defined in Section 5.3). The temperature and CO_2 time series data for one zone, for the same three days as those of Figure 5.2.1, are illustrated in Figure 5.2.4.

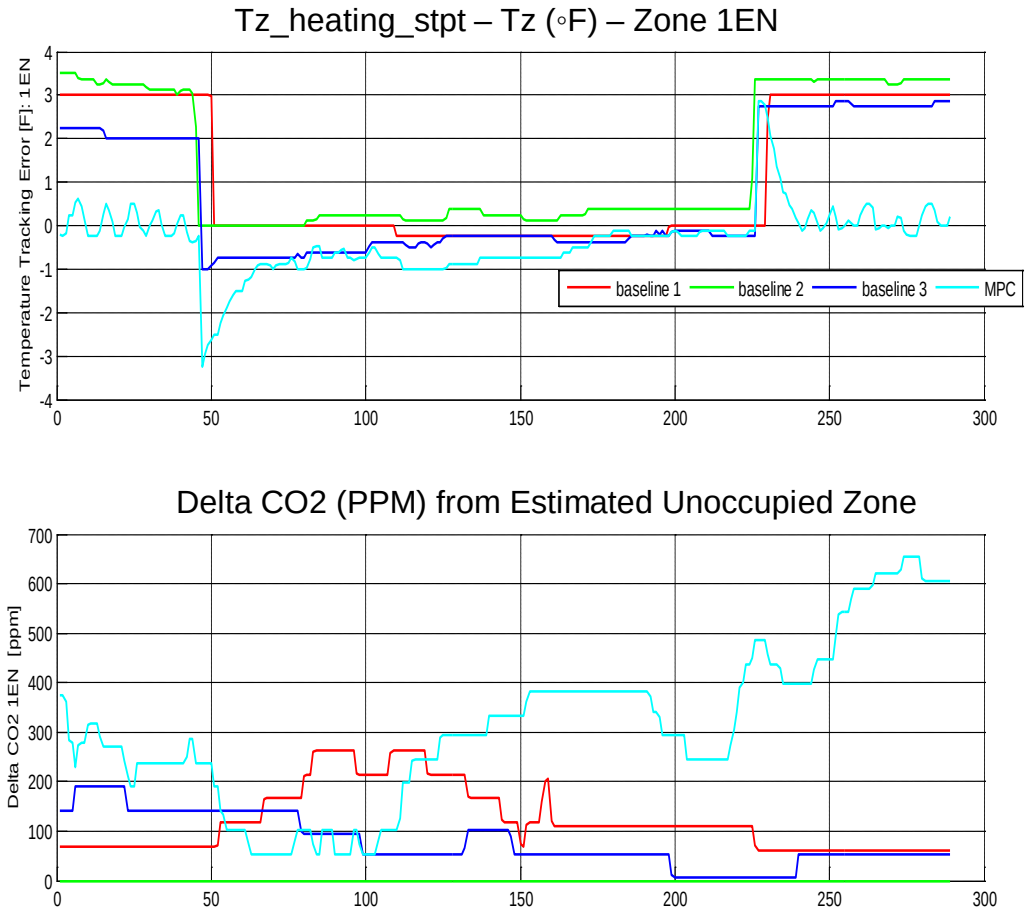

Figure 5.2.4 Zone temperature and set point (top) and CO_2 values (bottom) for EPMO (cyan) and baselines (blue, red, and green)

- Further, the overall performance estimate for each AHU_i is calculated as the average of performance values corresponding to all demonstration days for the respective AHU:

$$Performance\_Relative\_Overall_{AHU_i} = Average_{DemoDay_i}\left(Performance\_Relative_{AHU_i,DemoDay_j}\right)$$

- The overall EPMO system performance was calculated as the average of all averages corresponding to the three AHUs, based on the following formulae:

$$Performance\_Relative\_Overall\_EPMO = Average_{AHU_i}\left(Performance\_Relative\_Overall_{AHU_i}\right)$$

These values are the overall results reported in Table 5.1. Further details are discussed for each performance in Section 5.3.

5.3 PERFORMANCE RESULTS DISCUSSION

Each performance objective included in the Table 5.1 is described in the following paragraphs. The performance metrics were calculated based on the method presented in Section 5.2. Additional details are provided in Appendix B.

The performance results reported in Table 5.1 pertain to two main technologies of the EPMO system: optimization-based control algorithm (the MPC algorithm) and the FDD algorithm.

Quantitative Performance Objectives

This section describes in more details the performance metrics calculations summarized in Table 5.1. The overall results are illustrated in Figure 5.3.1 for the following objectives: energy consumption reduction, peak power reduction, discomfort reduction, and fault diagnostics system robustness. Figure 5.3.1 illustrates the overall performance of the EPMO system relative to the baseline HVAC control schedules as averages for all AHUs and all demonstration days. The EPMO system performance for each AHU is illustrated in Figure 5.3.2.

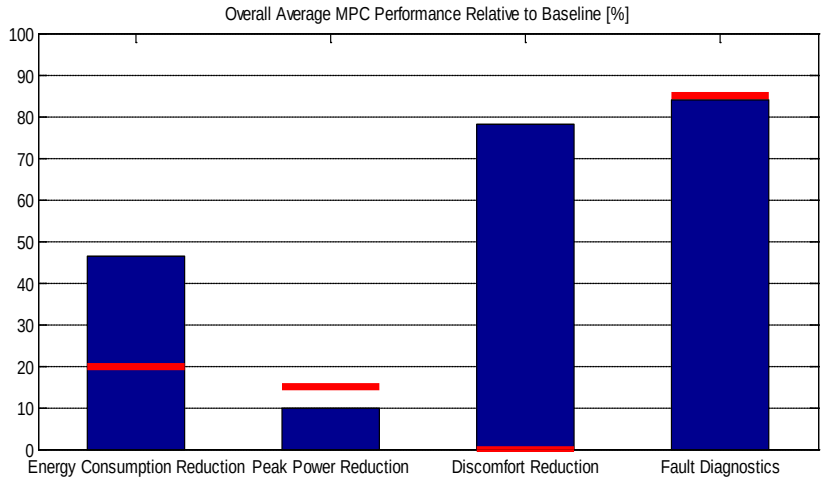

Figure 5.3.1 Illustration of overall EPMO system performance relative to baseline schedules.

Figure 5.3.1 shows the overall performance as averages across all AHUs and demonstration periods. The targets are illustrated as horizontal red lines.

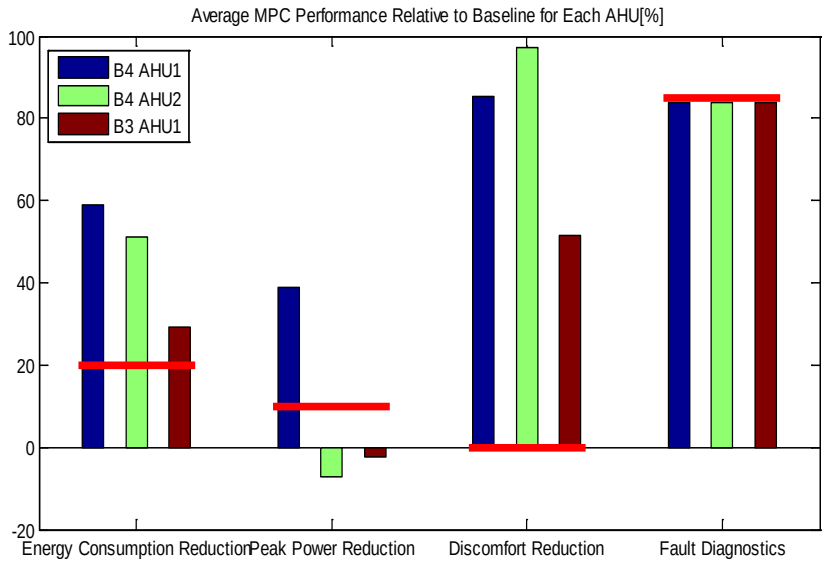

Figure 5.3.2 EPMO system performance relative to baseline schedules for each AHU

The methods and data used to estimate EPMO system performance is detailed below for each quantitative objective.

1. *Reduce Building Energy Consumption (Energy) & Greenhouse Gas Emissions (CO_2).*
   Purpose: The ultimate goal of EPMO system is to reduce energy consumption, peak electric demand, and greenhouse gas emissions in DoD facilities. The objective is to reduce building total energy consumption including HVAC, lighting and equipment (i.e. plug loads).
   Metrics and Success Criteria: The metrics used to assess this objective and the success criteria are listed as following:
   - Total electric consumption (kWh/(ft^2-year)): 20% reduction over the baseline as explained above
   - Building peak demand power (kW): 15% reduction over the baseline
   - Total equivalent carbon dioxide (CO_2) emissions (kg): 20% reduction over the baseline

   Data: The metrics were assessed with actual measurements and where measurements were not available they were assessed with models. The baseline building is the building without any energy fault corrective actions. The data required to calculate these energy-related metrics are metering data for HVAC heat water meter. The simulation data was used for calculation of equivalent CO_2 emissions.
   Results: Quantitative comparisons were done between measured data from the baseline building and the post-commissioning building based on the analytical methodology explained in Section 5.2. As Figure 5.3.1 illustrates, the EPMO system reduces energy consumption on average by more than 40% and peak power by 10%. The detailed data for each demonstration period is discussed in Appendix C.2. Although the peak power was reduced significantly, the 15% target was not achieved. The MPC algorithm generates large peak power levels in

particular when the set point changes from unoccupied to occupied periods in order to meet thermal comfort during these transient periods. The MPC-algorithm-generated peaks are larger than those for the baseline algorithm because the BMS schedules do not meet thermal comfort as well as the MPC algorithm does.

2. *Reduce HVAC Equipment Specific Energy Consumption*. The intent was to evaluate the energy consumption reduction at HVAC equipment level for heating plant, pumps, AHU heat exchangers, and fans. Although this component-level metric is less critical than the overall energy consumption of Objective #1, it is expected that these measurements could provide more insight into the specific energy trade-offs made by the MPC algorithm. Due to the lack of power sub-metering data and HVAC equipment measurements, these objectives could not be evaluated. The large cost of the instrumentation purchase, installation and commissioning necessary to calculate all the equipment specific energy consumption precluded the installation of all the required meters.
    - Heating plant instrumentation cost: $24,000 (cost of steam-side sensors and water-side thermal meter)
    - Pump instrumentation cost: $12,600 (cost of flow and pressure sensors, and electrical meter)
    - Fan instrumentation cost: $8,850 (for one fan)

These costs are relatively large in view of the overall sensor commissioning cost for the EPMO system ($72,580).

3. *Reduce Building Loads (Energy).* The intent was to reduce building loads in order to reduce building demand energy and therefore reduce HVAC system energy consumption. The types of loads that were considered at the beginning of the project were plug and lighting loads. The objective was to reduce these loads during unoccupied times. Two challenges were encountered and could not be overcome: (1) lack of sub-metering data for lighting and plug loads at zone level, and (2) lack of integration of lighting control into the overall site BMS.

4. *Maintain/Improve Temperature Regulation.*
   Purpose: Maintain the thermal comfort throughout the demonstration period. Thermal comfort is met when the zone temperatures remain within the comfort band set in the BMS. Instead of focusing on the thermal comfort we selected the thermal discomfort and aimed to minimize it.
   Metrics and Success Criteria: Thermal discomfort was selected as the appropriate metric because it was observed that the BMS HVAC schedule (the baseline control algorithm) did not meet comfort at all times. Discomfort is measured as the sum of the magnitudes of the zone temperature excursions outside the comfort band for all times when this happens. The exact formula is described in Appendix C.1.
   Data: The detailed data is presented in Appendix C.2 for each AHU and demonstration period.
   Results: As illustrated in Figure C.3.1 the MPC algorithm decreased the thermal discomfort by more than 75% relative to the BMS HVAC control schedules.
   Remark: The comfort metric used does not address the zone CO_2 values because first the baseline schedule did not explicitly control the outdoor airflow volume rate based on zone CO_2 values, and second no other CO_2-based constraints were communicated by the facility management team. As a result, it was decided that the EPMO system did not include these explicit constraints. The demonstration results show that the MPC algorithm increased the

zone CO_2. This is a result of decreased outdoor airflow volume rate during the heating season. The EPMO system can accommodate CO_2 constraint when these are made available.

5. *Energy Performance Monitoring and Optimization System Robustness.*
   Purpose: Diagnose the HVAC system faults during the demonstration period. These faults are primarily related to HVAC system actuators: dampers, fans, valves.
   Metrics and Success Criteria: Percentage of the correctly detected and isolated faults during the demonstration period.
   Data: Measurements recorded during the demonstration period for real faults and injected faults. The real faults were determined by an expert after demonstration by analyzing the data. These faults were then compared against those diagnosed by the on-line FDD algorithm. There are 31 fault events and they are categorized as follows:
   - Event type: injected faults: 15 events; actual faults: 16 events
   - HVAC equipment type: VAV: 13 faults; AHU: 18 faults.

   Results: As Figure C.3.1 illustrates FDD algorithm correctly diagnosed 84% of all events aforementioned, very close to the 85% target. The FDD performance was non uniform across the three AHUs, partially caused by the difference in the instrumentations installed for each AHU.

6. *Energy Performance Monitoring and Optimization System Payback Time.*
   Purpose: Evaluate the cost and benefits of the demonstrated EPMO system.
   Metrics and Success Criteria: Payback Time, Savings-to-Investment Ratio, and Net Present Value for the EPMO system.
   Data: The data used as input to the NIST BLCC tool pertains to sensor costs and commission costs, EPMO system maintenance as well as energy savings. All the inputs, as used directly in the BLCC software tool, are included in Appendix C.4. The overall instrumentation costs are included Table 5.3.1 and further discussed in Section 6.0. The relative energy consumption reduction values are included in Table 5.3.2 for each AHU and HVAC subsystem based on demonstration data detailed in Appendix C.2.

Table 5.3.1 Sensor costs (including commissioning) for each HVAC subsystem and EPMO system technology

System	Calibration /Validation Cost	MPC Demo Sensor cost	Fault-accommodating MPC demo
Chiller Plant	0	0	0
Building	13500	0	13600
AHU & VAVs	59350	0	8450
Space	0	0	0
Total	**72850**	0	22050

Table 5.3.2 Estimated energy consumption reduction for the main HVAC subsystems and for each AHU

B7114	B7114AHU1 (kWh)	B7114AHU2 (kWh)	B7114 Total (kWh)	Relative energy savings (%)	Absolute Value of Energy Savings (kWh)
Fan energy	47058	37793	84851	6%	5091
Heating coil energy	364160	438370	802530	62%	497569
Total VAV reheat energy	94534	32604	127138	17%	21613
B7113	**B7113AHU1 (kWh)**	**B7113AHU2 (kWh)**	**B7113 Total (kWh)**		
Fan energy	72682	77000	149682	6%	8981
Heating coil energy	519050	552980	1072030	62%	664659
Total VAV reheat energy	61568	49380	110948	17%	18861

Results: The detailed output of the NIST BLCC 5.3 software tool used to estimate the Payback Time and the Savings-to-Investment ratios are included in Appendix C.4. The final results are included in Table 5.1.

The NPV is calculated using the following formula:

$NPV = PV(EC_0) - PV(EC_1) + PV(OM_0) – PV(OM_1) + PV(REP_0) – PV(REP_1) –PV(IC)$

where

subscript “0” denotes the baseline conditions
subscript “1” denotes the EPMO system
ICs is the installation cost of the EPMO system
ECs is the annual energy cost savings
OMs is the annual non energy O&M savings, and
REPs is the future replacement savings

Based on the results of the BLCC 5.3 software tool included in Appendix C.4 the PV values are:

$PV(EC_0) - PV(EC_1) = \$36,682$
$PV(OM_0) – PV(OM_1) = \$0$ (although the O&M cost are expected to decrease for the EPMO system due to the automated FDD and fault-accommodating features, these cost cannot be estimated at the time when this report was written, due to incomplete performance data)
$PV(REP_0) – PV(REP_1) = \$0$ (we assume these cost to be equal)
$PV(IC) = \$122,850$

Therefore NPV = -$86,168.

Qualitative Performance Objectives

1. *Ease of Use.*
   Purpose: The intent was to train potential users (building managers, HVAC engineers) to use the EPMO system, and use their feedback on the usability of the technology and time required to learn and use the EPMO system to help the project team to develop, evaluate, and refine the technology.
   Results: The objective was not achieved. The technology was matured to level TRL 6 but during demonstration the system had to be monitored by experts to ensure it operated robustly. Although the EPMO system can operate automatically for many hours, there might be occasions where the system may slow down for various reasons: loss of communication with BMS, delays in reaching the optimal combination of set points, etc. For these reasons, combined with the time constraints caused by the chiller plant malfunctions, led to a TRL level inadequate for non-expert usage. The main focus of this effort was to demonstrate that the EPMO system's benefits make worthwhile further technology development efforts.

2. *Prioritization of Energy Faults and Corresponding HVAC System Operation Strategies.*
   Purpose: The main objective was to help the energy manager to (i) detect, classify and prioritize the building energy faults and (ii) prioritize the alternative HVAC operating strategies for the investigated fault types based on the strategies' estimated impacts for each fault and corresponding alternative strategies.
   Results: This goal was partially accomplished by re-using the visualization tool developed under the effort in [38] for the project ESTCP EW-1015 for the same building, Building 7114. This tool was installed at the site and was being executed in parallel with the EPMO system. Although the system operated for a few months, no feedback was received from facility management related its performance and need for improvements.

Discussion on the Benefits of Fault-Accommodating Control

A third technology, described in Section 2.2, was demonstrated that integrated MPC and FDD algorithms, referred to in this report as Fault-Accommodating MPC. The demonstration data for this technology is detailed in Appendix C.4 but not used to generate the performance metrics of Table 5.1. The main reason is that the technology was demonstrated for only two days, which is considered to be insufficient to generate a realistic indicator of performance. A second reason is that the targets for such a fault-accommodating control system were challenging to be defined, in particular because this was a first-of-a-kind system development and demonstration effort. It is expected that such a fault-accommodating technology will provide a greater synergy of control and diagnostics algorithms because both use similar sensors, models, and computational platforms. This synergy is likely to results in higher benefits than the sum of the individual control and diagnostics benefits. It remains challenging however to calculate what the cost benefits are in the absence of quantitative data. One such benefit for which there is only minimal data available is the labor cost saved to diagnose an HVAC system fault and to modify the control schedules until the equipment can be repaired. The fault-accommodating feature of the EPMO system accomplishes these tasks automatically. In view of the large diversity of faults and implications on comfort and energy consumption, it remains an open problem to determine the overall benefits.

6.0 COST ASSESSMENT

This section details the cost assessment used to estimate the Simple Payback and Savings-to-Investment Ratio provided in Table 5.1.

6.1 COST MODEL AND DRIVERS

The cost model used for the EPMO system cost-benefits analysis is provided in Table 6.1.1. This data was entered in the NIST Building Life Cycle Cost software tool for estimating the mentioned objectives. The two largest costs are associated with sensor and EPMO system commissioning.

The sensors installed at the site are standard: BTU meters; valve and damper position sensors; temperature sensors. It should be noted that only one AHU (out of three AHUs used for demonstrations in this effort) and its associated VAVs were instrumented with additional sensors. For the other two AHUs, several models were re-used directly (from the first AHU) with limited validation data. When the systems have similar features in terms of configuration, usage, and size, instrumenting only one component from each category benefits directly the EPMO system. If these AHUs differ significantly in at least of these features, additional sensors may be required and this leads to larger Payback Time and smaller Savings-to-Investment Ratio values than calculated here.

The EPMO system commissioning estimate is based on approximately 2-3 months needed by an expert (the required skills are detailed in Section 7.0) to integrate the models, calibrate, map points, set up the optimization solver components and customize them for the EPMO technology for a specific building.

Table 6.2.1 Cost Model EPMO System

Cost Element	Data Tracked During the Demonstration	Estimated Costs ($)
Instrumentation capital costs plus commissioning cost	Estimates made based on component costs for demonstration; Labor and material required to install	$72,850
Software cost	Engineering computational tool, such as MATLAB, and components of the optimization solver	$4,000
EPMO system commissioning cost	Estimate based on time required for expert installation	$50,000
Consumables	Estimates based on rate of consumable use during the field demonstration	N/A
Facility operational costs	Reduction in energy required vs. baseline data	N/A
Maintenance	• Frequency of required maintenance • Labor and material per maintenance action	$2,000
Hardware lifetime	Estimate based on components degradation during demonstration	0
Operator training	Estimate of training costs	$2,000

[1] The sensor costs are provided in Table 5.3.1

6.2 COST ANALYSIS

The overall benefits of the EPMO system were evaluated using the NIST BLCC software tool based on the costs of Table 6.1.1 and the energy consumption reduction provided in Table 5.1. The complete output of the BLCC tool is included in Appendix C.4. The technology can be applied to the buildings with the following characteristics:

- Medium and large-scale commercial buildings located in geographical areas with similar weather pattern as in Chicago area. Similar HVAC system configuration, e.g. central heating plants serving AHUs that are connected to multiple VAVs.
- The EPMO system can be installed on the same workstation as the BMS. If this is not possible, the costs of the workstation and BACnet gateway, for connecting the new computer with the site BMS, have to be included in the cost-benefit analysis. For example, adding $3,000 to the non-annually recurring costs decreases the Simple Payback to 2.01 and increases the SIR to 3.64. The information from Table 6.2.1 can be used to estimate the investment cost for the EPMO system implementation which is approximately $0.9/sq.ft. for the demonstration buildings. This value is expected to vary for other buildings, depending on the level of existing instrumentation, functionality of the BMS, building insulation, load conditions, etc.
- On-line access to weather forecast data is assumed in the benefit analysis. Due to Internet connection constraints at the Navy site, the forecasts were manually downloaded from the NOAA website.

7.0 IMPLEMENTATION ISSUES

This section includes a discussion of the implementation issues in the areas of instrumentation, modeling, BMS integration, network communication, user interfaces and required skills issues.

Instrumentation

All instrumentation used in this demonstration is standard Commercial Off-the-shelf (COTs) products. The recommended measurement accuracies for the power meters and thermal meters are given in *A Specifications Guide for Performance Monitoring Systems* [39]. If the BMS is not a 'native' BACnet system, a BACnet gateway will be required to implement the technology. Care is needed when setting up the BACnet gateway. The change of value (COV) for updating the measurement for the weather station, power meters and thermal meters should be as small as possible while not overloading the data communication network. Currently, the instrumentation cost is relatively high. The largest components are the equipment and installation costs due to the large number of zones in large commercial buildings.

Modeling

Matlab was used in this project as the platform for simulation and optimization algorithm execution. For a technology demonstration project, the use of Matlab is appropriate. For broader deployment, existing Matlab code can be compiled and distributed as an executable program. In other words, the EPMO system can be deployed on computers without Matlab.

For some equipment models, including cooling coil, lack of good quality data created some issues for model calibration and validation. Currently, considerable time is spent dealing with issues related to sensor data quality (e.g., sensor bias and drifting) for modeling and diagnostics. Real-time sensor health monitoring provides a means to dramatically reduce the cost related to the commissioning of energy monitoring systems to ensure data quality. Also, information related to building current control sequences was not totally open due to a proprietary BMS on site.

BMS Integration

In this demonstration, real time building operational data was collected through a BACnet gateway via a customized middleware software package that enabled applications to programmatically extract data from the system, perform calculations outside of the middleware and finally write data back to the middleware. Examples of such applications are building performance simulation programs, FDD tools, visualization, controls and optimization tools.

Network Communication

Significant challenges were encountered in the development and testing of the advanced building energy management system tool because of remote access problems. Network security constraints prevented the team from having remote access to the computers at Great Lakes. This presented a significant challenge for coding and debugging. Team members could do efficient debugging only while visiting the site. This made it harder for the team to troubleshoot and fix complex and unforeseen issues with the code. It is recommended that remote access be granted for developers implementing similar systems at other sites. This access should be in compliance with DoD IT policy including Navy Public Service Network. Also, a secured and integrated DoD network should be established for building applications.

Robustness of Optimal Control Technology

The EPMO system was implemented on three AHUs and during the demonstrations there were several occasions when the solver delayed in reaching optimal set point values for the AHUs and VAVs. The frequency of these occurrences is not yet fully understood. Although at these times the recommended optimal set-point values did not change significantly, there is a need for more demonstration data (during load changes and season transitions) to modify the EPMO system accordingly. These modifications can be in same cases as simple as interrupting the solver when it takes longer than a pre-established duration and re-using the previous set points. These are the simple type of rules that can resolve many of the cases when the algorithm converges slower to the optimal solution.

Required Skills

The current version of the EPMO system requires the following skills for implementation:

- Creating building and HVAC component models as described in Appendices B.1-B.3. These models can be standardized for all similar buildings and HVAC subsystems. This project offered direct example of the extent to which these models can be re-used. The models from a project-instrumented AHU were re-used for two other AHUs with less instrumentation.
- Setting up the BACnet gateway and middleware software for bi-directional communication with the BMS. The middleware is described in Appendix B.4 and is a critical component of scalable BMS solutions.

- Setting up the set-point optimization problem with the HVAC component constraints, energy models, and performance objectives. To a large extent the BLOM tool [37], developed partly with resources from this project, automates the optimal control problem formulation based on expert inputs. Such an environment can be further developed to automate this process to the extent that it requires only standard building and HVAC configuration information.

8.0 REFERENCES

1. Office of the Under Secretary of Defense For Acquisition, Technology, and Logistics, Report of the Defense Science Board Task Force on DoD Energy Strategy, More Fight – Less Fuel, Feb 2008.
2. DoD Base Structure Report – Fiscal year 2008
3. DoD Facilities and Vehicles Energy Use, Strategies and Goals – Program Overview, GovEnergy 2008, August 6, 2008
4. G. P. Henze, Kalz, D. E., Liu, S., and Felsmann, C., Experimental Analysis of Model-Based Predictive Optimal Control, *HVAC&R Research*, Vol. 11, No. 2, 2005, pp. 189-213.
5. M. A. Piette, S. Kinney, and P. Haves. Analysis of an Information Monitoring and Diagnostic System to Improve Building Operations, *Energy and Buildings* 33 (8) (2001), 783-791.
6. TIAX LLC *Energy Impact of Commercial Buildings Controls and Energy Diagnostics*.. For DOE, May 2005. http://www.epa.gov/cleanenergy/energy-resources/refs.html
7. http://www.whitehouse.gov/news/releases/2007/01/20070124-2.html
8. M. E Brand. Pattern Discovery via Entropy Minimization. *In Uncertainty 99: AISTATS 99*, 1999.
9. M. E. Brand. Structure Learning in Conditional Probability Models via an Eutropic Prior and Parameter Extinction in *Neural Computation Journal*, Vol. 11,No. 5, pp. 1155-1182, July 1999.
10. L. Chiang, E. Russell, R. Braatz, *Fault Detection and Diagnosis in Industrial Systems*, Springer Verlag, London, 2000.
11. Pokrajac, A. Lazarevic, L.J. Latecki, "Incremental local outlier detection for data streams," *Proc. IEEE Symposium on Computational Intelligence and Data Mining*, 2007, pp. 504-515.
12. N. Pejcic, N. Reljin, S. McDaniel, D. Pokrajac, A. Lazarevic, Detection of Moving Objects using Incremental Connectivity Outlier Factor Algorithm, *Proceedings of ACM Southeast Conferenc*e, Clemson, SC, March 19-21, 2009
13. J. D. Spitler, D.E. Fisher and D.C. Zietlow. 1989. A Primer on the Use of Influence Coefficients in Building Energy Analysis. *Proceedings of the Building Simulation '89 Conference*, pp. 299-304.
14. Kaplan, M., and P. Canner.1992. *Guideline for Energy Simulation of Commercial Buildings*. Portland: Bonneville Power Administration.
15. Tuluca, A. 2010. Modeling for Existing Buildings. *ASHRAE Existing Building Conference*. New York, NY.
16. Keranen, H., Suur-Uski, T. and Vuolle, M. 2007. Calibariton of Building Simulation Model by Using Building Auotmation System- a Case Study. *Proceedings of Clima 2007 WellBeing Indoors*. Helsinki, Finland. June 10-14, 2007

17. Dudley, J.H., Black, D., Apte, M., Piette, M.A. and Berkeley, P. 2010. Comparison of Demand Response Performacnr with an EnergyPlus Model in a Low Energy Campus Building. *2010 ACEEE Summer Study on Energy Efficiency in Buildings*. Pacific Grove, CA. August 15-20, 2010.
18. NIST Handbook 135 – *Life Cycle Costing Manual for the Federal Energy Management Program*. 1995.
19. DOD *Energy Manager's Handbook*. http://www.wbdg.org/ccb/DOD/DOD4/dodemhb.pdf. August 25, 2005.
20. US Army Corps of Engineers. *EM385-1-1 Safety and Health Requirements Manual*. September 15, 2008.
21. T. Bailey and P. Haves. *ESTCP SI-0929 Automated Continuous Commissioning of Commercial Buildings Demonstration Plan*. February 2010.
22. ANSI/ASHRAE Standard 140-2007. *Standard Method of Test for the Evaluation of Building Energy Analysis Computer Programs*. American Society of Heating, Refrigerating and Air-Conditioning Engineers, Inc. Atlanta, GA. 2007.
23. Crispieri, G. 2008. Data Quality Evaluation Methods. *International SEMATECH Manufacturing Initiative*, Technology Transfer #08074943A-ENG. July 2008. [Available at http://www.sematech.org/docubase/document/4943aeng.pdf]
24. N. Bourassa. Automatic Diagnosis for Ailing Rooftop Air Conditioners, *PIER Technical Brief*, July 2005.
25. R. Radhakrishann, D. Nikovski, K. Peker, and A. Divakaran. Locally Weighted Regression for Fault Detection and Diagnosis of HVAC Equipment", *IEEE Intl. Conf. on Industrial Electronics*, 2006.
26. A. Lazarevic and Z. O'Neill. United Technology Research Center Real Time Decision Support Project Internal Report. 2008.
27. M. Giering. "Carrier Building Decision Support Internal Project Report". 2009, 2010.
28. EPA. Energy Star Building Manual http://www.energystar.gov/index.cfm?c=business.EPA_BUM_CH3_InvestAnalysis
29. Ma, Y., Borrelli, F., Hencey, B., Coffey, B., Bengea, S., Packard, A., Haves, P., "Model Predictive Control for the Operation of Building Cooling Systems", in Proceedings of the American Control Conference, July 2010, Baltimore, MD.
30. F. Borrelli and T. Keviczky. "Distributed LQR design for identical dynamically decoupled systems". IEEE Transaction on Automatic Control, 53(8):1901-1912, September 2008.
31. F. Borrelli, J. Pekar, M. Baotic and G. Stewart. "On The Computation Of Linear Model Predictive Control Laws". Automatica, 46(6):1035-1041, June 2010.
32. F. Borrelli. "Constrained Optimal Control of Linear and Hybrid Systems", Lecture Notes in Control and Information Sciences, vol. 290. Springer, 2003.
33. M. Baotic, F. Borrelli, A. Bemporad, and M. Morari. "Efficient on-line computation of constrained optimal control". SIAM Journal on Control and Optimization, 5:2470–2489, September 2008
34. Lennart Ljung, "System Identification: Theory for the User", Prentice Hall
35. Roth, K. W., Westphalen, D., Feng, M. Y., Llana, P., and Quartararo, L. (2005). "Energy impact of commercial building controls and performance diagnostics: market characterization, energy impact of building faults and energy savings potential". *Report prepared for U.S. Department of Energy*. TIAX LCC, Cambridge, MA.

36. S. Sarkar, A. Srivastav, and M. Shashanka, “Maximally Bijective Discretization for Data-driven Modeling of Complex Systems”, Proceedings of American Control Conference, (Washington, D.C.), 2013
37. Kelman, A., Vichik, S., Borrelli, F., “BLOM: The Berkeley Library for Optimization Modeling and Nonlinear Predictive Control”, Internal report, Department of Mechanical Engineering, University of California, Berkeley, 2013. Website: http://www.mpc.berkeley.edu/software/blom
38. Adetola, V., Ahuja, S., Bailey, T., Dong, B., Khawaja, T., Luo, D., O’Neil, Z., Shashanka, M., “Scalable Deployment of Advanced Building Energy Management Systems”, ESTCP-EW-1015 Project, Technical Report.
39. http://cbs.lbl.gov/performance-monitoring/specifications/
40. Narayanan, S., Bengea, S., Lin, Y., Taylor, R., Vrabie, D., Yuan, S., Killough, S., Kuruganti, Manges, W., Woodworth, K., T., Borrelli, F., Kelman, A., “A Wireless Platform for Energy-Efficient Building Control Retrofits”, Final report, ESTCP Project EW-200938, July 2012.

APPENDICES

APPENDIX A: Points of Contact

All the important points of contact (POC) involved in the demonstration are included in Table A.1.

Table A.1 Point of contact information

POINT OF CONTACT Name	ORGANIZATION Name Address	Phone Fax E-mail	Role in Project
Trevor Bailey	United Technologies Research Center 411 Silver Lane, MS 129-78 East Hartford, CT, 06108	Ph. (860) 610-1554 Fax (860) 660-1014 Email: BaileyTE@utrc.utc.com	Project Leader
Peter Behrens	Great Lakes Naval Facility &Eng CMD 525 Bronson Street BLDG 112 Great Lakes IL 60088	Ph. (847) 688-2121 x28 Email: peter.behrens@navy.mil	Navy Great Lakes Energy Manager

APPENDIX B: TECHNOLOGY DETAILED DESCRIPTION

B.1 CONTROL-ORIENTED BUILDING ZONE TEMPERATURE MODELS

In this section, dynamic models for compartments are discussed. The main goal is to obtain simple models to capture essential behavior in compartment areas for model based control design. Ideally, detailed and possibly complex models will be necessary to describe accurate dynamics in the compartments. However, they will not be suitable for model based control design (MPC in our case). Therefore, we employ a fairly simple model structure from System Identification theory [34]. In modeling, we mainly focus on relation between compartment temperature, outside air temperature, VAV air flow, VAV discharge air temperature. The diagram of compartments is shown in Figure B.1.1.

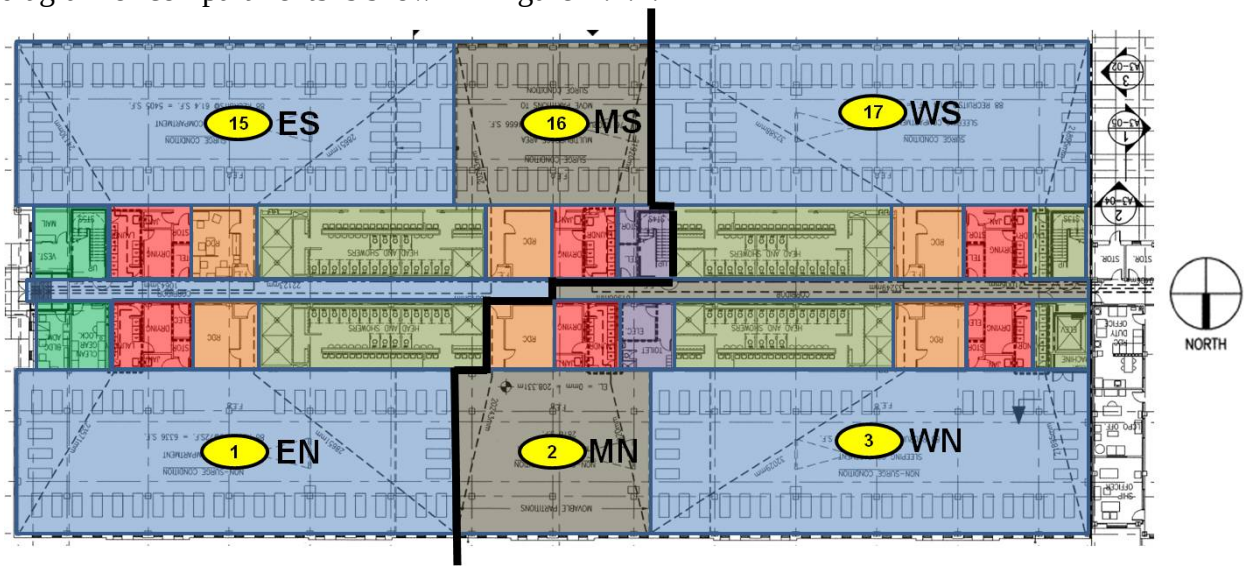

Figure B.1.1. Compartment areas of B7114 first floor are shown.

The compartments were are identified by numbers and orientation. AHU1 provides controlled air to 1 East North (EN), 15 East South (ES), and 16 Middle South (MS), while AHU2 supplies air to 2 Middle North (MN), 3 West North (WN), and 17 West South (WS). In addition, AHU1 takes care of half second floor compartments (31 EN, 45 ES, and 46 MS) and half third floor compartments (61 EN, 75 ES, and 76 MS). Likewise, AHU2 deals with the other half second floor compartments (32 MN, 33 WN, and 47 WS) and the other half third floor compartments (62 MN, 63 WN, and 77 WS).

Model structure

For each compartment, at current time *k*, we use the following discrete time (5 min sample rate) model structure

$$T_{k+1} = \alpha_1 T_k + \alpha_2 T_{k-1} + \alpha_3 T_{k-2} + \beta_1 OAT_k + \beta_2 OAT_{k-1} + \gamma\ \dot{m}_k (VDAT_k - T_k) + d, \quad \text{(B.1.1)}$$

where

T : *compartment temperature*,

OAT : *Outside Air Temperature*,

$\dot{m}$: *VAV air flow to compartment*,

$VDAT$: *VAV Discharge Air Temperature*,

$\alpha_1, \alpha_2, \alpha_3, \beta_1, \beta_2, \gamma, d$: *parameters to be identified*.

With normal operation data, functional test data, or mixture of two, we attempt to calculate model parameters that can best describe the compartment behavior.
Remarks:

- The inputs in this model structure are *OAT,* $\dot{m}$, and *VDAT*. *OAT* is an input that is not controllable (i.e. disturbance) and the others are controllable. Therefore, by using this model, we may able to calculate inputs to mitigate impact of high or low *OAT to* compartments if *OAT* is predictable.
- The model structure (B.1.1) has a nonlinear term associated with $\dot{m}, VDAT$, and *T*. However, it is linear in their combined term.
- In cooling season, AHU Discharge Air Temperature (DAT) can be used at the place of *VDAT*.
- *VDAT* is measurable for the building 7114 AHU1 compartments. However, *VDAT* cannot be measured directly for the other compartments. For these compartments, we use VAV models in order to estimate *VDAT* and it is used for the model parameter calculation of (B.1.1).
- There are several components that can influence compartment temperature: lights, electronic equipment such as computer, sun light, occupancy, and any indoor activities such as physical training (PT). These variables are not included in the model as they are not easily measurable or predictable. Their impact will be revealed by compartment temperature heating (or cooling) set point violation and it should be compensated by our controller design in terms of feedback.
- By having current (*k*) and previous (*k-1*, *k-2*) compartment temperature terms, the model tries to capture effect of thermal inertia in compartment.
- It would take time for *OAT* to influence compartment temperature. Therefore, we use not only OAT_k, but also OAT_{k-1}.
- The constant term *d* exists as the input and output data has non-zero dc values. If the dc values are removed in the data, the *d* term may not be necessary. More aspects on this parameter will be discussed in later subsections.

Experiment Design for System Identification Data

Several functional tests were performed to obtain data sets for identification of model parameters in (B.1.1). Large amount of data is desired in order to obtain a good model [34]. However, due to limited numbers of site visits and the seasonal constraint (e.g. data for heating season should be collected in winter.), limited number of data sets were collected. Mainly data collection for heating season is discussed here. But the main idea in this section is also applied to data collection for cooling season.

Measured *OAT* is collected via BAS, while we manipulate

1. AHU Hot water Coil Valve (HCV) position,
2. VAV Re-Heat Coil Valve (RCHV) position,
3. VAV air flow via damper position,

simultaneously by pre-determined sequences. The first two variables changes discharge air temperature (*VDAT)* and the last intends to change air flow ($\dot{m}$). Note that, in cooling season, one may manipulate AHU Cooling Coil Valve position to change *VDAT*. Input sequences for the above variables are randomly chosen with consideration that their combination should cover the typical ranges of *VDAT* and $\dot{m}$. Exemplary profiles and corresponding input and output data are shown in Figure B.1.2 and B.1.3.

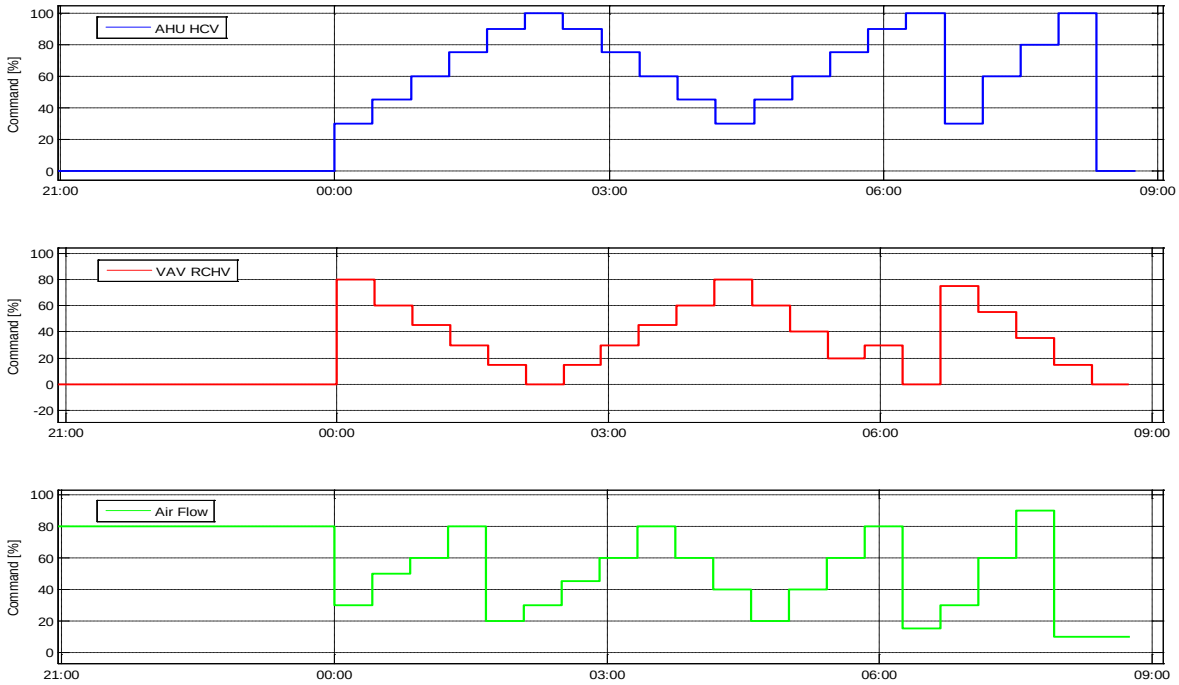

Figure B.1.2. Input sequences selected during October 25th~26th 2012 functional test.

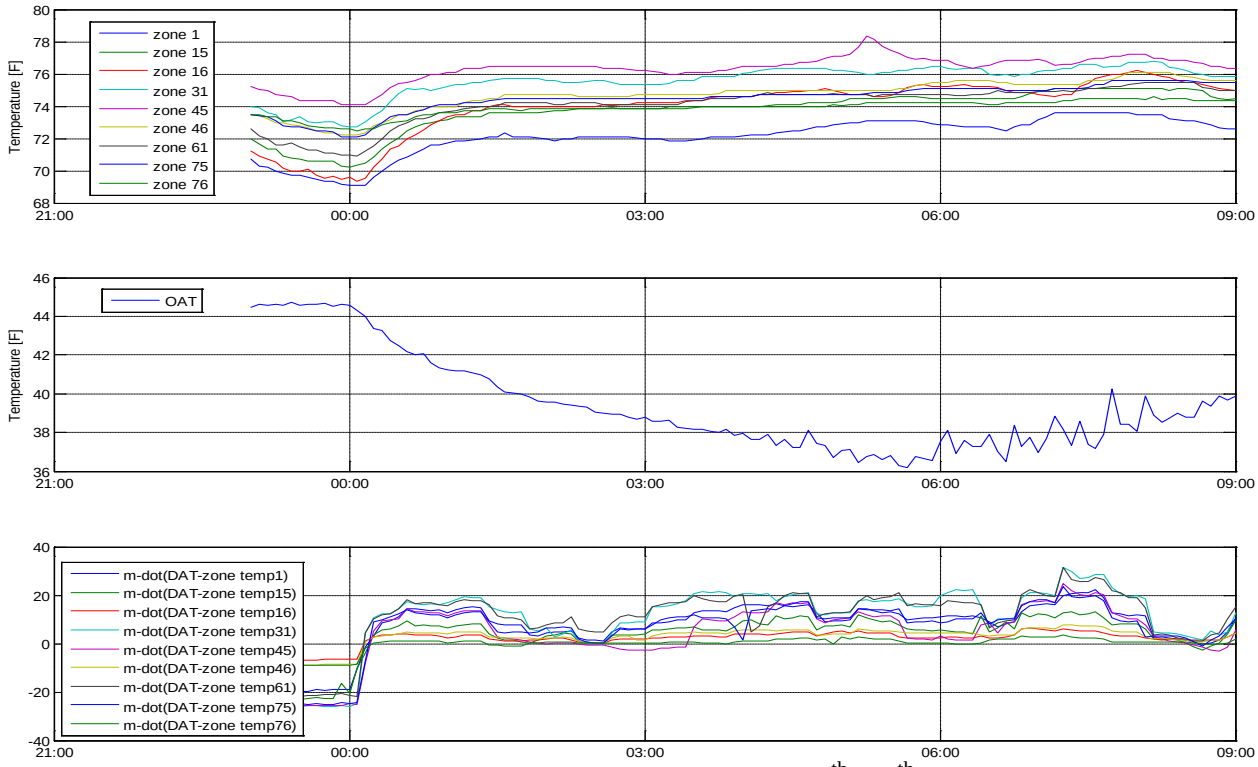

Figure B.1.3. Data collected and calculated from October 25th~26th 2012 functional test.

The top plot in figure B.1.3 shows the temperature of B7114 AHU1 compartments, OAT, and calculated value of each compartment. The input sequence was updated every 25 min. Reasoning behind this update rate choice is that it would allow each compartment zone time to react to given input conditions without requiring too much time to test all cases.

Identification and validation of model with data

With the model structure as in Equation B.1.1 and functional test data, model coefficients were calculated using MATLAB System Identification toolbox. The high level identification process is shown in Figure B.1.4.

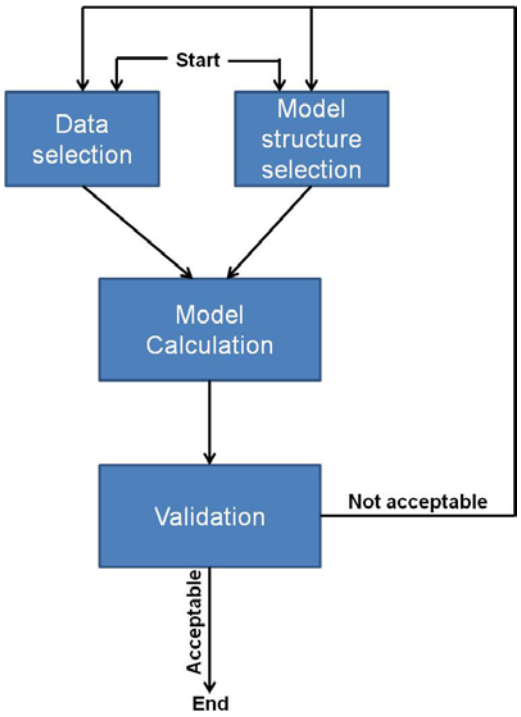

Figure B.1.4. System identification procedure

In the next subsections, procedures we took to generate models for February and March 2013 demonstration are discussed.

Data selection

For the first two demonstrations (November and December 2012), models were estimated using the functional test data sets that were collected in October 2012. However, analysis with November and December demonstration data suggested that models need a careful review. Some open-loop prediction results of the models are shown below with the December MPC demonstration data.

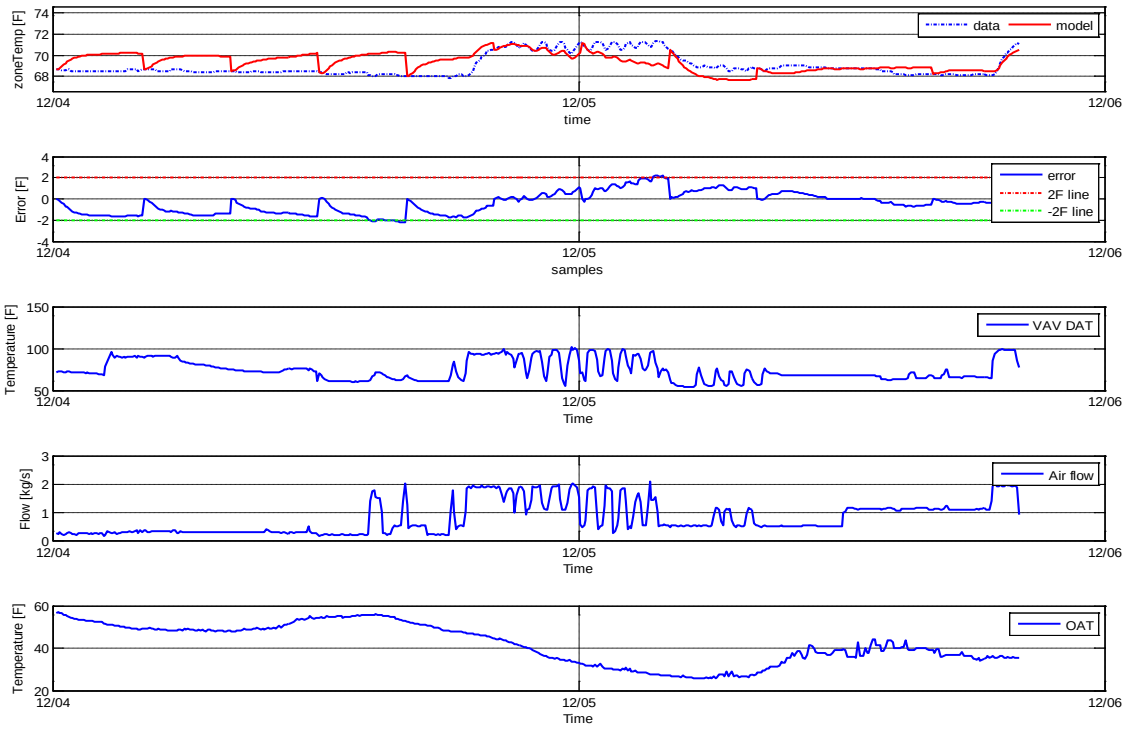

Figure B.1.5. Four-hour, open-loop prediction by the model using December 4th and 5th data.

In Figure B.1.5, the result for the 1 EN compartment is shown. MPC was active from mid-December 4th to end of December 5th. Note that baseline VAV DAT and air flow inputs are very low frequency while those by MPC have more various frequency contents. Given initial temperature from the data, 4 hour open loop prediction was calculated and the model was re-initialized with a new initial temperature from the data. Then the prediction curves are compared to the real temperature profile. One can see that the model predicts real temperature fairly well when VDAT and air flow show relatively high frequency contents while it does poor job when VDAT and air flow are almost dc. The reason is that the model was trained with dynamic inputs illustrated in Figure B.1.2 and Figure B.1.3. Therefore, the calculated compartment models would not be able to predict temperatures accurately for the extremely low frequency inputs seen in Figure B.1.5. See also Figure B.1.6.

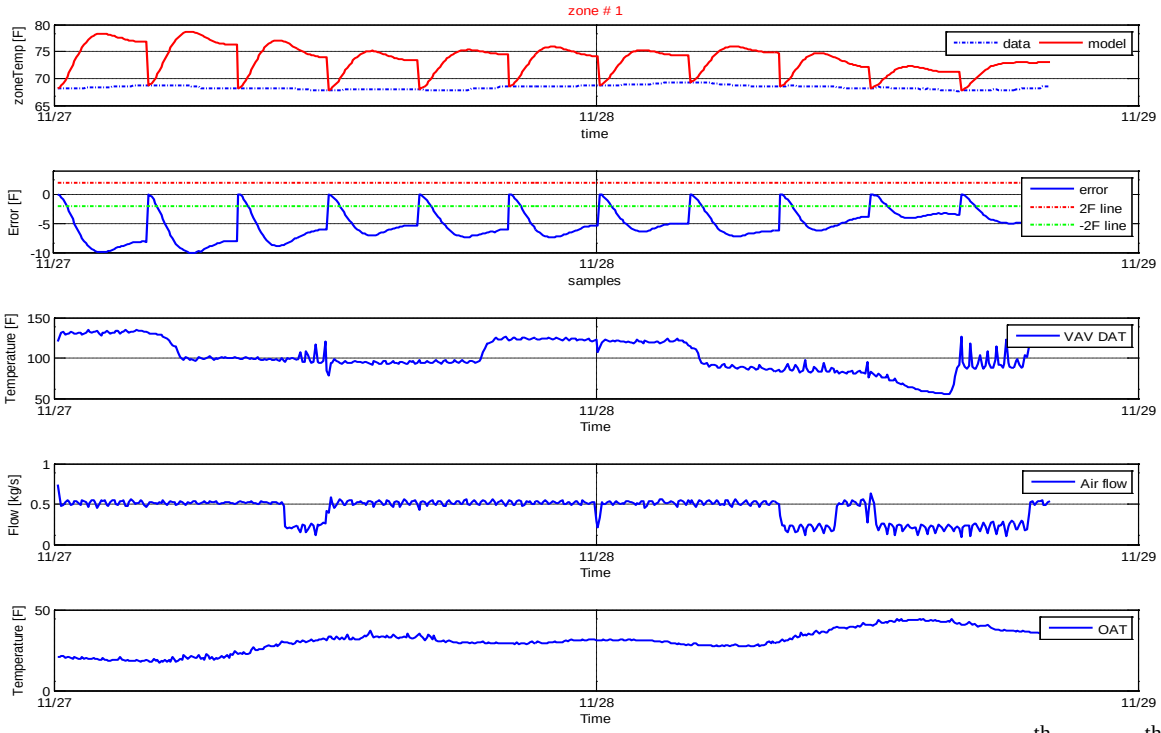

Figure B.1.6. Four-hour, open-loop prediction by the model using November 27th and 28th data for 1 EN compartment.

This may results in non-optimal set points calculations when MPC computes its open loop input solution, it is much like what's seen in early December 4th and later December 5th shown in Figures B.1.5 and B.1.6. In Figure B.1.7, temperature of each compartment went up even when discharge air temperature was lower than compartment temperatures. For model improvement, we selected several data sets of normal operation in addition to the functional test data for model parameter calculation as their input profiles contain much lower frequency contents.

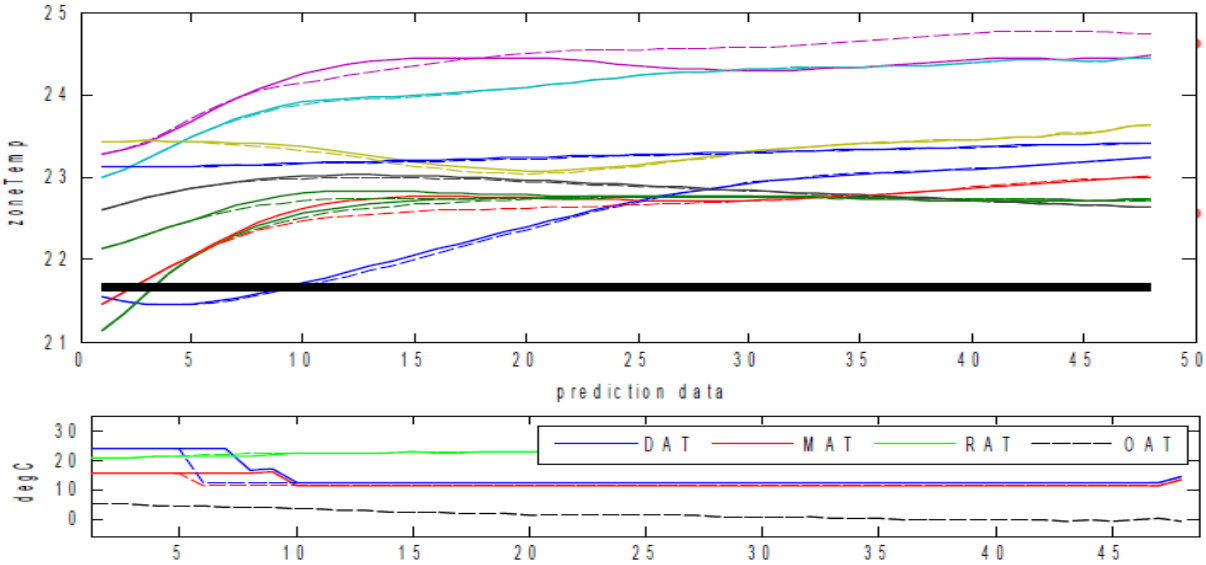

Figure B.1.7 Compartment temperature prediction using the models (top figure) and open loop MPC solutions (bottom figure).

In Figure B.1.7, corresponding individual VAV DAT open loop profiles were omitted. In most cases, the AHU DAT solution by MPC is very similar to what's shown in early December 4th and late December 5th data shown in Figure B.1.5 in terms of frequency content. Temperature is shown in [^{0}C].

Model Calculation

For model calculation, Matlab System Identification Toolbox was used. As seen in the model structure, there is a nonlinear component in (B.1.1)

$$m_k^i (VDAT_k^i - T_k^i). \tag{B.1.2}$$

Therefore, an additional step to construct (B.1.2) from data is required (i.e. regressor). The System ID toolbox provides a function to construct a custom regressor such as (B.1.2). Once the term (B.1.2) is computed, Equation B.1.1 becomes linear in compartment temperature, outdoor air temperature, and the term in (B.1.2).

Validation

Several sets of data were used to validate the new model compartment models. Validation results with the same data set used in Figure B.1.5 (Figure B.1.6) is shown in Figure B.1.8 (Figure B.1.9). The new model improved its ability to predict temperature for very low frequency inputs.

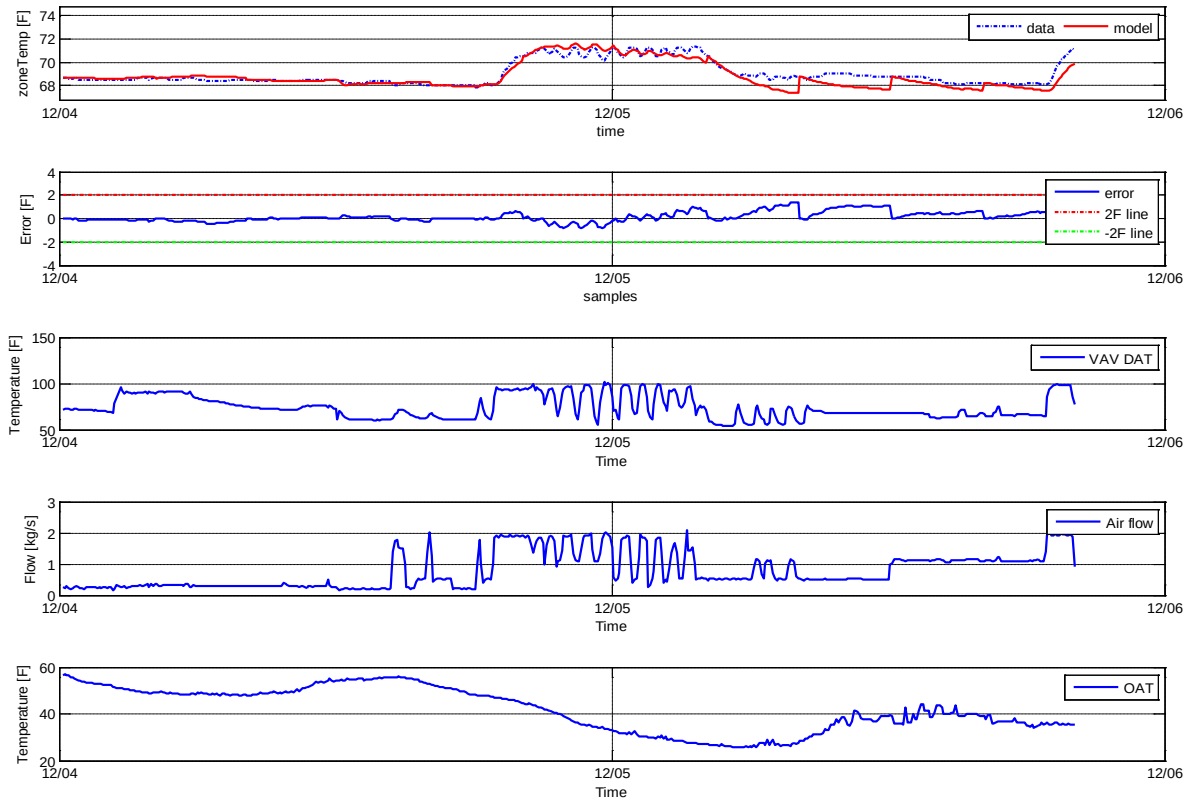

Figure B.1.8. Four hour open loop prediction by the new model using December 4th and 5th data for the 1st floor North East compartment.

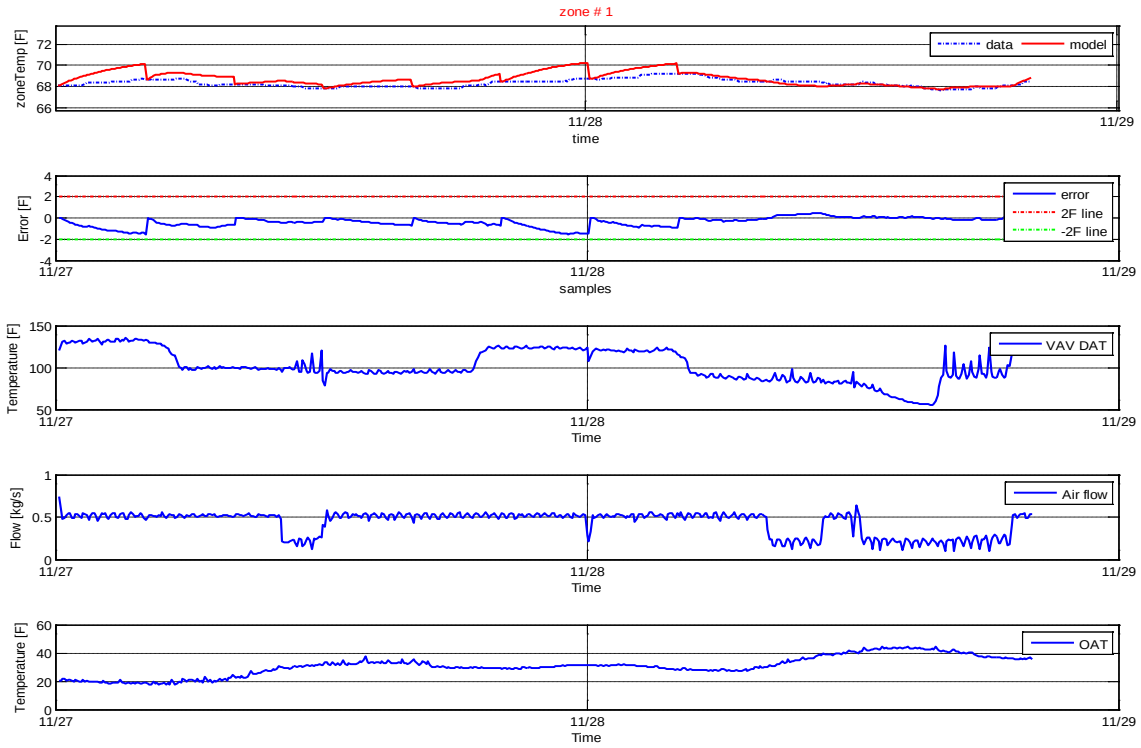

Figure B.1.9. Four-hour, open-loop prediction by the new model using November 27th and 28th data for the 1st floor North East (1EN) compartment.

Conclusion and Remarks

In this section, the dynamic models and their parameter calculation process were described for the compartments in Buildings 7113 and 7114. The effectiveness of our model structure selection and model parameters should be finally judged by reviewing the outcome of the MPC control performance that will be discussed in the other section. The model computation process is iterative so that model parameters can be updated fairly easily as new and more informative data sets are available. The down side of this approach is that one needs to carefully monitor and control tests for data collection in order to obtain high quality data sets that have strong correlation between inputs and outputs. In addition, even using normal operation data requires careful inspection as some abnormal events (e.g. open windows) can significantly affect the temperature in compartments.

For more realistic implementation of the models we developed, one may develop models for different compartment and outdoor average temperatures. As we try to approximate nonlinear behavior of compartment temperatures in a simple model structure (B.1.1), the model parameters including *d* would be different with respect to what the average compartment and outdoor temperatures were at the duration of data collection and tests. In this way, the models for control can be switched depending upon these leading to potentially better control performance.

B.2 CONTROL-ORIENTED HVAC SYSTEM MODELS

For building control and optimization at supervisory level, it was assumed that the dynamics of HVAC equipment, such as AHU mixing box, cooling and heating coils, fans, have a faster dynamics relative to building envelope and zones. Thus, HVAC component model can be considered as quasi-steady state within the time-scale of interest for building supervisory control.

Motivated by the objective of rapid model development and deployment for optimal building control demonstrations, a data-driven based approach was employed to generate, calibrate, and validate HVAC models for Model Predictive Control design and implementation. Specifically, the following HVAC models were developed, validated, and implemented into the MPC problem formulation:

- Outdoor air fraction model
- Mixed air temperature model
- Heating coil model
- AHU total flow rate model
- Fan model
- VAV reheat coil model

Figure B.2.1 shows the schematic layout of the air handling unit (AHU) system in Builidngs 7113 and 7114. Note that the four AHUs employed in this study, AHU1 and 2 from Buildings 7113 and 7114, are all identical in terms of capacity and areas served. The AHU system includes outdoor/mixed/return air dampers, cooling and heating coils with face bypass damper control, a supply and a return fan with static pressure controls.

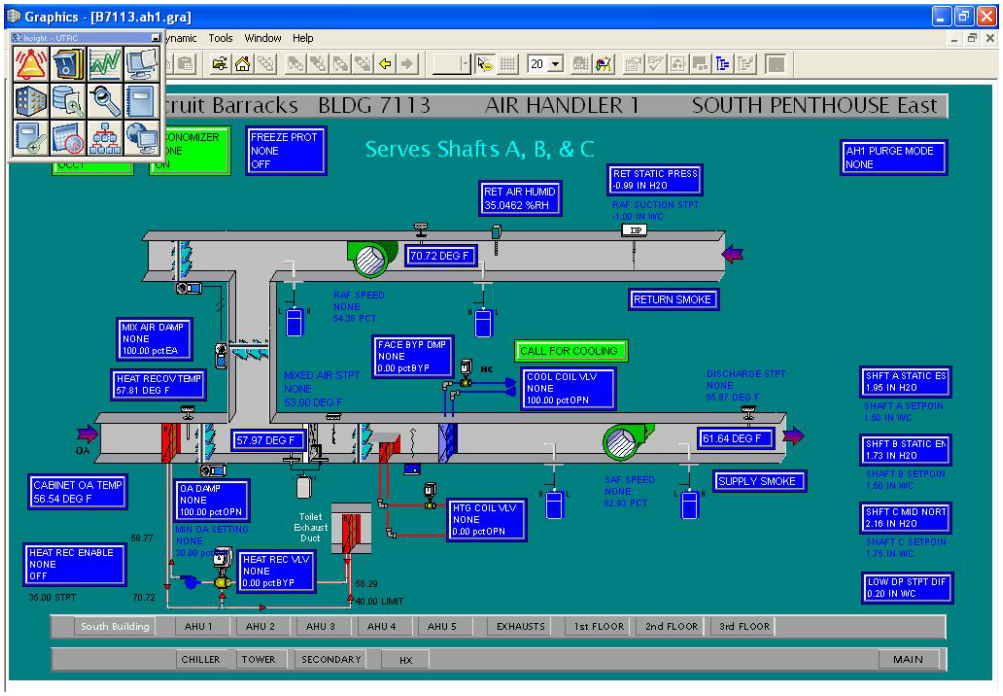

Figure B.2.1: Schematic of AHU system in Building 7113 and Building 7114

Outdoor Air Fraction and Mixed Air Temperature

The outdoor air fraction is modeled as a function of outdoor air damper position (OAD) only. Due to the distinct differences in outdoor air temperature and thus the mixed air temperature in heating and cooling seasons, it was found that better model predictions could be obtained if separated models were calibrated to cooling and heating season shown below, respectively.

For cooling season:

$$OAF = 0.844 \cdot OAD + 0.1096$$

For heating season:

$$OAF = \text{-}2.3694 \cdot OAD^2 + 4.3066 \cdot OAD - 1.008$$

The mixed air temperature is determined as:

$$T_{MA} = OAF \cdot T_{OA} + (1\text{-}OAF) \cdot T_{RA} \ ,$$

where *OAD* is the outdoor air damper position, *OAF* is the outdoor air fraction, T_{OA}, T_{RA}, T_{MA} are the outdoor, return and mixed air temperature, respectively. Figure B.2.2 shows the calibration and validation results of the mixed air temperature model.

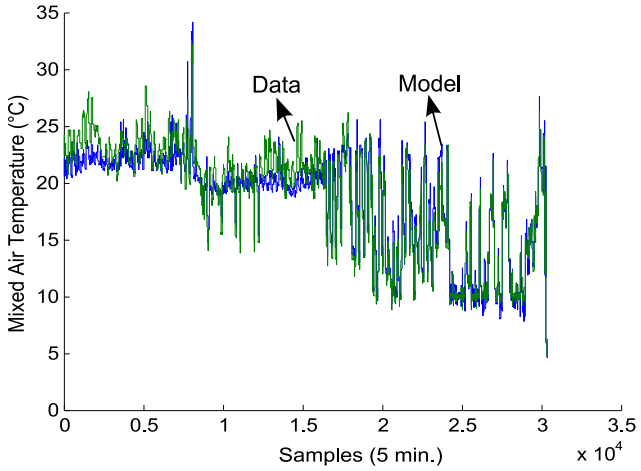

(a) Comparisons of mixed air temperature measurement and prediction

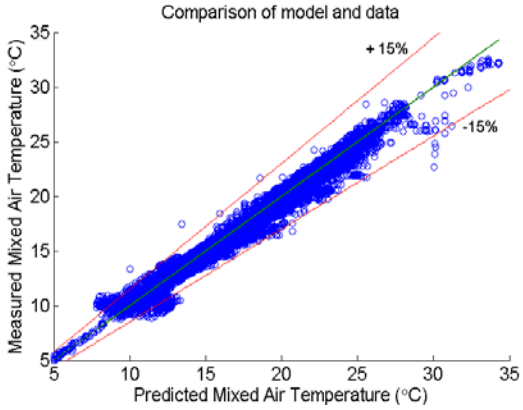

(b) Scatter plot of model and data comparisons

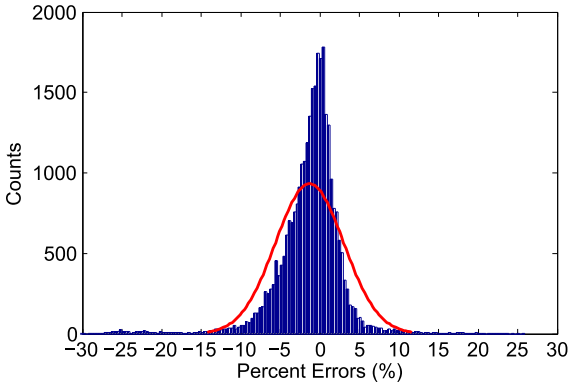

(c) Histogram of percent errors

Figure B.2.2: Validation results of mixed air temperature predictions

Heating Coil

The purpose of the heating coil modeling for predictive control design is to provide accurate thermal power consumption prediction through the heat transfer process from hot water to air. Assume we draw a control volume across the heating coil with mixed air as inlet flow and the distributed air after the heating coil as the outlet flow. When the first law of thermodynamics is applied to this control volume and assume that the flow crossing the boundaries are in steady-state, no changes in latent energy and no thermal energy generation, the thermal power consumption of the heating coil is given by:

$$P_{hc} = \dot{m}_{sa} \cdot c_{pa} \cdot (T_{DA,AHU} - T_{MA} - \Delta T_{fan})$$

where P_{hc} is the thermal power consumption of the heating coil, c_{pa} is the specific heat capacity of air, $T_{DA,AHU}$ is the discharge air temperature of the AHU, and ΔT_{fan} is the temperature rise across the fan. Figure B.2.3 shows the calibration and validation results of heating coil power consumption predictions.

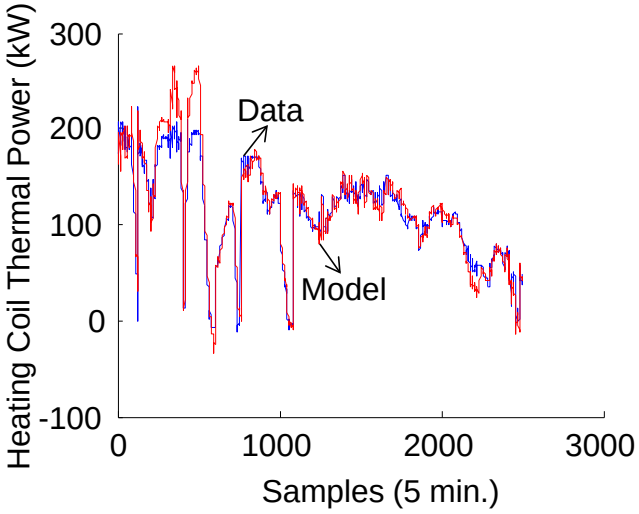

(a) Comparisons of heating coil thermal power measurement and prediction

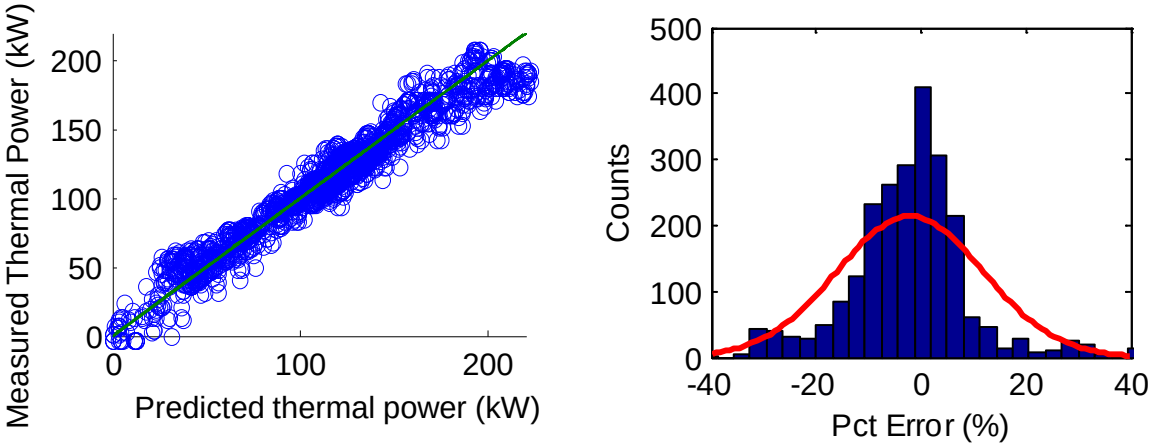

(b) Scatter plot of model and data comparisons (c) Histogram of percent errors

Figure B.2.3: Validation results of heating coil thermal power predictions

AHU Air Flow Rate Estimation

To accurately estimate the thermal power consumption of the heating coil and fan power consumption, an accurate estimate of the AHU supply air flow rate is needed. A correlation is considered for the total AHU supply flow rate and the summed supply VAV flow rates to all the compartments for a given AHU. Figure B.2.4 shows the calibration and validation results of the total AHU flow rate as a function of the summed supply VAV flow rates.

$$\dot{m}_{a,AHU} = 0.90501 \cdot \sum_{i=1}^{N_{Comp}} \dot{m}_{a,CompVAVi} + 7.4491$$

where $\dot{m}_{a,AHU}$ is the total AHU supply air flow rate (kg/s) and $\dot{m}_{a,CompVAVi}$ is the VAV supply flow rate (kg/s) for a given compartment, and N_{Comp} is the total number of compartments.

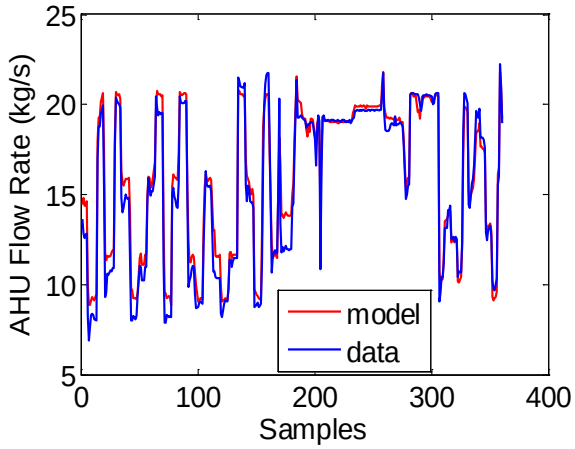

(a) Comparisons of AHU air flow rate measurement and prediction

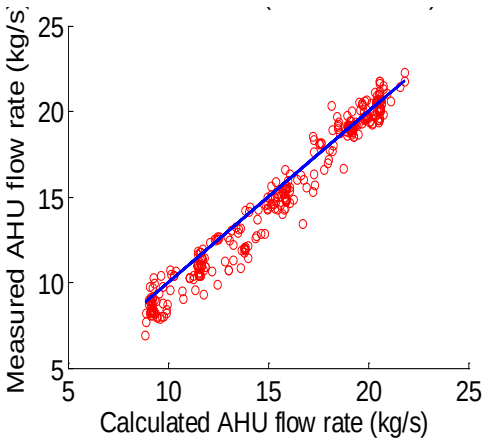

(b) Scatter plot of model and data comparisons

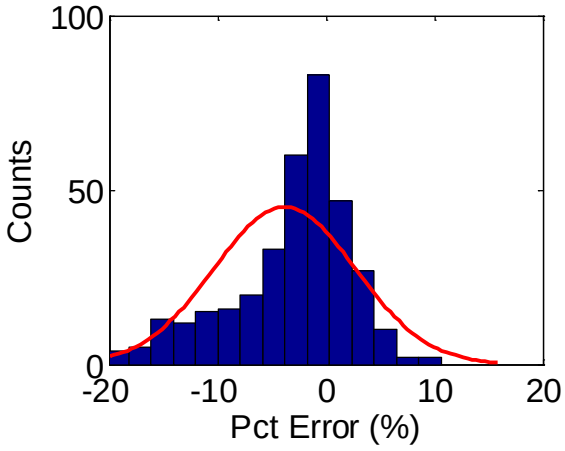

(c) Histogram of percent errors

Figure B.2.4: Validation results of mixed air temperature predictions

Supply Fan

The fan model is used to estimate the supply fan power consumption. For this project, the supply fan model is modeled as a cubic polynomial of the AHU supply air flow rate

$$P_{SF,AHU} = 0.007418 \cdot \dot{m}_{a,AHU}^3 - 0.1732 \cdot \dot{m}_{a,AHU}^2 + 2.207 \cdot \dot{m}_{a,AHU} - 5.847$$

where $P_{SF,AHU}$ is the supply fan power consumption (kW) and $\dot{m}_{a,AHU}$ is the total AHU supply air flow rate (kg/s).

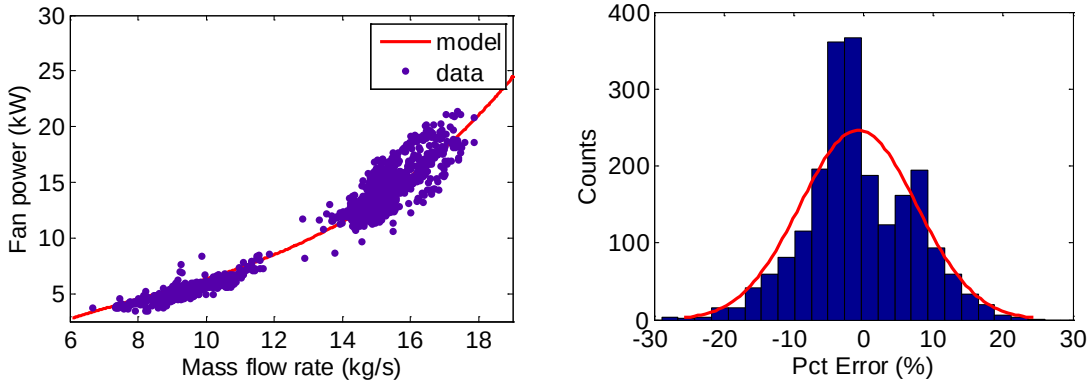

(a) Fan power consumption (b) Histogram of percent errors

Figure B.2.5: Supply fan model validation results

Variable Air Volume (VAV) with Reheat Coil

For VAV units, the flow set points and reheat valve position are control variables, based on which the discharge air temperature can determined from the following equation:

$$T_{A,VAV,Supply} = T_{DA,AHU} + a \frac{T_{W,HC,in}}{\dot{m}_{a,CompVAVi}^b} v_{HC,valve}^c$$

where $T_{DA,AHU}$ is the discharge air temperature (◦C) of the AHU, *a*, *b*, *c* are coefficients determined during model calibration, $T_{W,HC,in}$ is the supply hot water temperature (◦C) from the boiler, $\dot{m}_{a,CompVAVi}$ is the VAV supply flow rate (kg/s), and $v_{HC,valve}$ is the VAV reheat coil valve position ([0-1]). The thermal power consumption of each VAV reheat coil is determined based on the sensible heat transfer at the air-side. Figure B.2.6 shows the calibration and validation results of the VAV discharge air temperature.

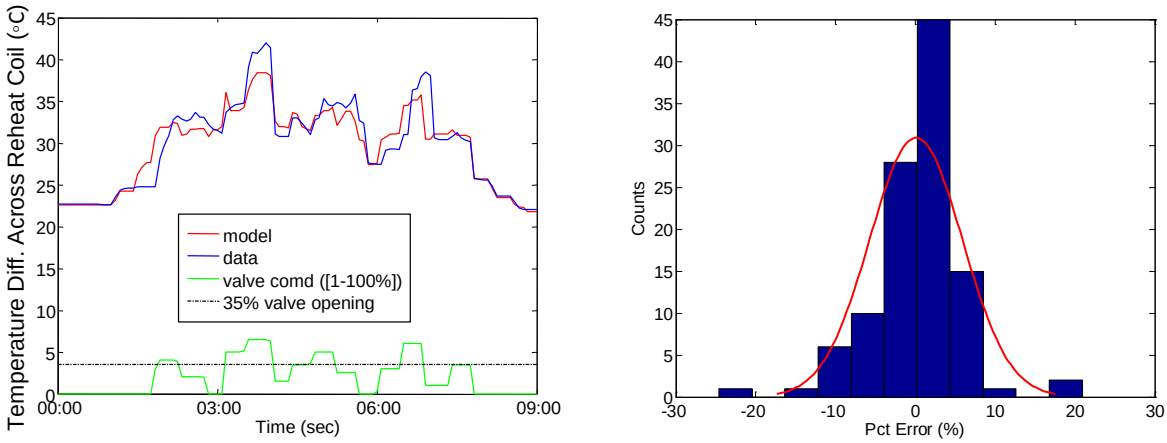

(a) Comparison of VAV reheat model with data (b) Histogram of percent errors

Figure B.2.6: Validation results of VAV reheat coil model

B.3 HVAC SYSTEM FAULT DETECTION AND DIAGNOSTICS METHODS

Fault Detection and Diagnostics (FDD) of Building Systems

FDD technologies can potentially reduce significant energy inefficiency resulting from faults and degradation of building equipment and materials; errors in operating schedules and critical design/planning flaws. A study shows that faults in mechanical and lighting equipment alone can increase the total energy consumption for commercial buildings by 2% to 11% [35]. The UTRC team selected an FDD system that uses a data-driven methodology integrated with certain amount of domain knowledge to detect and diagnose faults. The FDD tool-chain includes an off-line step of learning the nominal behaviors and an on-line step of detecting off-nominal behaviors. Since modeling a complex system, such as a building with various integrated systems, using first principles can be a challenging task, data-driven behavior learning can be a practical choice for many cases.

Among the data-driven methods the project team selected a Graphical Network based approach for fault detection and diagnosis. This approach allowed encoding the background domain knowledge and physics-based understanding of the system, while allowing discovery of new relationships within data streams using structure learning algorithms. Thus this approach for FDD provided a framework for a hybrid approach that utilized data-generated information, domain knowledge and physics-based understanding of a system. A whole building graphical network model may be too complex for tractability and fault isolation. Therefore, a hierarchical approach to diagnostic model building was adopted.

FDD Tool Chain

The FDD tool-chain used in this project primarily has the following steps:

(1) Data acquisition
(2) Data pre-processing
(3) Model learning
(4) On-line detection

(1) Data acquisition: As described above, the methodology down selected for FDD is primarily data-driven. Although data-driven methodologies have the advantages of low-cost commissioning, enhanced scalability, quick adaptability to system variation/evolution and limited requirement of domain knowledge, they require sufficient data in order to reliably model a complex system. Data sufficiency involves two major aspects: 1) Spanning the operating space and 2) Statistically significant amount of data. Whether a data set is statistically significant or not really depends on the type of data-driven technique chosen for modeling. For example, typically continuous space models require lesser amount of data compared to discrete space models. However, continuous space models often need restrictive assumptions regarding the distribution of data. On the other hand, discrete space data-driven techniques can model data with arbitrary distributions that is extremely helpful in complex nonlinear building operation scenarios. In the current study, both historical data and functional tests have been used in order to generate enough data to model discrete graphical models for different building subsystems.

(2) Data pre-processing: Data pre-processing is an important step towards building a reliable data-driven diagnostics model. The two major aspects of data pre-processing are (a) data quality verification and (b) data abstraction for modeling. In the data quality verification step, sensor

observations are checked for data ranges, rate of changes and communication reliability. Data abstraction process depends on the type of model chosen. In order to prepare data for discrete probabilistic graphical models, continuous sensor observations need to be discretized. Discretization has been performed using various techniques including equal-width, equal frequency and Maximally Bijective Discretization (MBD). The MBD methodology has been developed under this project and is described in detail in [36].

(3) Model learning: The first step in the modeling procedure, the graphical structure of the FDD model is learned in a completely data-driven manner to discover relationships between variables inherent in the data. The learned graphical structure is then validated against domain knowledge and physics based understanding of the system. At this step, several spurious connections may be removed and some critical ones enforced, the graphical structure is also pruned to keep only necessary variables for dimensionality reduction. Using a goodness-of-fit metric that is based on accuracy of prediction of certain critical variables, model parameters are adjusted to achieve a good fit. At this point the graphical network model for FDD is used to analyze new validation data to generate an anomaly score quantifying the extent of departure from the nominal performance of variable, given the measurement of other related variables. Based on the anomaly scores and a suitably chosen threshold, faults can be detected in any variable of the FDD model. The flagged events can then be verified against ground truth.

(4) On-line detection: After the FDD model learning step, the tool is deployed to perform on-line fault detection and estimation of fault level. Probabilistic graphical models are built for each relevant building sub-system. Therefore, a hierarchical decision making can be performed based on decisions from each of the FDD models. Real faults are random and it is often difficult to obtain ground truth for large building systems. Therefore, in order to validate a diagnostic system, it is important to have the capability of electronic fault injection. This capability is essentially similar to the ability to perform functional tests on building subsystems.

Using the above procedure, graphical network models were developed for FDD at the building system and sub-system level. The following sections provide the details for the FDD modeling, the results obtained and the lessons learned.

FDD of AHU-VAV based Building HVAC Systems

The team has developed graphical network models for AHU-VAV based building HVAC systems in order to demonstrate the FDD capability on the demonstration site (Buildings 7113, 7114 at Navy Campus, Great Lakes, IL).

(1) VAV Diagnostics: Variable Air Volume (VAV) boxes are typically located at the zone level where they receive conditioned air from Air Handling Unit (AHU) s and further condition the air before it reaches the zones. In the demonstration site, VAVs have two actuators: dampers and reheat coil valves (see Figure B.3.1). The dampers control the amount of air flow to be supplied to the zones where as reheat coil valves occasionally reheat the air if needed before it enters the zones. Therefore, the typical faults in such VAVs are: (a) Damper system faults (stuck, leaky and sticky) and (b) Reheat coil valve system faults (stuck, leaky and sticky). Typically, sufficiently instrumented VAVs have the following sensors: (i) air flow, (ii) supply air temperature (at AHU

level) and (iii) discharge air temperature. Figure B.3.2 shows a graphical model based on these sensors where, damperPosition and hwValve nodes signify the control commands for damper and reheat coil valve positions respectively. On the other hand, airFlowInd and Power denote air flow measurement and calculated air-side power (using supply and discharge air temperatures and air flow).

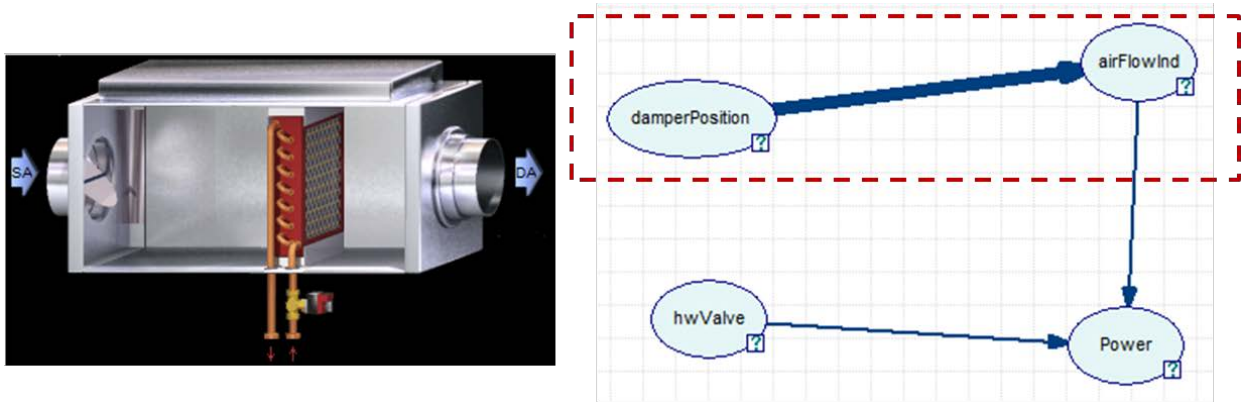

Figure B.3.1 Typical VAV configuration and corresponding graphical model

Although discharge air temperature sensors are typically available in VAVs, most of the VAVs in the demonstration site did not have them. Instead the zones had zone temperature sensors. It is understood that zone temperature is correlated with discharge air temperature. Still, it is observed that it is not sufficient for VAV reheat coil valve diagnostics. Therefore, only VAV damper system diagnostics has been demonstrated.

Figure B.3.2 shows typical VAV air flow characteristics (Damper position vs. Air flow) at nominal health. Essentially such behavior is encoded in the graphical model using historical and functional test data.

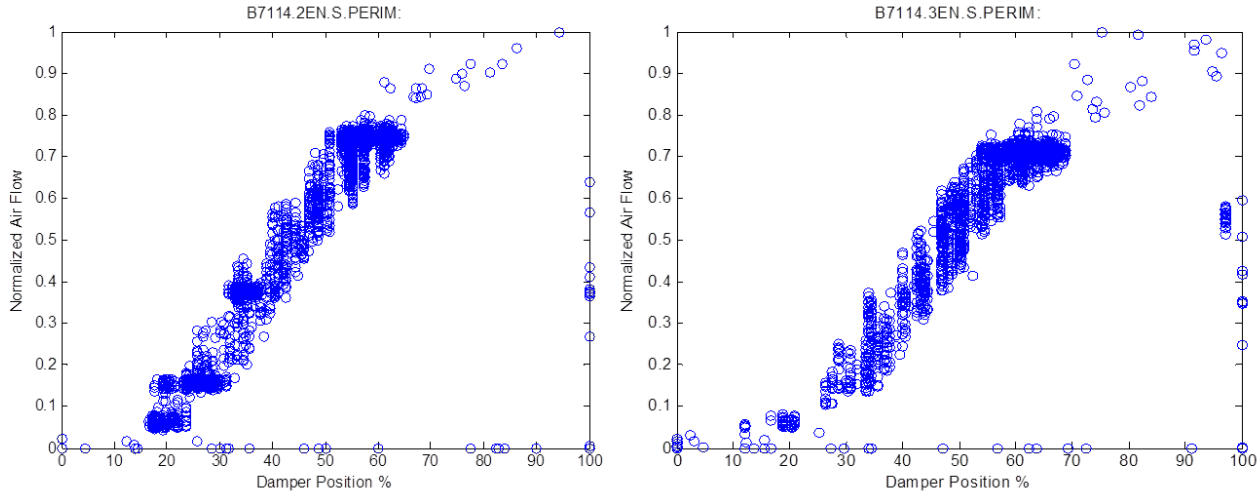

Figure B.3.2 Nominal VAV air flow characteristics

Despite different size/capacity of different VAVs, normalized air flow characteristics are similar across VAVs in the building; few healthy VAVs are chosen to learn the parameters of the model. When such model is applied for all other VAVs in the building, quite a few VAVs were found to have damper system issues.

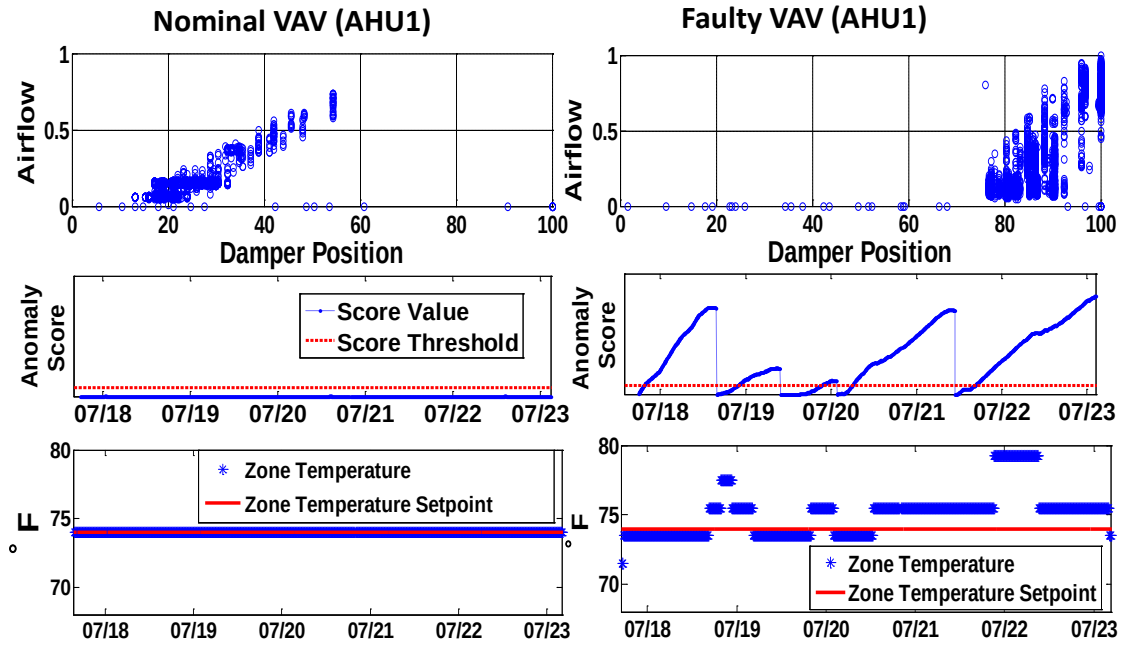

Figure B.3.3 Real VAV fault in Building 7114

For example, Figure B.3.3 shows comparative results for two VAVs in Building 7114 AHU1. It is clear from the figure that VAV on the right hand side has damper system issues as it does not seem to open until 75% damper opening. Consequently, comfort in the corresponding zone cannot be met as well. It should be noted that although VAV faults typically do not have significant energy impact, they still have considerable comfort impact.

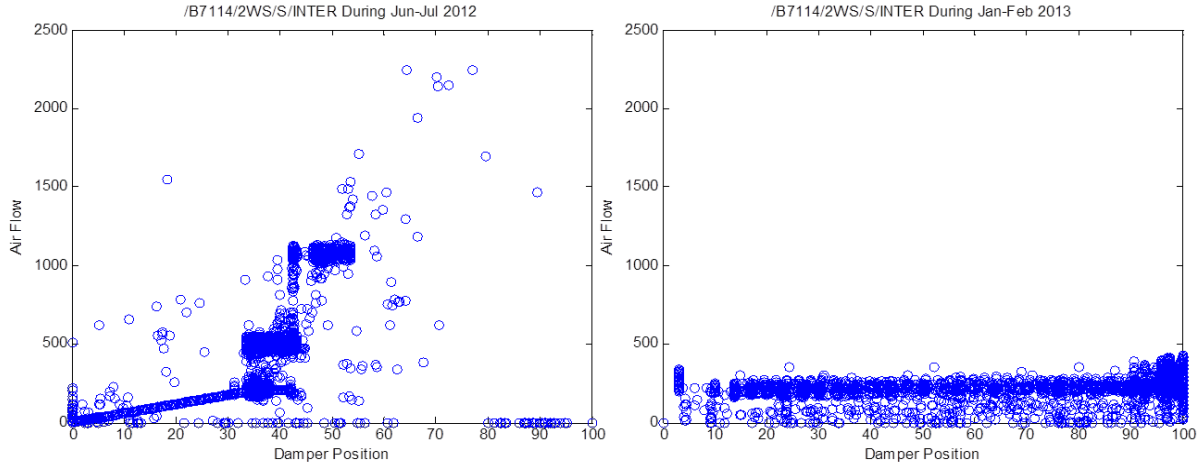

Figure B.3.4 Development of VAV fault/degradation

The last scenario is described in Figure B.3.4, where, a VAV was healthy during middle of 2012, but it degraded as time progressed. During early 2013, it seems to have a stuck (at zero position) damper issue. However, it can be an issue with the air flow sensor too. Unfortunately, due to lack of sensor redundancy the issue cannot be further isolated without manual isolation.

(2) AHU Diagnostics: AHUs typically condition air for multiple zones before it is supplied through the VAVs. Primarily, there are four major actuator sections for an AHU (see Figure B.3.5), namely Damper, Hot deck, Cold deck and Fan section. In order to be able to isolate an AHU fault, separate graphical models are built for these four sections.

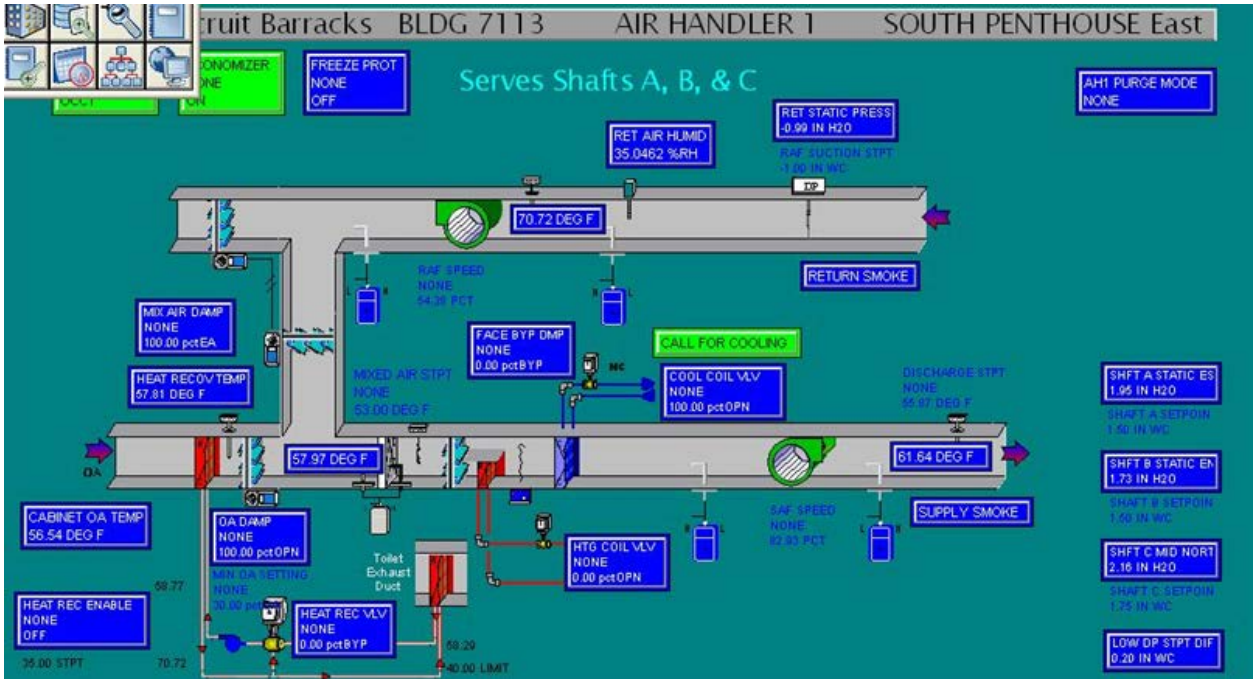

Figure B.3.5 Typical AHU configuration in the demonstration site

Damper section diagnostics: Typically, AHUs have three dampers to control the ratio between fresh and recycled air flowing into the building. They are outside air damper (OAD), mixed air damper (MAD) and exhaust air damper (EAD). Usually, the damper positions are mechanically or electronically coupled to maintain a certain outside air fraction (OAF). Therefore, faults in the damper system (dampers stuck, leaky, sticky) will affect the OAF. The graphical model shown in Figure B.3.6 essentially captures the correlation between OAD and OAF (note, the model does not have explicit MAD, EAD nodes as they are deterministically coordinated with OAD).

Ideally, OAF can be calculated using fresh and total supply air flow measurements. However, due to lack of fresh air flow sensor, OAF has been estimated using three temperatures, outside air temperature (OAT), mixed air temperature (MAT) and return air temperature (RAT).

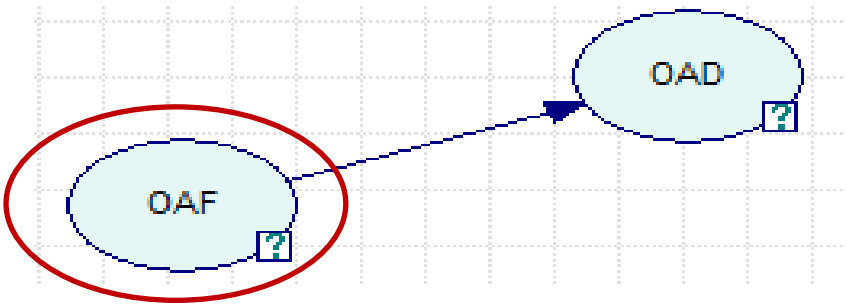

Figure B.3.6 AHU damper system graphical model

The graphical model has been trained using both functional test and historical data. Figure B.3.7 shows diagnostics result for a week window in February 2013, when four faults were electronically injected at different times. Two were injected for very short period of time and the other two faults were injected for much longer period of time. As seen in Figure B.3.7, all the injected faults were detected successfully and no false alarm occurred during this time period.

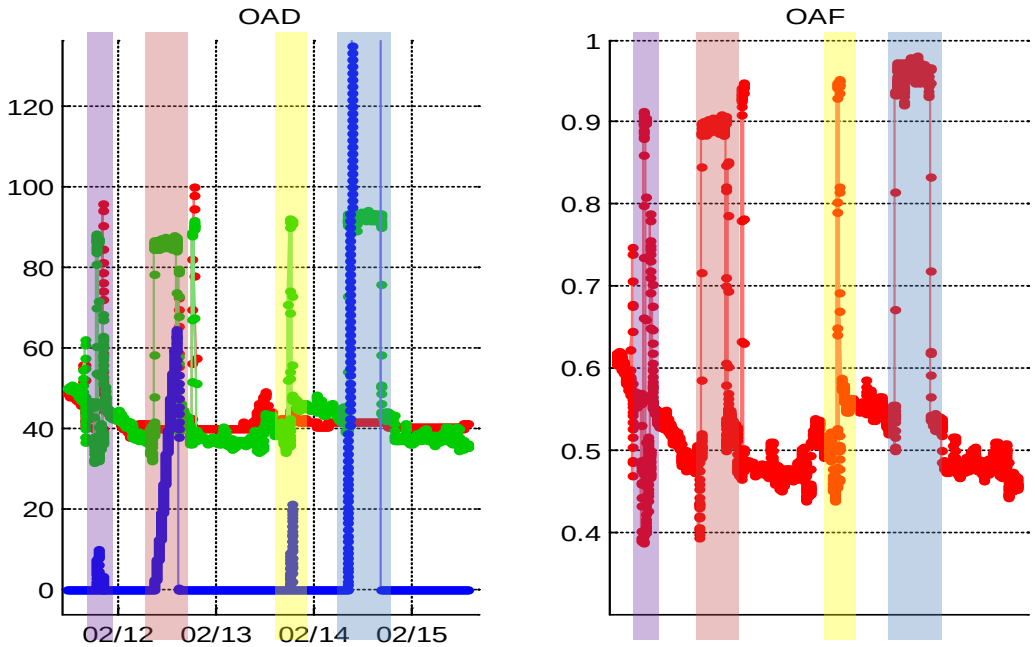

Figure B.3.7 AHU Damper system diagnostics result with electronically injected faults

Similar to the VAV scenario, sensor faults can also occur in this case. However, due to the under-sensed environment in buildings, it is very difficult to distinguish between sensor and plant fault without active perturbation. For example, in B7113 AHU2, there was an issue with the MAT sensor. Ideally, MAT values should lie between OAT and RAT values (note, here OAT is represented by heat recovery discharge air temperature (HRDAT)). Although it was not detected automatically, but manual observation suggested that this basic rule gets violated sometimes for this AHU. To make sure, OAD was moved to 0% and 100% opening. In the first case, MAT should be equal to RAT and in the second case MAT should be equal to HRDAT. However, both of these conditions failed (see Figure B.3.8) and it was concluded MAT sensor had a positive bias although that bias was variable in nature.

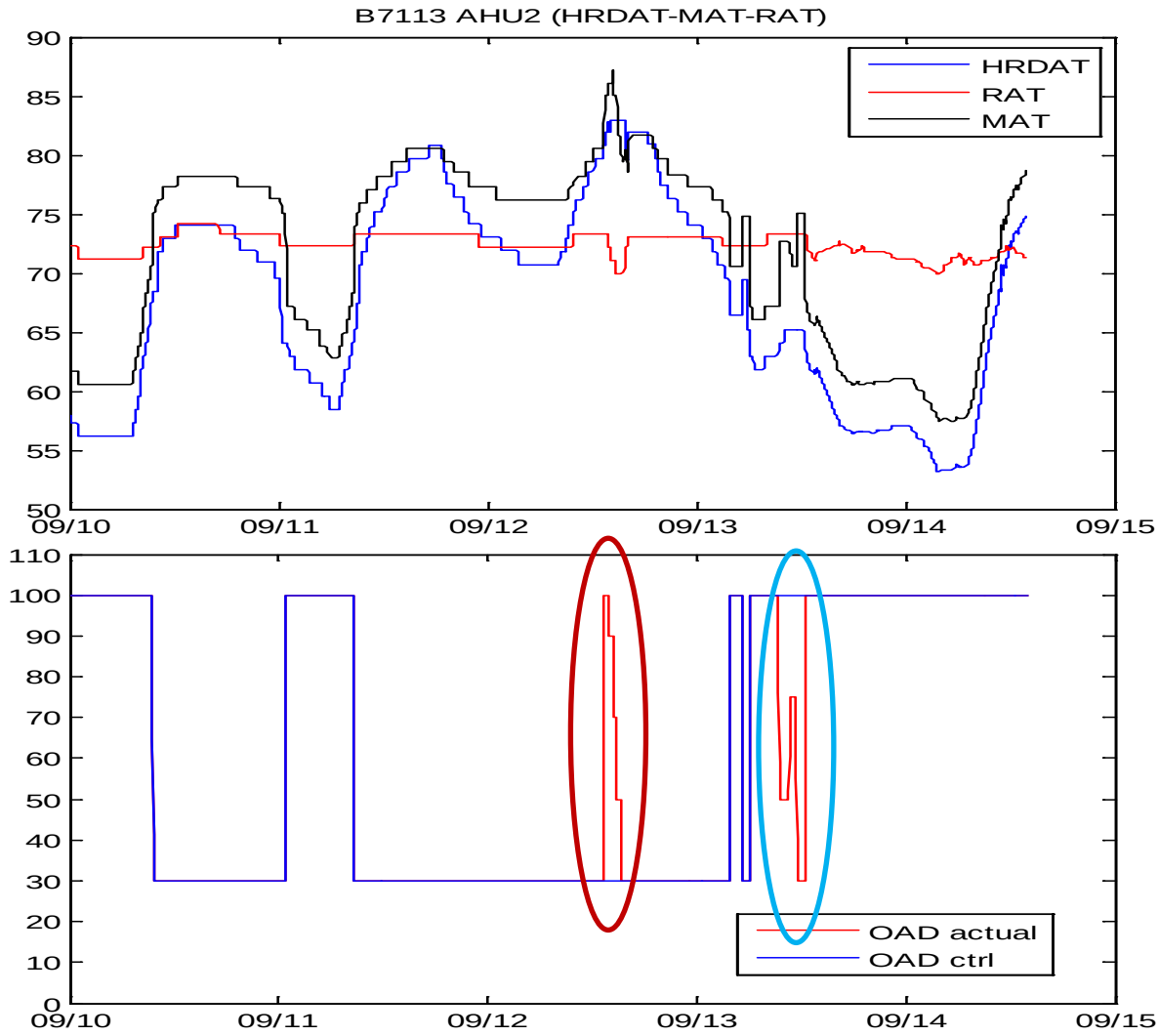

Figure B.3.8 MAT sensor fault in B7113 AHU2

Figure B.3.9 shows results of an off-line analysis to estimate energy impact of an AHU damper system fault. Here the estimation was based on an OAD stuck (at 70 %) fault. While the nominal power consumption was actually measured over the time period, faulty power consumption was estimated using a physics-based model.

Note, the energy impact of an OAD fault really depends on the fault severity and the season (outside air condition). For example, during winter when the OAT is significantly lower than typical zone temperatures, controller demands OAD to be at low positions (enough to meet the minimum ventilation requirement).

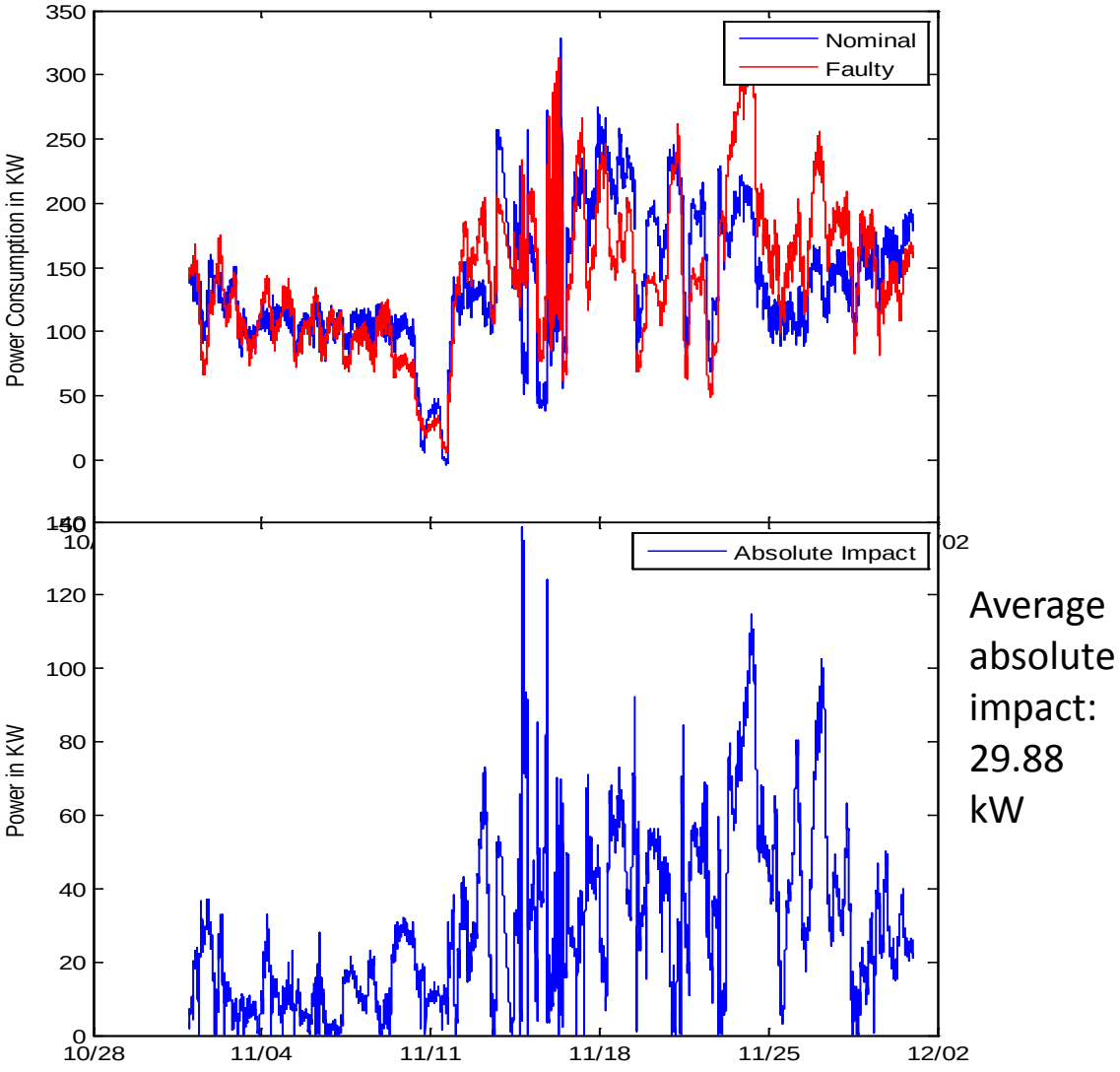

Figure B.3.9 Estimation of energy impact of an OAD stuck (at 70%) fault in winter

In such a condition, if OAD gets stuck in a high position (say 70%), then heating coil at AHU level and reheat coils at VAV level have to work very hard to meet the comfort requirement. Hence, the energy impact is going to be very high. On the other hand, the same fault will have much less energy impact during spring/fall time when controller demanded OAD positions also remain high.

Finally, for the purpose of fault tolerant control, upon detection of a damper system fault, the diagnostics system conveys an estimated range of OAF under the faulty condition (as shown in Figure B.3.6) to the control module. Then the control module adapts the set points accordingly.

Heating system diagnostics: AHUs typically have a heating deck in order to heat up air before supplying to the VAVs in the heating season. Heating deck is composed of a heat exchanging mechanism where energy is exchanged between a hot water stream and an air stream. The air stream enters the cooling deck with mixed air temperature (MAT) and exits with discharge air temperature (DAT). Similarly, hot water enters with hot water inlet temperature (T_in_hw) and exits with hot water outlet temperature (T_out_hw). There is a valve that controls the water flow which is called the heating coil valve (HCV). It is clear that during heating, DAT should be higher than MAT and T_in_hw should be higher than T_out_hw. In addition, AHUs in the demonstration site have a face bypass damper (FBD) just before the heating coil that bypasses air around the heating coil if necessary. This is particularly useful in extreme cold conditions in order to prevent the heating coil from freezing. Typical faults in the heating system include HCV stuck, leaky or sticky, clogged pipes and fouling. The FBD actuator can also get stuck, leaky or sticky.

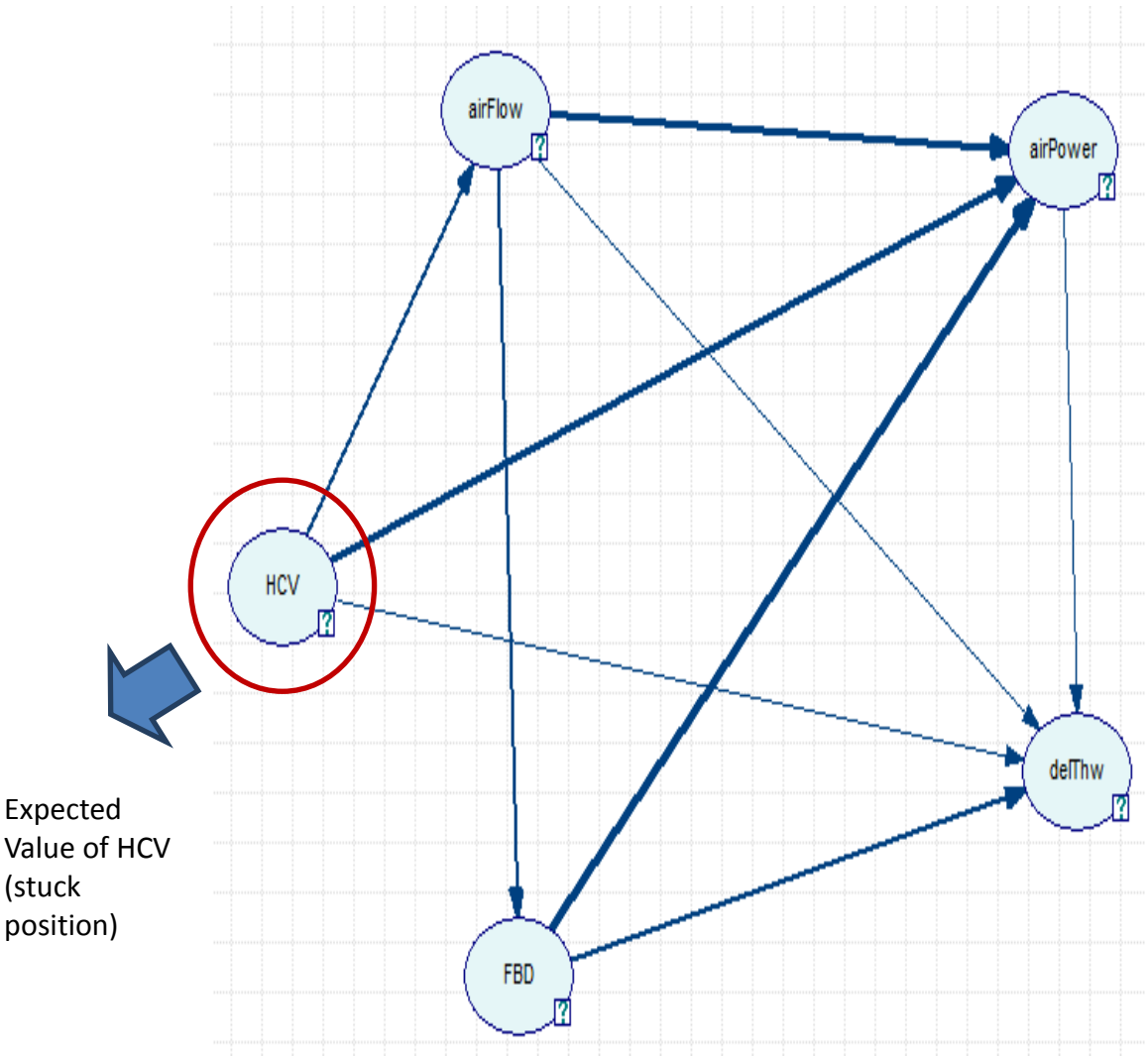

Figure B.3.10 AHU heating system graphical model

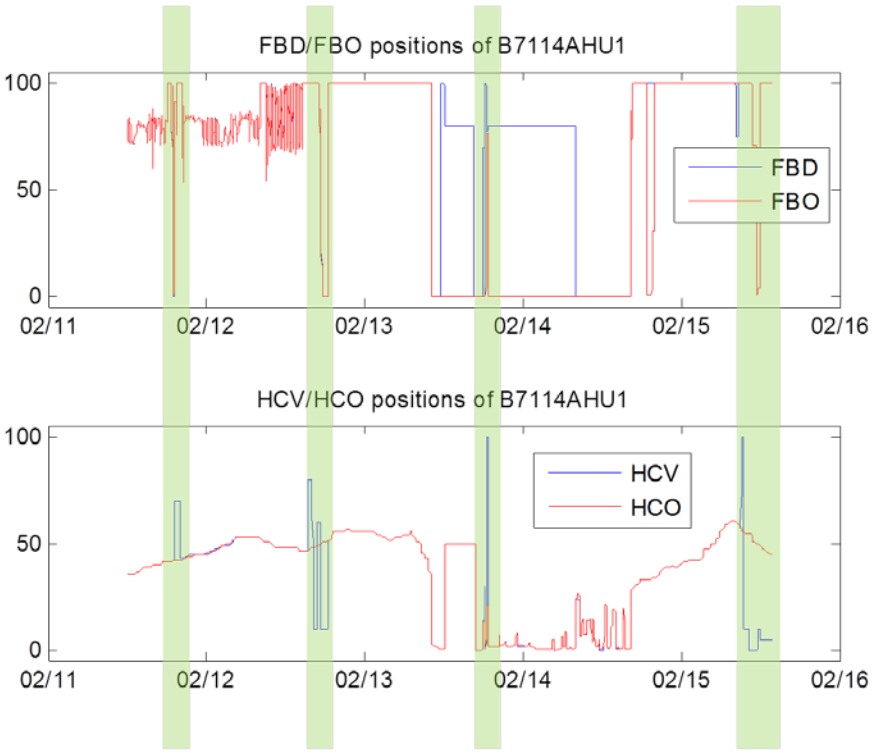

Figure B.3.11 AHU heating system electronic fault injection

To detect such faults graphical model is created as shown in Figure B.3.10 where the nodes include HCV position (controller command), FBD position (controller comand), airFlow (air flow over the heating coil), delThw (difference between T_in_hw and T_out_hw) and airpower (air side power that is calculated using air flow and the difference between DAT and MAT). The graphical model is trained based on historical and functional test data.

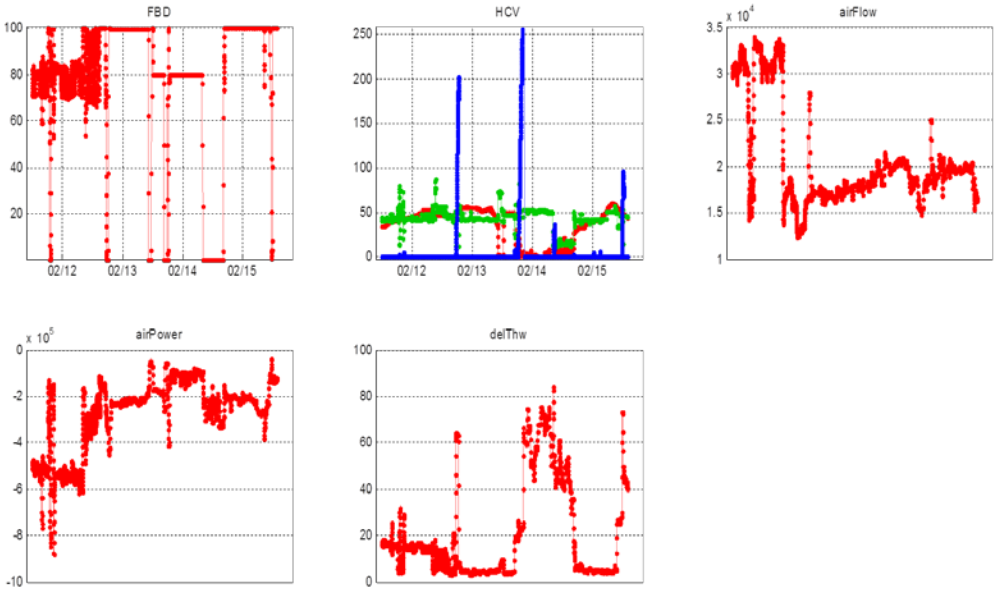

Figure B.3.12 AHU Heating system diagnostics results

To validate the diagnostic performance of such a model heating coil stuck faults were injected in B7114 AHU1 as shown in Figure B.3.11 (note, HCO is the controller command before override and HCV is the position after override; similarly, FBO is the controller command before override and FBD is the position after override). It was observed that when the HCV stuck faults (stuck at 70% or 100%) were injected; due to the local control loop FBD was getting moved to 100% in order to bypass the entire air flow around the heating coil. Due to this, HCV stuck faults can get unobservable and similarly FBD faults can get unobservable if HCV moves to 0% via the local control loop. This is essentially a local fault accommodation scheme. However, electronic fault injection becomes really difficult in this case which is observed in the diagnostic results shown in Figure B.3.12. Although all the injected faults are detected, the ability to observe faults could not be sustained for longer periods in order to demonstrate diagnostics-control integration.

Figure B.3.13 shows results of an off-line analysis to estimate energy impact of an AHU heating system fault. Here the estimation was based on an HCV stuck (at 100 %) fault. While the nominal power consumption was actually measured over the time period, faulty power consumption was estimated using a physics-based model.

Finally, for the purpose of fault tolerant control, upon detection of a damper system fault, the diagnostics system conveys an estimated range of HCV under the faulty condition (as shown in Figure B.3.10) to the control module. Then the control module adapts the set points accordingly.

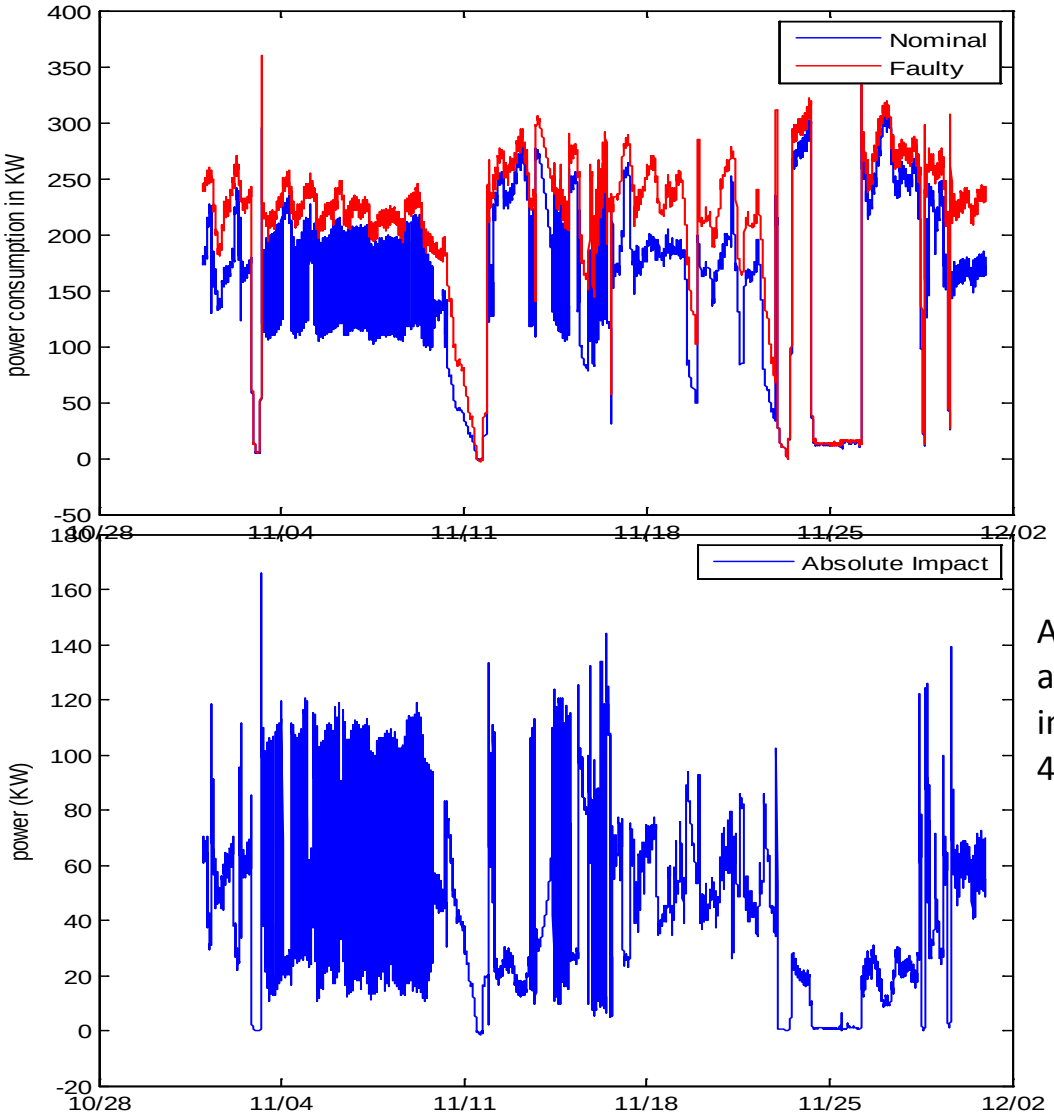

Average absolute impact: 44.8 KW

Figure B.3.13 Estimation of energy impact of an HCV stuck (at 100%) fault in winter

Cooling system diagnostics: AHUs typically have a cooling deck in order to cool down air before supplying to the VAVs in the cooling season. Cooling deck is composed of a heat exchanging mechanism where energy is exchanged between a chilled water stream and an air stream. The air stream enters the cooling deck with mixed air temperature (MAT) and exits with discharge air temperature (DAT). Similarly, chilled water enters with chilled water inlet temperature (T_in_chw) and exits with chilled water outlet temperature (T_out_chw). There is a valve that controls the water flow is called the cooling coil valve (CCV).

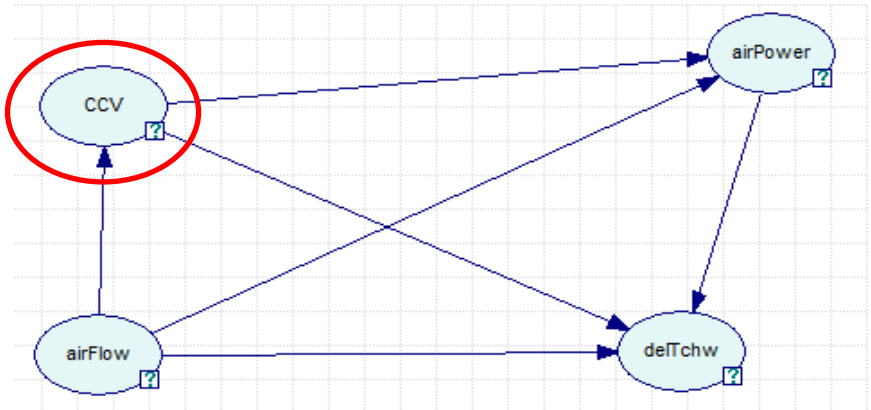

Figure B.3.14 AHU cooling system graphical model

It is clear that during cooling, DAT should be lower than MAT and T_in_chw should be lower than T_out_chw. Typical faults in the cooling system include CCV stuck, leaky or sticky, clogged pipes and fouling.

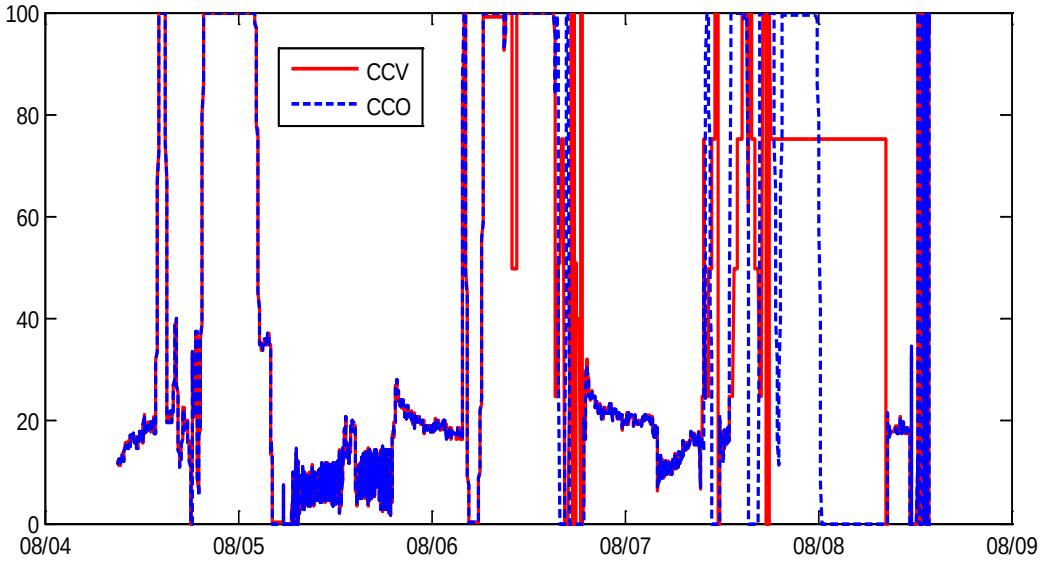

Figure B.3.15: AHU cooling system electronic fault injection

To detect such faults graphical model is created as shown in Figure B.3.14 where the nodes include CCV position (controller command), airFlow (air flow over the cooling coil), delTchw

(difference between T_in_chw and T_out_chw) and airpower (air side power that is calculated using air flow and the difference between DAT and MAT). The graphical model is trained based on historical and functional test data.

To validate the diagnostic performance of such a model cooling coil stuck faults were injected in B7114 AHU1 as shown in Figure B.3.15 (note, CCO is the controller command before override and CCV is the position after override).

Figure B.3.16 shows that the diagnostic system detects all the faults that were injected (sweep experiments, stuck at 75% overnight). However, there are some other fault flags that are not necessarily injected. Among them two flags (mornings of 08/05 and 08/06) seem to be false alarms and they occurred due to large transience in the system in the morning. They can be masked using a persistency check on the flag. The other flag on 08/06 afternoon resulted from few minor fault injections as well as due to a chiller shut down. This shows the necessity of a hierarchical system-wide diagnostic system that suppresses down-stream alarms when there is an issue with an upstream component.

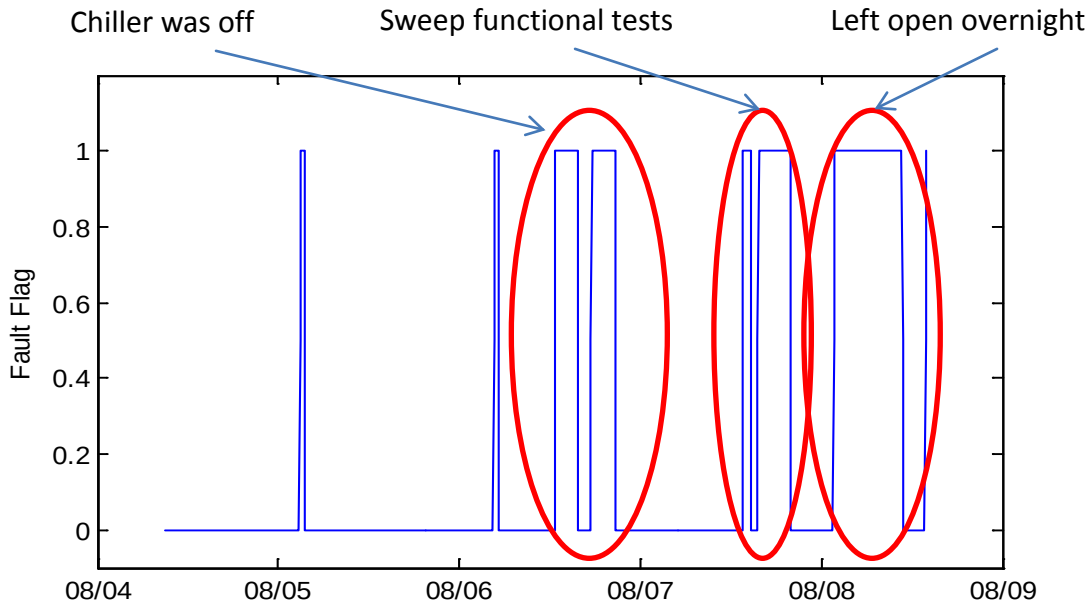

Figure B.3.16 AHU cooling system fault detection results

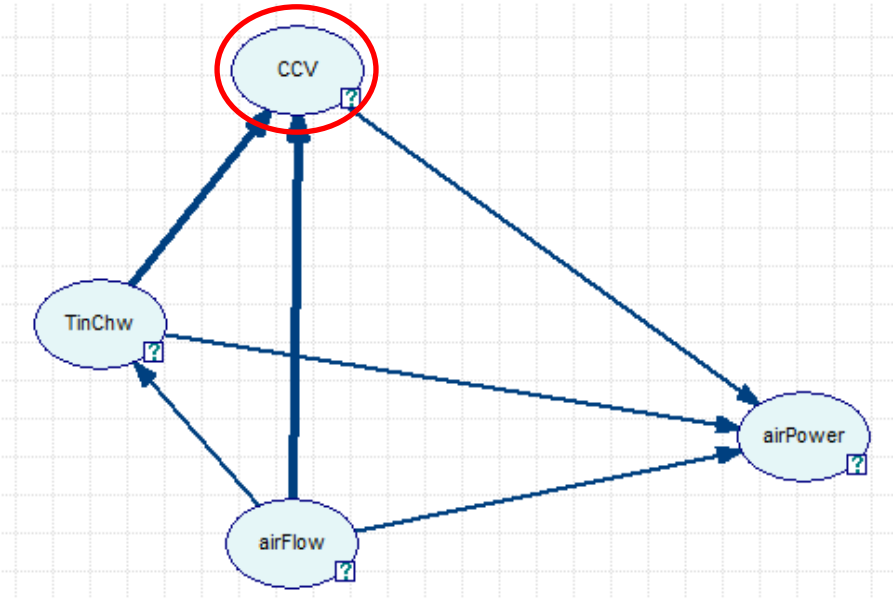

Figure B.3.17 AHU cooling system graphical model (with a reduced sensor suite: without T_out_chw)

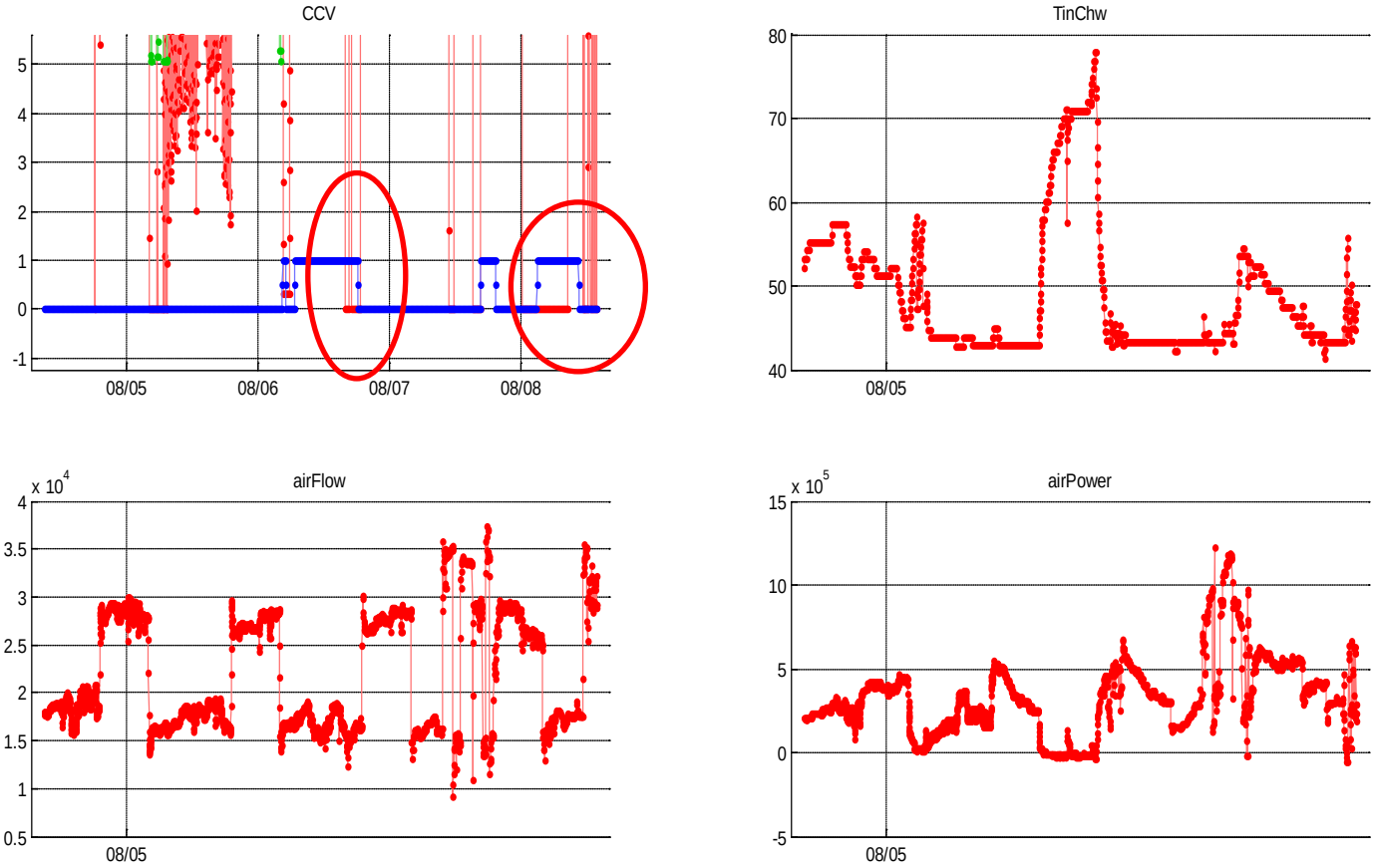

Figure B.3.18 AHU cooling system fault detection results without using T_out_chw

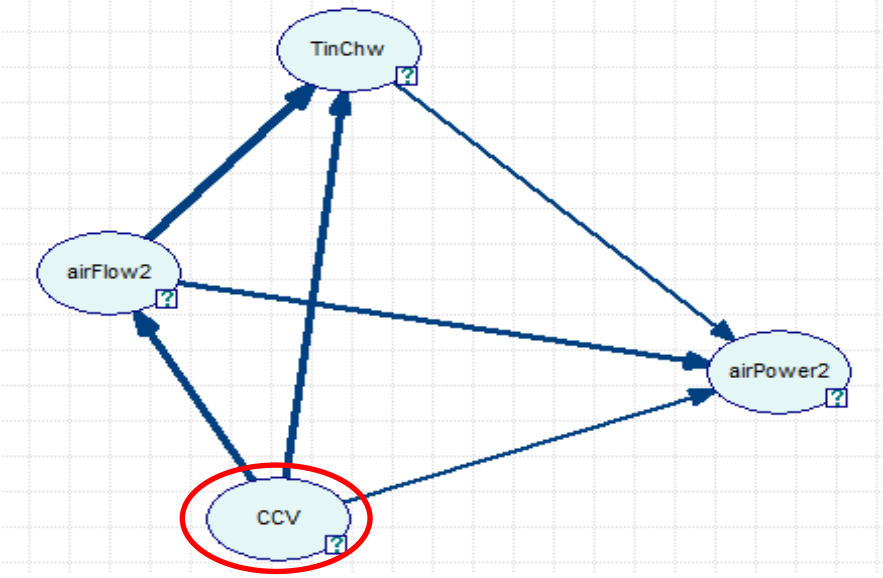

Figure B.3.19 AHU cooling system graphical model (with a reduced sensor suite: without AHU air flow sensor, AHU air flow estimated from VAV air flows)

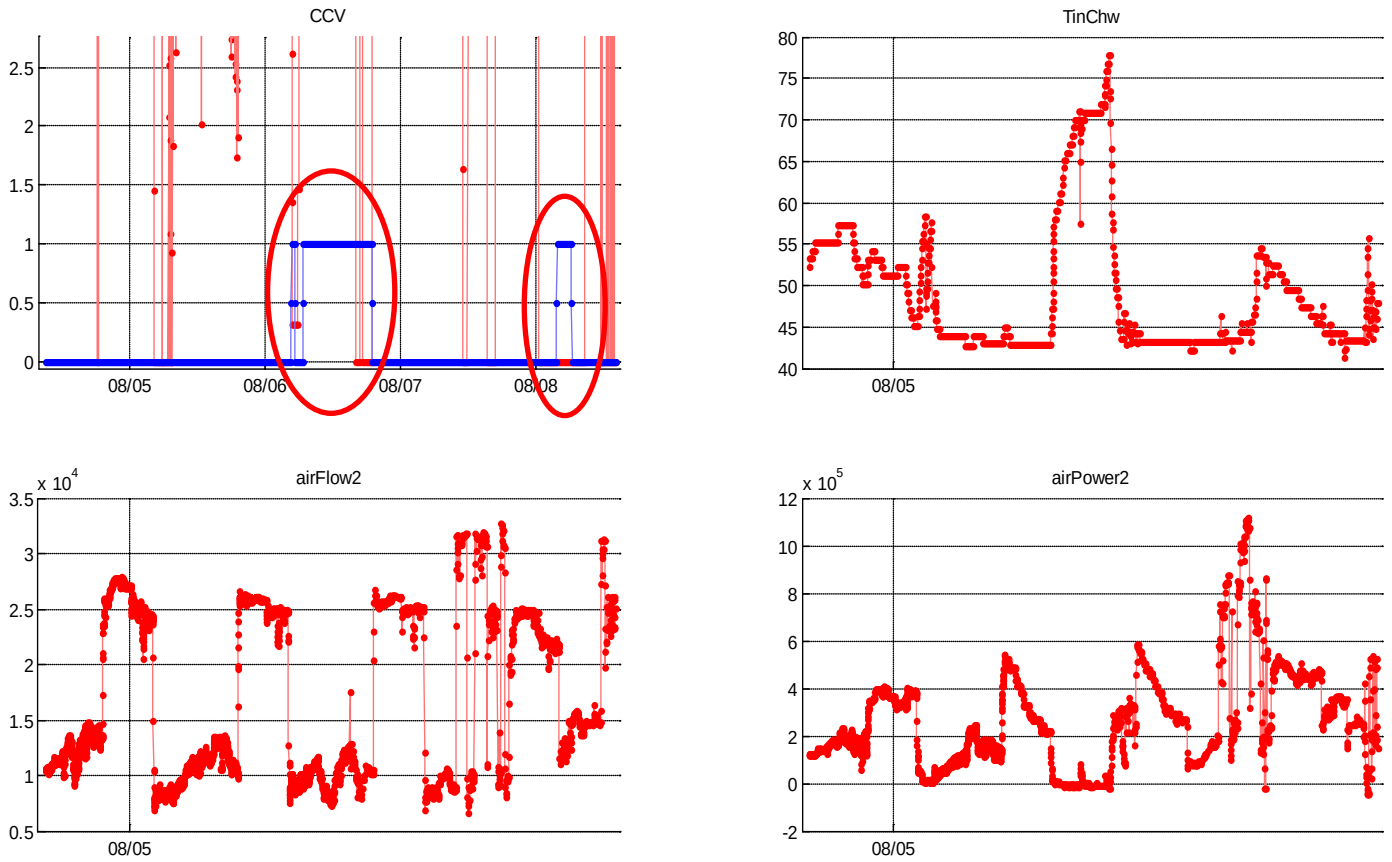

Figure B.3.20 AHU cooling system fault detection results without using T_out_chw and direct AHU air flow measurement

The above results show that the diagnostics model is sufficient to capture typical anomalies in the cooling system. However, the graphical model uses both T_in_chw and T_out_chw that may not belong to a common sensor suite available for an AHU cooling deck. While T_in_chw can be approximated from chiller outlet temperature, T_out_chw sensor needs to be installed for every AHU. However, it should be noted that both inlet and outlet chilled water temperatures are important to account for both sensible and latent heat transfer. Still, a graphical model was created without using T_out_chw as shown in Figure B.3.16 and the corresponding result is shown in Figure B.3.17. As expected, the diagnostics model becomes less sensitive. However, it may be enough to capture large anomalies in the system.

Beyond the availability of temperature sensors, often there is no air flow sensor for AHUs as it is required to have multiple averaging sensors in order to measure air flow in an AHU reliably. However, AHU air flow can be estimated by summing VAV air flows. Figure B.3.19 and Figure B.3.20 shows the graphical model and the corresponding results while AHU air flow was approximated by summing VAV air flows (affected nodes: airFlow2, airPower2). As expected, the diagnostics model sensitivity further drops due to this approximation. Such analysis can be performed more rigorously for every HVAC component to determine optimal sensor suites for diagnostics.

Fan system diagnostics: Typically, AHUs have two fans: supply and return fan. They are either coordinated in order to maintain a static pressure in the air duct or they are separately controlled to maintain supply and return static pressure in the ducts respectively. The latter is the case for the demonstration site: there are three shafts (air ducts) for the supply fan and it is required to maintain a minimum static pressure in these shafts; return fan is required to maintain a return static pressure in the return shaft. Both fans are variable frequency drives (VFDs), hence both speed command from the controller as well as fan power measurements are available for both the fans. The faults in the fan system can be: efficiency degradation for fans, belt slippage, bearing failure, increase in blade tip clearance, cracks in fan blades etc. All such faults essentially result in a changed correlation among fan speed, power and air flows. Also, due to degradation fans may not be able to maintain required shaft static pressures.

Based on this basic domain knowledge, a graphical model is created as shown in Figure B.3.21. The nodes are SAFspeed, SAFpower (Supply air fan speed and power), RAFspeed, RAFpower (Return air speed and power), airflow (supply air flow through the AHU), minSSP (minimum supply static pressure) and RSP (return static pressure). The graphical model is trained based on historical and functional test data. Figure B.3.22 shows that B7114 AHU1 had return fan issues. Although the anomaly is observed with a reduced strength in other nodes, the anomaly score for RSP node is most dominant. Essentially the problem was that the return fan was not being able to maintain RSP under certain operating conditions. It was concluded to be a control related fault.

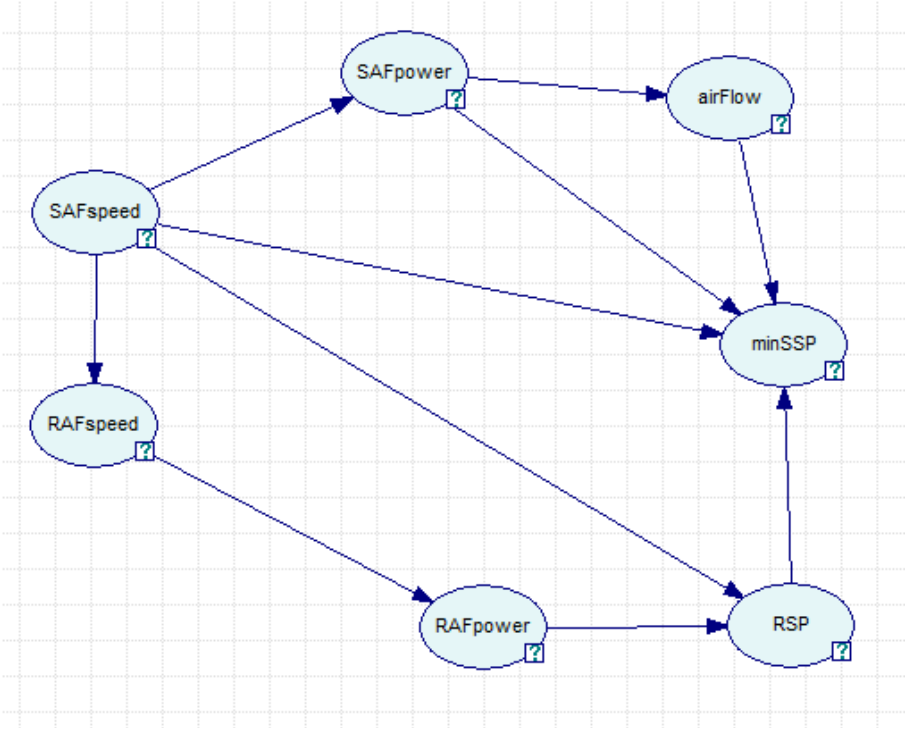

Figure B.3.21 AHU fan system graphical model

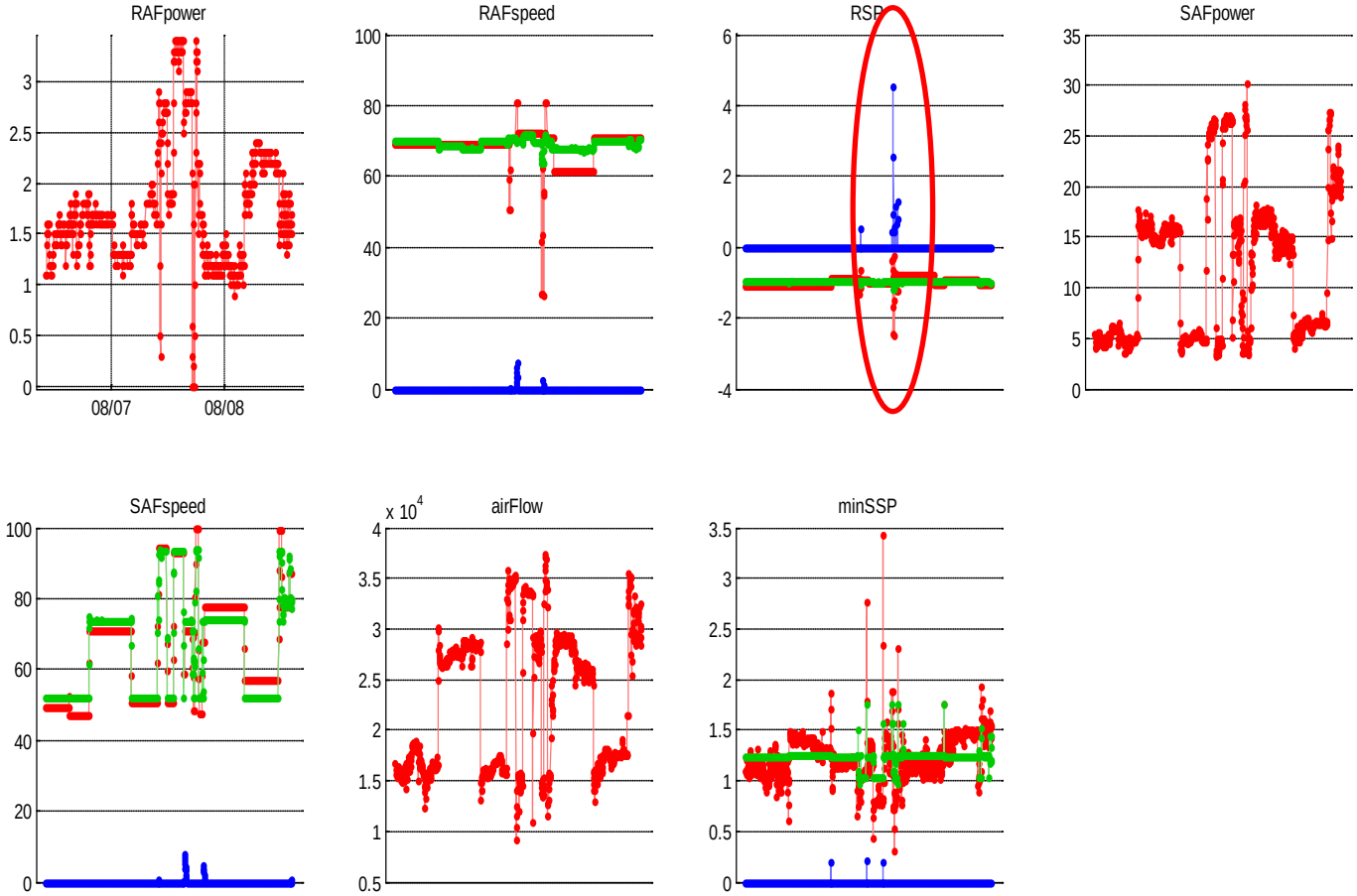

Figure B.3.22 AHU Fan system diagnostics result with real faults

B.4 MIDDLEWARE IMPLEMENTATION

UTRC Data Management Software

The UTRC Data Management Software allowed the seamless communication of control and diagnostics applications with the Siemens Apogee Insight Building Management System (BMS). It also provided facilities to store historical data-points and experiment logs in a local database. Figure B.6.1 depicts the overall software architecture employed in the experiments. A Dell PowerEdge™ T410 server, running Linux RedHat, hosted the UTRC Data Management Software. This computer was connected to the Siemens Apogee Insight BMS through a local network. Both machines were located in the Building 7114 mechanical room. Control and diagnostics applications, written in Matlab, were executed on another test computer attached to the same local network. Applications communicated to the UTRC Data Management Software through Web-services. UTRC Data Management Software exploited the Siemens Apogee Insight BACnet server to access the BMS data-points.

The UTRC Data Management Software was customized and expanded to support the particular needs of this activity. In particular, new drivers were developed; failsafe features were conceived and implemented and a capability to log experiment information was added.

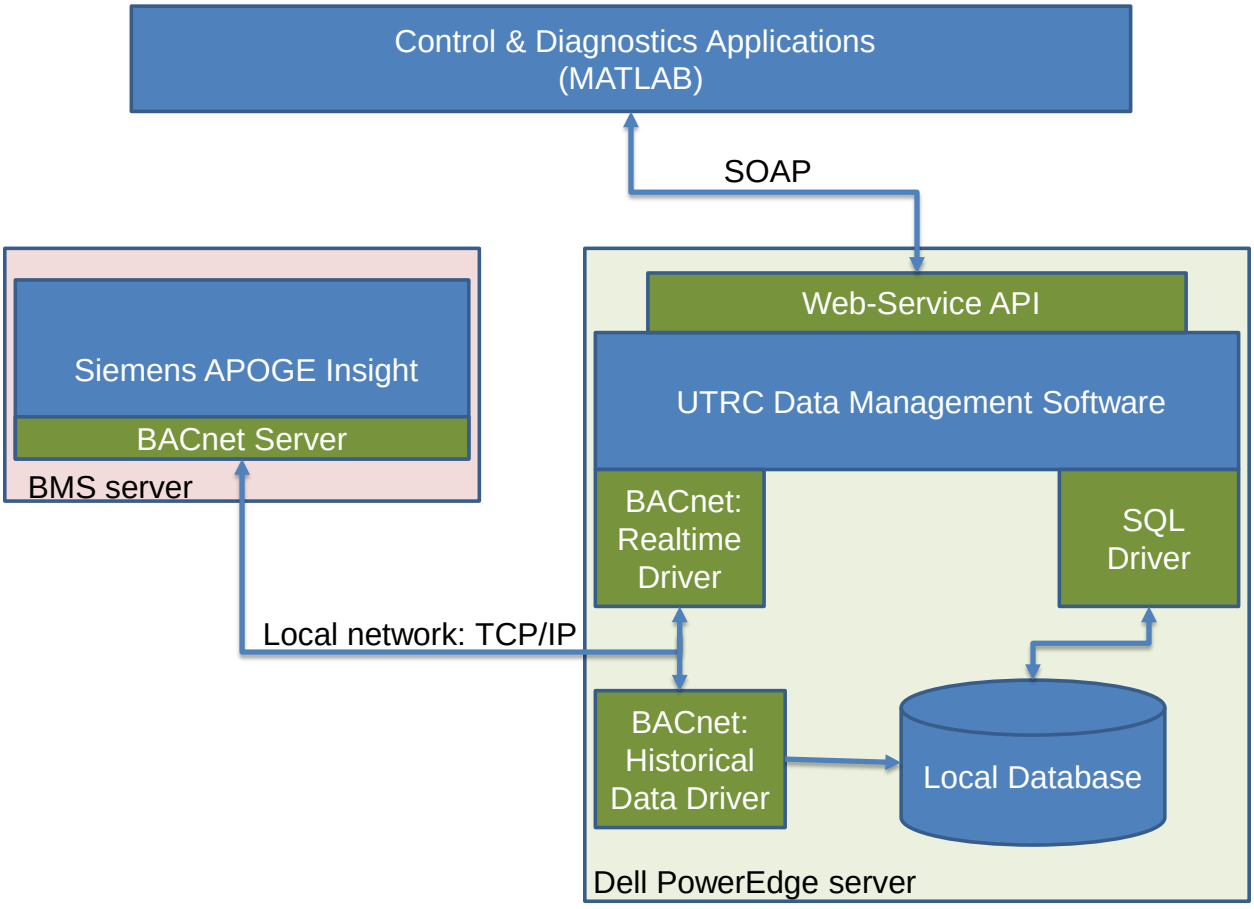

Figure B.6.1: System Architecture

Drivers

The UTRC Data management SW comprises drivers to talk to the BMS and to the local database. In order to communicate with the Siemens Insight BMS two drivers (Historical Data Acquisition and Real-time Data Access) were developed. Both are built on top of an open-source BACnet protocol stack library (http://bacnet.sourceforge.net/).

1. Historical Data Acquisition: A daemon runs in background to periodically acquire all BMS data-points that are exposed on BACnet and to store them into the local database for future access and analysis.
2. Real-time Data Access: Application requests to read and override specific data points are handled by this dedicated driver that generates the appropriate BACnet commands.

The SQL Driver is used to talk to the local database to retrieve historical data-points and logs.

Failsafe features

Unattended data acquisition data-points and executing advanced control and diagnostic experiments for an extended period of time, require mechanisms to 1) recover from an unexpected conditions (e.g. power loss); 2) Fail back on the default BMS operations when those conditions occur. To address the first issue, a daemon was created to start and monitor the UTRC data management SW and all the required SW at startup. It also ensures that all the needed SW components are properly running. To address the second issue a heart-beat concept was used: an application intending to override BMS operations needs to periodically notify the BMS of its alive status. When the application fails to do so, the BMS recognizes an error condition and fails back to its default operations. The BMS logic was modified to support this capability.

Logging

The UTRC data management SW was extended to provide a logging capability. This allows applications to log about experiments and other particular conditions. A log is defined by the following fields: “timestamp” (when the log was generated), “type” to simplify indexing of tags, “username” the user who generated the log, “message” a text field with additional information about the log.

Interfacing to the UTRC Data Management Software

The UTRC Data Acquisition Software exposes its API through Web-services. Applications can use this API remotely (and locally).

APPENDIX C: DETAILED PERFORMANCE ANALYSIS

C.1 METHOD FOR CALCULATION OF QUANTITATIVE PERFORMANCE OBJECTIVE METRICS

Calculation of Energy Consumption

The methods employed to compute the savings will follow the recommendations in ASHRAE Guideline 14-2002.

Calculation –

$$kWhbase\_e = \sum_{t=1}^{b} kWhfan\_b + \sum_{t=1}^{b} MMBtuCC\_b * \text{ Typical chiller eff } + \sum_{t=1}^{b}(MMBtuHC\_b) * \text{Typical eff} * mk$$

$$kWhnew\_e = \sum_{t=1}^{p} kWhfan\_n + \sum_{t=1}^{p} MMBtuCC\_n * \text{ Typical chiller eff } + \sum_{t=1}^{p}(MMBtuHC\_n) * \text{Typical boiler eff} * mk$$

$$Savings_{kWh\_e} = (kWh_{base\_e} - kWh_{new\_e})/kWh_{base\_e} * 100\%$$

with the symbols defined as follows:

mk = MMBtu to kWh conversion coefficient

Typical chiller eff = 0.8 kW/Ton (information from facility manager at CERL)

Typical boiler eff = 0.75 (information from facility manager at CERL)

t = time step

b = baseline control strategy time frame

p = proposed control strategy time frame

kWh_{base_e} = Total fan electrical energy consumption (in kWh) during the time frame when baseline control strategy is being implemented

kWh_{new_e} = Total fan electrical energy consumption (in kWh) during the time frame when proposed control strategy is being implemented

kWh_{fan_b} = Fan electrical energy consumption (in kWh) at each time step during the time frame when baseline control strategy is being implemented

kWh_{fan_n} = Fan electrical energy consumption (in kWh) at each time step during the time frame when proposed control strategy is being implemented

$Savings_{kWh\_e}$ = Percentage savings in fan electrical energy consumption due to the proposed control strategy

$MMBtu_{CC\_b}$ = Cooling energy consumption (in MMBtu) at each time step during the time frame when baseline control strategy is being implemented

$MMBtu_{CC\_n}$ = Cooling energy consumption (in MMBtu) at each time step during the time frame when proposed control strategy is being implemented

$MMBtu_{HC\_b}$ = Heating energy consumption at AHU heating-coil (in MMBtu) at each time step during the time frame when baseline control strategy is being implemented

$MMBtu_{HC\_n}$ = Heating energy consumption at AHU heating-coil (in MMBtu) at each time step during the time frame when proposed control strategy is being implemented

Calculation of Peak Electrical Power Demand

Same assessment method as the one employed for Objective 1.

Calculation –

kW_{base_e} = Max(kW_{fan_b} + $MMBtu_{CC\_b}$* Typical chiller eff)

kW_{new_e} = Max(kW_{fan_n}+ $MMBtu_{CC\_n}$* Typical chiller eff)

$Savings_{kW\_e}$ = (kW_{base_e} – kW_{new_e})/kW_{base_e} x 100%

With the symbols defined as follows:

kW_{base_e} = Peak electrical power (in kW) during the time frame when baseline control strategy is being implemented

kW_{new_e} = Peak electrical power (in kW) during the time frame when proposed control strategy is being implemented

kW_{fan_b} = Fan electrical power (in kW) at each time step during the time frame when baseline control strategy is being implemented

kW_{fan_n} = Fan electrical power (in kW) at each time step during the time frame when optimal control strategy is being implemented

$MMBtu/hr_{CC\_b}$ = Cooling demand (in MMBtu/hr) at each time step during the time frame when baseline control strategy is being implemented

$MMBtu/hr_{CC\_n}$ = Cooling demand (in MMBtu/hr) at each time step during the time frame when optimal control strategy is being implemented

$Savings_{kW\_e}$ = Percentage savings in peak electrical power due to optimal control strategy

Calculation of CO_2 Emissions

Same assessment method as the one described for Objective 1. The CO_2 emissions were calculated by multiplying the electric and gas usage with CO_2 emissions factors.

Calculation –

$$CO_{2base} = \sum_{t=1}^{b}(kWhfan\_b + MMBtuCC\_b * \text{Typical Chiller eff}) * e\_co2 + \sum_{t=1}^{b}(MMBtuHC\_b) * \text{Typical boiler eff} * h\_co2$$

$$CO_{2new} = \sum_{t=1}^{b}(kWhfan\_n + MMBtuCC\_n * \text{Typical Chiller eff}) * e\_co2 + \sum_{t=1}^{b}(MMBtuHC\_n) * \text{Typical boiler eff} * h\_co2$$

$Savings_{CO2}$ = (CO_{2base}–CO_{2new})/ CO_{2base} x 100%

Where

h_co2 = CO_2 emissions for natural gas (120.593 lbs/MMBtu) [13]

e_co2 = CO_2 emissions for electricity (1.16 lbs/kWh for Illinois) [14]

Calculation of Temperature Regulation

The temperature regulation error (absolute value) was integrated during the periods of occupancy on a daily basis. This calculation was repeated for baseline control operation and operation with the EPMO system strategy. The two values were compared to ensure that temperature regulation performance is not sacrificed when realizing the energy savings.

Calculation –

Zone_occupancy = 0 or 1 based on occupancy schedule

Temperature_error = $\sum_{all\ zones} \sum_{\substack{occupied\ time \\ in\ a\ week}} \left| T_{measured} - T_{setpoint} \right| \Delta t_{sampling}$

Calculation of Payback Time, Savings-to-Investment Ratio, and Net Present Value

A practical SIR formula for building related project, recommended by NIST [18], will be used in this project:

$$\boldsymbol{SIR_{A:BC}} = \frac{\Delta \boldsymbol{E} + \Delta \boldsymbol{W} + \Delta \boldsymbol{OM\&R}}{\Delta \boldsymbol{I_0} + \Delta \boldsymbol{Repl} - \Delta \boldsymbol{Res}}$$

Where all amounts are calculated in their present values:

$\boldsymbol{SIR_{A:BC}}$: Ratio of operational savings to investment-related additional costs, computed for the alternative relative to the base case;
$\Delta \boldsymbol{E} = (\boldsymbol{E_{BC}} - \boldsymbol{E_A})$: Savings in energy costs attributable to the alternative;
$\Delta \boldsymbol{W} = (\boldsymbol{W_{BC}} - \boldsymbol{W_A})$: Savings in water costs attributable to the alternative;
$\Delta \boldsymbol{OM\&R} = (\boldsymbol{OM\&R_{BC}} - \boldsymbol{OM\&R_A})$: Difference in OM&R costs;
$\Delta \boldsymbol{I_0} = (\boldsymbol{I_A} - \boldsymbol{I_{BC}})$: Additional initial investment cost required for the alternative relative to the base case;
$\Delta \boldsymbol{Repl} = (\boldsymbol{Repl_A} - \boldsymbol{Repl_{Bc}})$: Difference in capital replacement costs;
$\Delta \boldsymbol{Res} = (\boldsymbol{Res_A} - \boldsymbol{Res_{Bc}})$: Difference in residual value.

Net present value (NPV) is the total net cash flow that a project generates over its lifetime, including first costs, with discounting applied to cash flows that occur in the future. NPV indicates what a project's lifetime cash flow is worth today. The formula below will be used to calculate NPV over a given period:

$$\boldsymbol{NPV} = \sum \frac{\boldsymbol{R_t}}{(\boldsymbol{1+i})^{\boldsymbol{t}}}$$

Where:

$\boldsymbol{t}$: is the time of cash flow (the elapsed time in years);
$\boldsymbol{i}$: is the discount rate;
$\boldsymbol{R}$: is the net cash flow (the amount of cash inflow minus outflow). In building related project, this will be energy savings minus investments in a given year[17].

If we assume that $\Delta \boldsymbol{E_t}$, ΔW_t $\Delta OM\&R_t$ to be the same in every year (i.e., there is no price escalation and quantities of energy and water saved each year are the same) and there are no

[17] Energy Star Building Manual
http://www.energystar.gov/index.cfm?c=business.EPA_BUM_CH3_InvestAnalysis

additional non-annually recurring OM&R or replacement costs, the following simplified formula can be used to compute simple payback time (SPB)[18]:

$$\boldsymbol{SPB} = \frac{\Delta \boldsymbol{I_0}}{[\Delta \boldsymbol{E_0} + \Delta \boldsymbol{W_0} + \Delta \boldsymbol{OM}\&\boldsymbol{R_0}]}$$

Where:

$\Delta \boldsymbol{I_0}$: Additional initial investment cost;
$\Delta \boldsymbol{E_0}$: Annual savings in energy cost;
$\Delta \boldsymbol{W_0}$: Annual savings in water cost;
$\Delta \boldsymbol{OM}\&\boldsymbol{R_0}$: Annual difference in OM&R costs.

C.2 PERFORMANCE ESTIMATION FOR NOMINAL MODEL PREDICTIVE CONTROL

This section describes the EPMO system performance evaluation for nominal, healthy HVAC system (in absence of HVAC system faults). The performance evaluation focuses on the Model Predictive Control technology assessment. The evaluation of the overall performance of MPC against baseline control for a given AHU through all demo days is accomplished based on calculated averaged values of the quantitative performance metrics of Table 5.1. For each MPC day, the results from three baseline days were averaged and used as the representative baseline.

In particular, the following performance metrics are considered for the overall MPC performance analysis for each demonstration AHU in the two mentioned campus buildings:

1. Comparison of total energy consumption
2. Energy consumption reductions from MPC
3. CO2 emission reductions from MPC
4. Peak demand reductions from MPC
5. Comparisons of mean CO2 level in compartment zones
6. Comparisons of comfort violations in terms of zone temperature

Building 7114 AHU 1

Table C.2.1 summarizes the demonstration schedule of Building 7114 AHU1 in Dec. 2012 and Mar. 2013.

Table C.2.1 Demonstration schedule of Building 7114 AHU1 in Dec. 2012 and Mar. 2013

Demo Days	**Demo Time Period**	**Mean Outdoor Air Temperature (◦F)**
Dec. 2012		
Day 1	12/04/2012 12pm - 24pm	48.7
Day 2	12/5/2012 0am to 24pm	34.1
Day 3	12/6/2012 0am to 24pm	40.9
Day 4	12/07/2012 0am to 15pm	42.2
Mar. 2013		
Day 1	03/11/2013 16pm to 24pm	34.5
Day 2	03/12/2013 0am to 24pm	31.7
Day 3	03/13/2013 0am to 24pm	27.0
Day 4	03/14/2013 0am to 24pm	30.7
Day 5	03/15/2013 0am to 13:30pm	34.6

As can be observed from Figure C.2.1, MPC brought promising energy consumption reductions across all test cases through demo days in 2012 and 2013 winter. In addition, MPC brought improved zone temperature regulation for comfort consideration. Note that in December 2012 demonstrations, the peak demand is increased for three MPC test days. One reason for this is that MPC tried to keep comfort as its priority and maintained the zone temperature beyond the heating set point most of the time compared to the baseline days. From Table C.2.1, MPC day 2 (Dec. 5, 2012, 24 hr.) was selected as an example to illustrate this point. As can be seen in Figure C.2.1, the zone temperature set point changed from 68°F to 71°F at evening around 6:50PM. During the set point transition time, MPC was able to respond to this and supplied higher heating power to lift the zone temperature to rise above the updated set point (see Figure C.2.1). By comparison, all the other three baseline cases failed to respond to this set point change and thus consumed less peak power during this period.

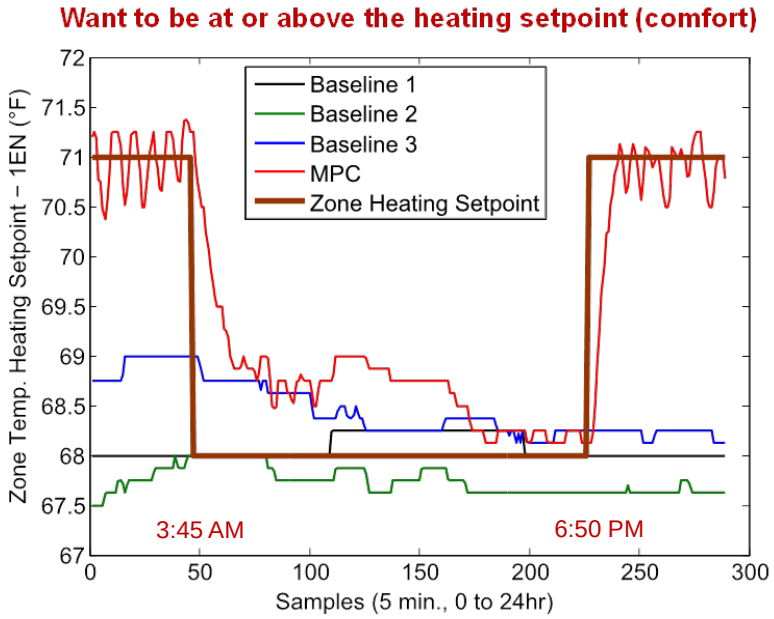

Figure C.2.1 Comparison of controlled zone temperature during set point changes

Figure C.2.2 shows the aggregated plots of comfort violations (temperature) and HVAC power consumption during the 24 hr. period. The 1st subplot shows the comfort violation in terms of zone temperature. The violation is calculated as $T_{heating}^{stpt} - T_z$, where $T_{heating}^{stpt}$ is the zone heating set point and T_z is the controlled zone temperature. This formula measures the distance of the controlled zone temperature to its heating set point. Ideally, the controlled zone temperature should always be equal or above the heating set point and thus a positive value means comfort is violated (i.e., $T_z < T_{heating}^{stpt}$).

As can be seen in Figure C.2.2, the peak demand (labeled by a "star" in the last subplot) happens around 7 PM right after the zone temperature set point was changed from 68°F to 71°F. By comparing with the 1st subplot, one could clearly infer the relations between power consumption and comfort violations during the set point changes, i.e., 3:45AM and 6:50PM.

Figure C.2.2 Example case of high peak demand from MPC to meet comfort conditions (Building 7114 AHU1 – Dec. 5, 2012, during a 24hr.-long demonstration window)

Figures C.2.3-C.2.7 present the comparison of total energy consumptions between MPC and averaged baseline, energy consumption reductions achieved by MPC, CO_2 emission reductions brought by MPC, peak demand reductions achieved by MPC, comparisons of mean CO_2 level in compartment zones, and comparisons of comfort violations in terms of zone temperature during Dec 2012 demo (subplot (a)) and Mar. 2013 (subplot (b)) demo of Building 7114 AHU1, respectively.

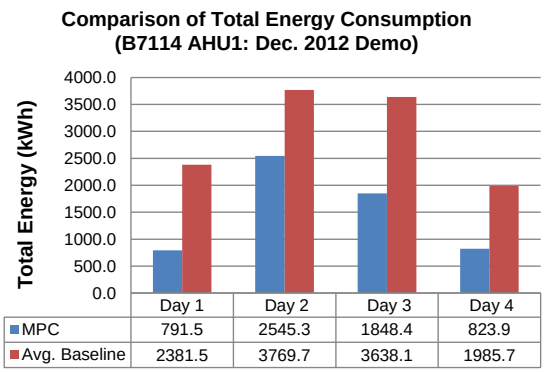

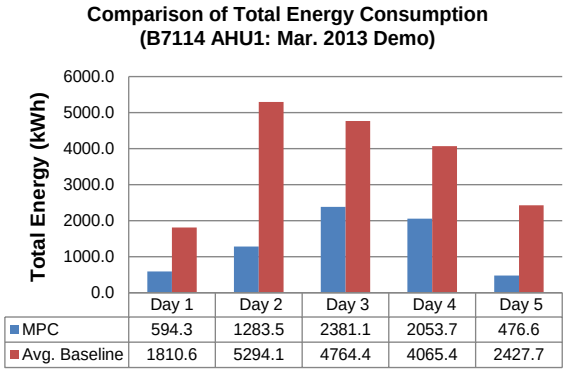

(a) Dec. 2012 Demo (b) Mar. 2013 Demo

Figure C.2.3 Comparisons of total energy consumption (B7114 AHU1)

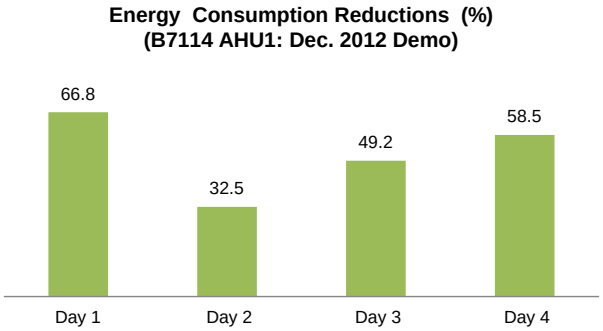

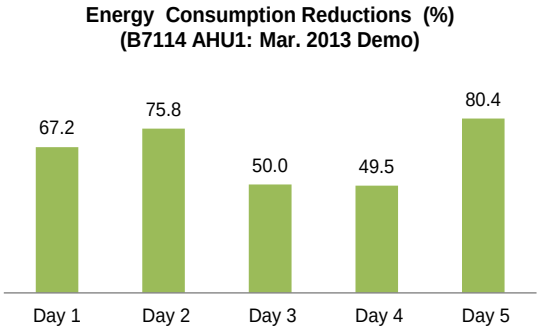

(a) Dec. 2012 Demo (b) Mar. 2013 Demo

Figure C.2.4 Energy consumption Reductions (B7114 AHU1)

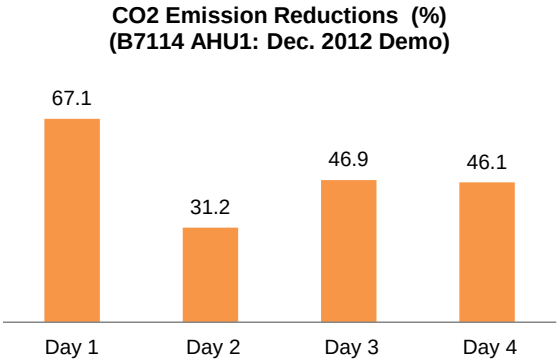

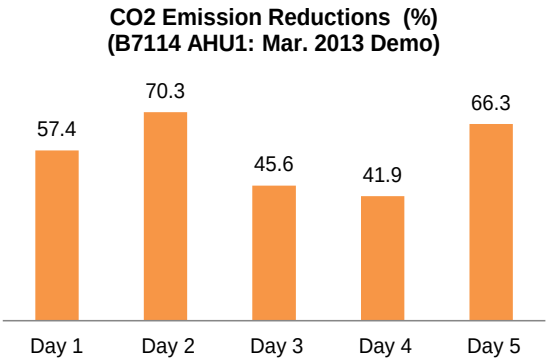

(a) Dec. 2012 Demo (b) Mar. 2013 Demo

Figure C.2.5 CO2 emission consumption reductions (B7114 AHU1)

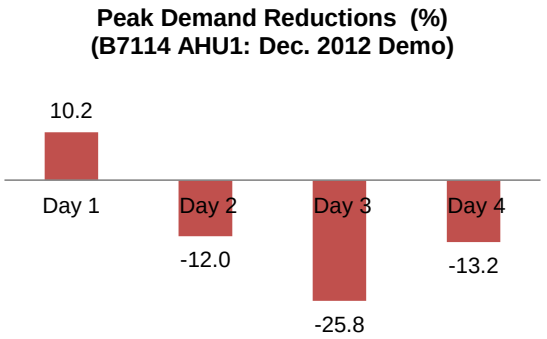

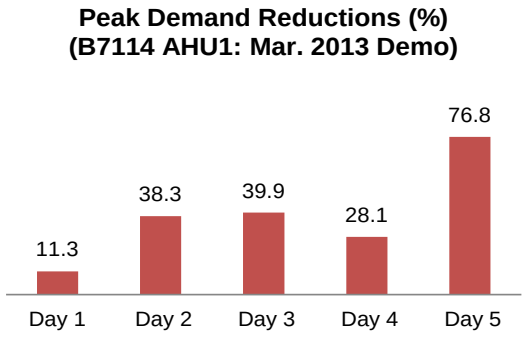

(a) Dec. 2012 Demo (b) Mar. 2013 Demo

Figure C.2.6 Peak demand reductions (B7114 AHU1)

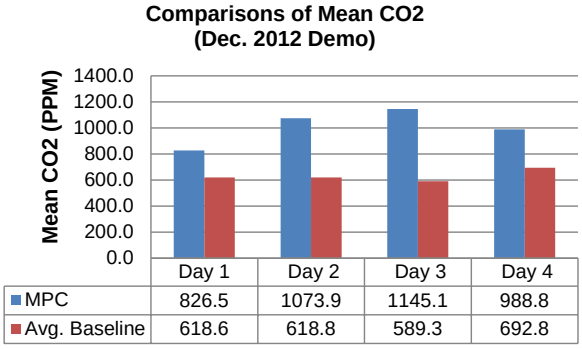

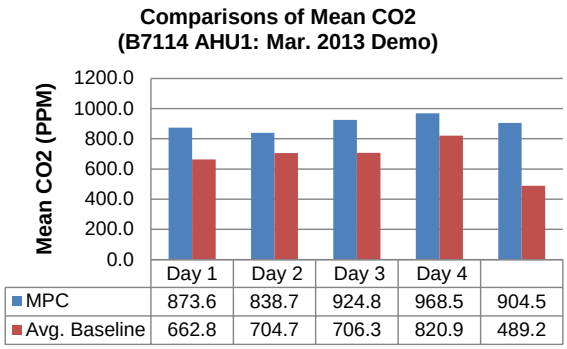

(a) Dec. 2012 Demo (b) Mar. 2013 Demo

Figure C.2.7 Mean CO2 in zones (B7114 AHU1)

To evaluate the comfort violations, the following criteria (degree hours of comfort violation) is considered in this study:

$$V_{comfort,temp} = \frac{1}{12}\int_{ts}^{te} \max(0, Tz^{stpt} - Tz)$$

where $V_{comfort,temp}$ is the comfort violation in degree hours ($°C \cdot hrs$), 1/12 is the conversion factor to convert the samples from 5 min. to 1hr, *ts* is the start time of a given demo day, *te* is the end time of a given demo day, *Tz* is the zone temperature of a given compartment, and Tz^{stpt} is the zone heating setpoint of a given compartment.

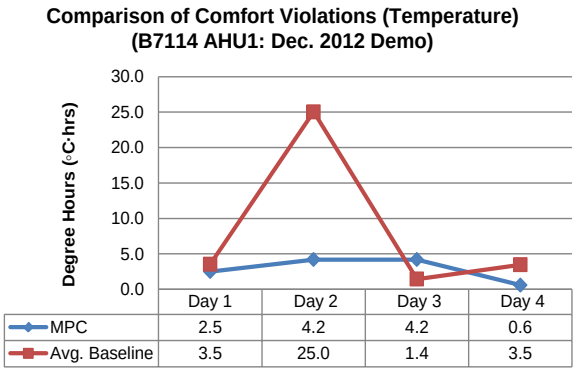

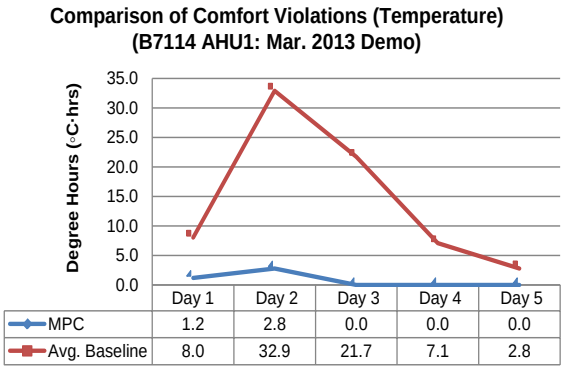

(a) Dec. 2012 Demo (b) Mar. 2013 Demo

Figure C.2.8 Comparison of comfort violations – zone temperature (B7114 AHU1)

Building 7114 AHU 2

Table C.2.2 summarizes the demonstration schedule of Building 7114 AHU2 in Nov & Dec. 2012, Feb. 2013, and Mar. 2013.

Table C.2.2 Demonstration schedule of Building 7114 AHU2 in Nov. & Dec. 2012 and Mar. 2013

Demo Days	**Demo Time Period**	**Mean Outdoor Air Temperature (◦F)**
Nov & Dec. 2012		
Day 1	11/14/2012 11am to 23pm	40.9
Day 2	12/04/2012 12pm - 24pm	48.7
Day 3	12/5/2012 0am to 24pm	34.1
Day 4	12/6/2012 0am to 24pm	40.9
Day 5	12/07/2012 0am to 15pm	42.2
Feb. 2013		
Day 1	2/12/2013 8am to 24pm	25.7
Day 2	2/13/2013 0am to 24pm	33.0
Day 3	2/14/2013 0am to 24pm	36.2
Day 4	2/15/2013 0am to 2pm	26.1
Mar. 2013		
Day 1	03/11/2013 16pm to 24pm	34.5
Day 2	03/12/2013 0am to 24pm	31.7
Day 3	03/13/2013 0am to 24pm	27.0

Day 4	03/14/2013 0am to 24pm	30.7
Day 5	03/15/2013 0am to 13:30pm	34.6

Figures C.2.9-C.2.12 present the comparison of total energy consumptions between MPC and averaged baseline days, energy consumption reductions brought by MPC, CO2 emission reductions brought by MPC, peak demand reductions brought by MPC, comparisons of mean CO2 level, and comparisons of comfort violations in terms of zone temperature during Nov & Dec 2012 demo (subplot (a)), Feb. 2013 (subplot (b)), and Mar. 2013 (subplot (c)) demo of Building 7114 AHU2, respectively.

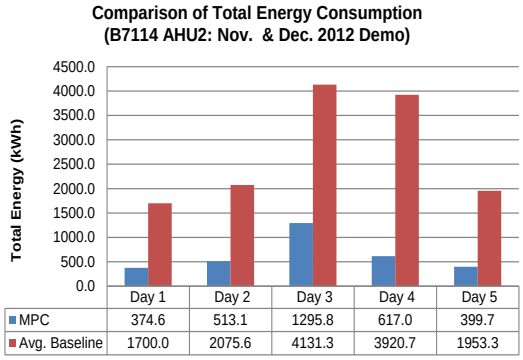

(a) Nov. & Dec. 2012 Demo

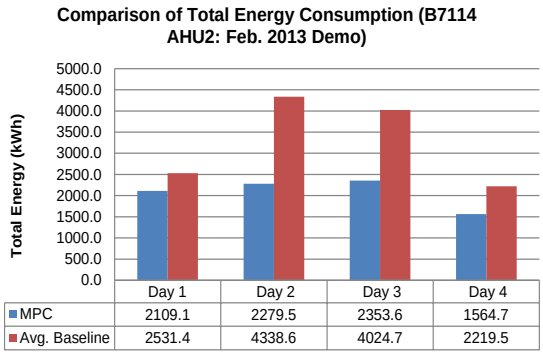

(b) Feb. 2013 Demo

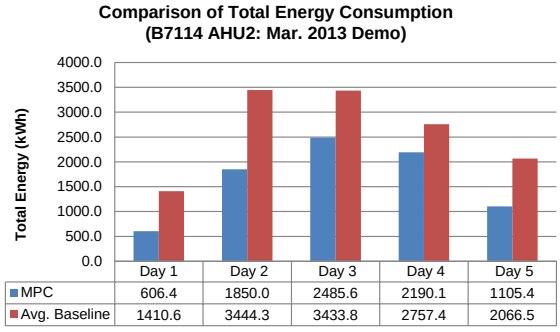

(c) Mar. 2013 Demo

Figure C.2.9 Comparisons of total energy consumption (Building 7114 AHU2)

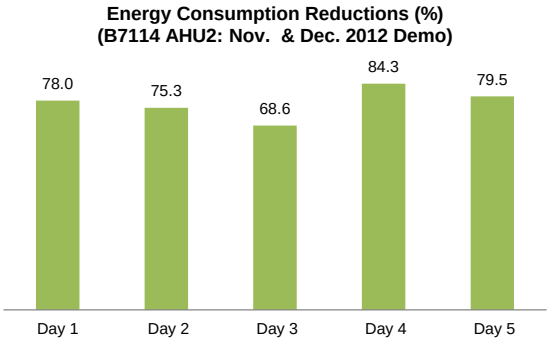

(a) Nov. & Dec. 2012 Demo

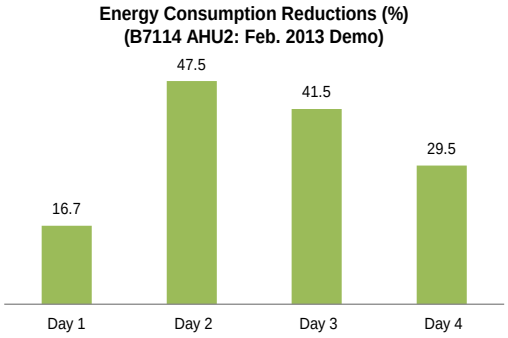

(b) Feb. 2013 Demo

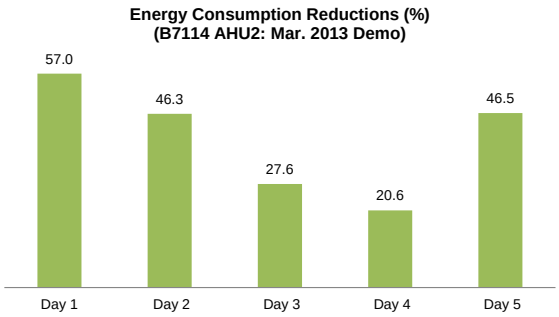

(c) Mar. 2013 Demo

Figure C.2.10 Energy consumption reductions (Building 7114 AHU2)

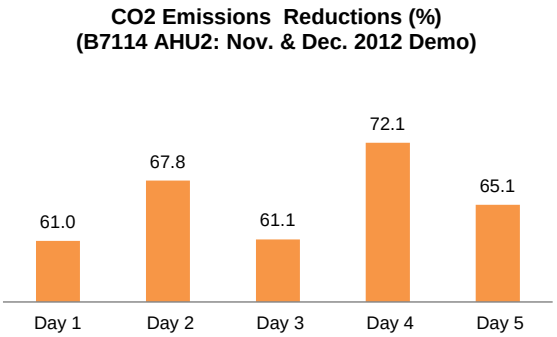

(a) Nov. & Dec. 2012 Demo

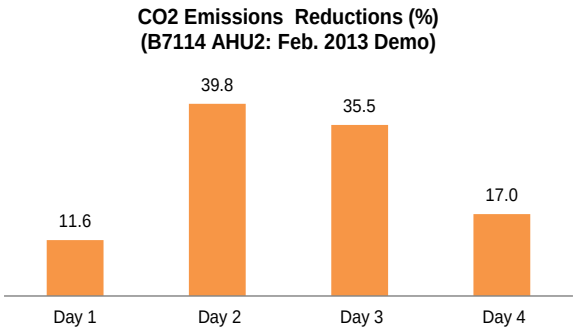

(b) Feb. 2013 Demo

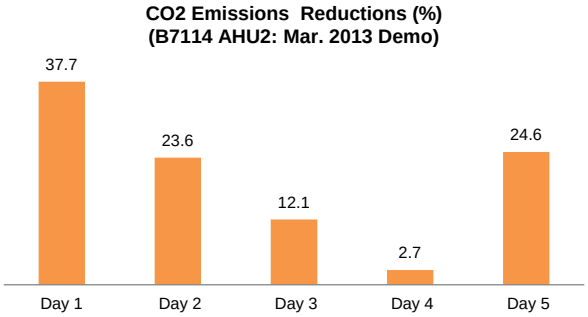

(c) Mar. 2013 Demo

Figure C.2.11 CO2 emission consumption reductions (Building 7114 AHU2)

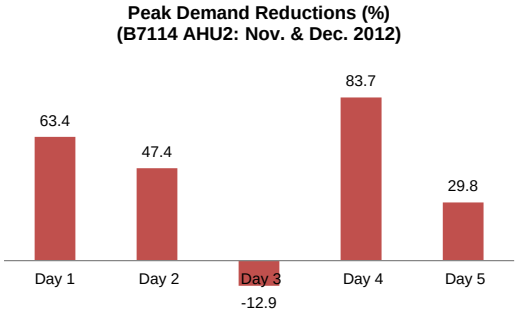

(a) Nov. & Dec. 2012 Demo

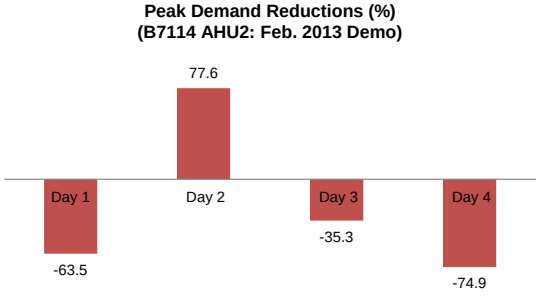

(b) Feb. 2013 Demo

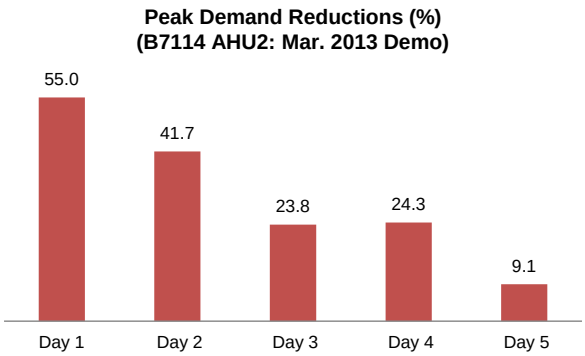

(c) Mar. 2013 Demo

Figure C.2.12 Peak demand reductions (Building 7114 AHU2)

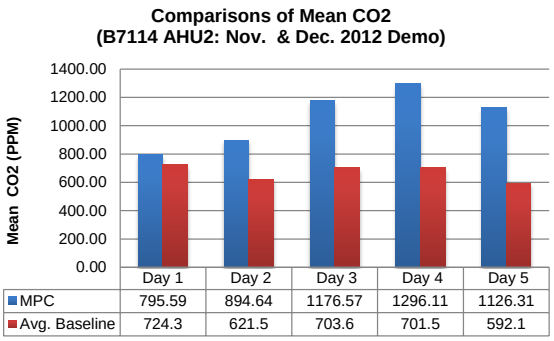

(a) Nov. & Dec. 2012 Demo

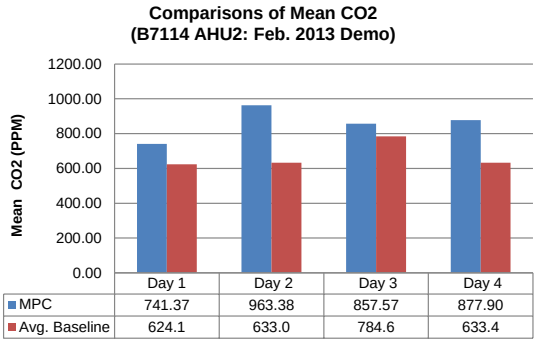

(b) Feb. 2013 Demo

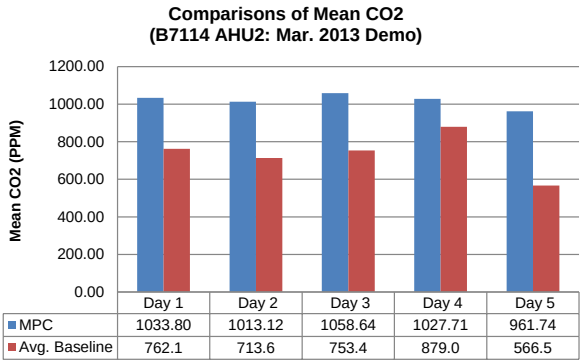

(c) Mar. 2013 Demo

Figure C.2.13 Mean CO2 in zones (Building 7114 AHU2)

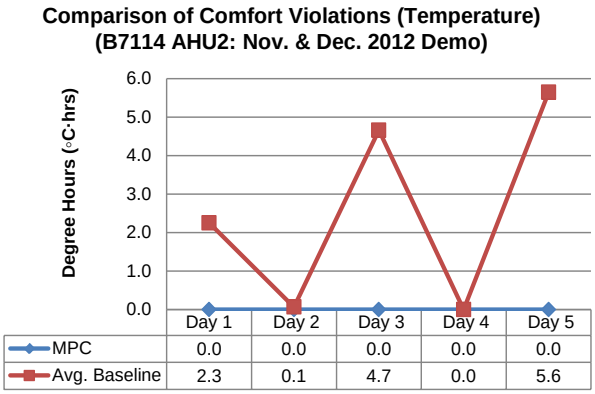

(a) Nov. & Dec. 2012 Demo

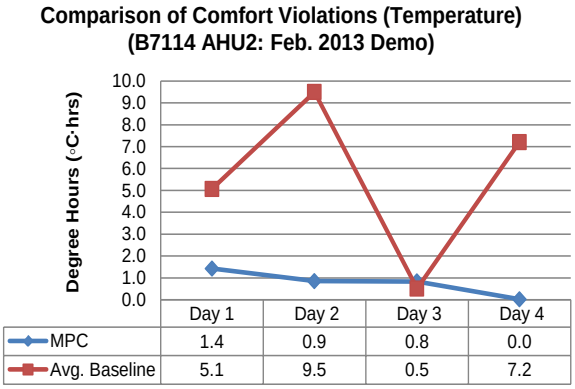

(b) Feb. 2013 Demo

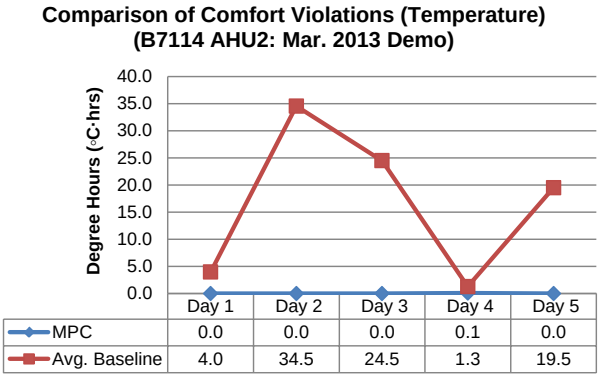

(c) Mar. 2013 Demo

Figure C.2.14 Comparison of comfort violations – zone temperature (Building 7114 AHU2)

Building 7113 AHU 1

Table C.2.3 summarizes the demonstration schedule of Building 7113 AHU1 in Nov & Dec. 2012 and Mar. 2013.

Table C.2.3 Demonstration schedule of Building 7113 AHU1 in Nov & Dec. 2012 and Mar. 2013

Demo Days	**Demo Time Period**	**Mean Outdoor Air Temperature (◦F)**
Nov & Dec. 2012		
Day 1	11/16/2012 0am to 16pm	39.3
Day 2	12/04/2012 0am - 24pm	50.0
Day 3	12/5/2012 0am to 24pm	34.1
Day 4	12/6/2012 0am to 24pm	40.9
Day 5	12/07/2012 0am to 15pm	42.2

Mar. 2013		
Day 1	03/11/2013 16pm to 24pm	34.5
Day 2	03/12/2013 0am to 24pm	31.7
Day 3	03/13/2013 0am to 24pm	27.0
Day 4	03/14/2013 0am to 24pm	30.7
Day 5	03/15/2013 0am to 13:30pm	34.6

Figure C.2.15-C.2.20 present the comparison of total energy consumptions between MPC and averaged baseline days, energy consumption reductions brought by MPC, CO2 emission reductions brought by MPC, peak demand reductions brought by MPC, comparisons of mean CO2 level, and comparisons of comfort violations in terms of zone temperature during Nov & Dec 2012 demo (subplot (a)) and Mar. 2013 (subplot (b)) demo of Building 7113 AHU1, respectively.

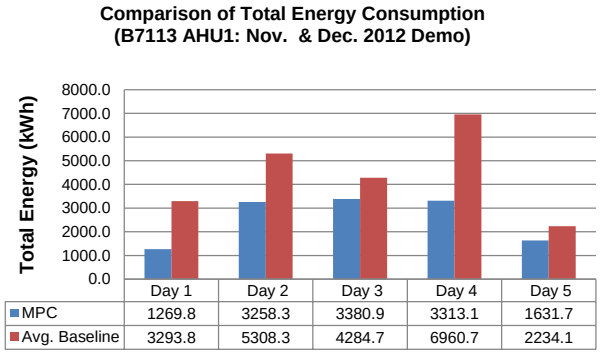

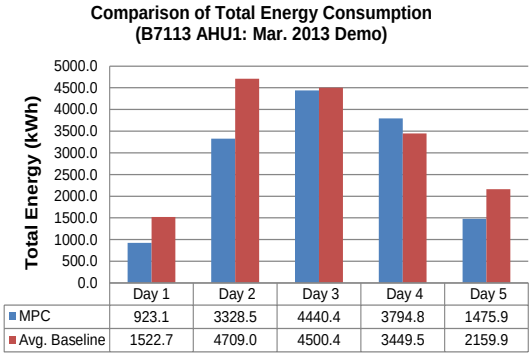

(a) Nov. & Dec. 2012 Demo (b) Mar. 2013 Demo

Figure C.2.15 Comparisons of total energy consumption (Building 7113 AHU1)

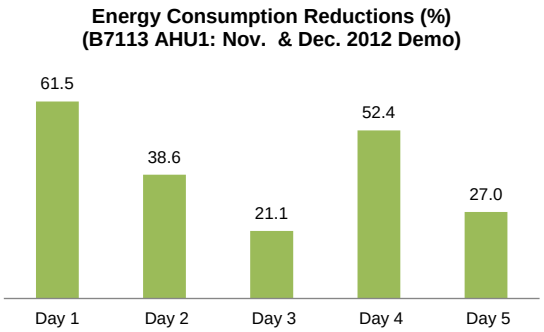

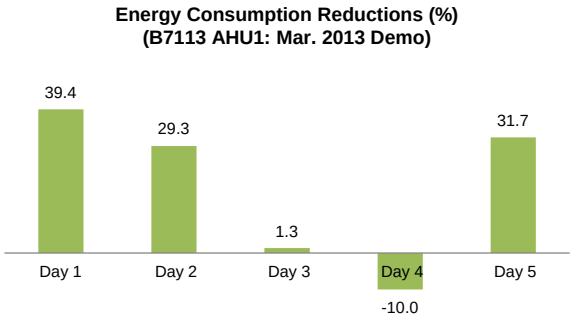

(a) Nov. & Dec. 2012 Demo (b) Mar. 2013 Demo

Figure C.2.16 Energy consumption reductions (Building 7113 AHU1)

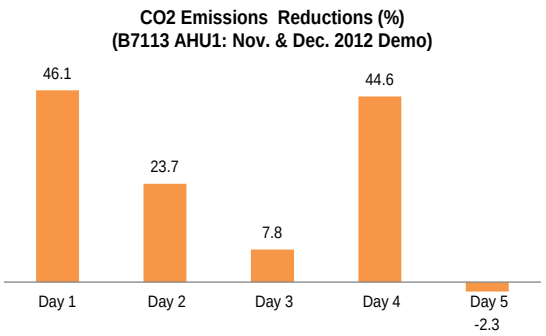

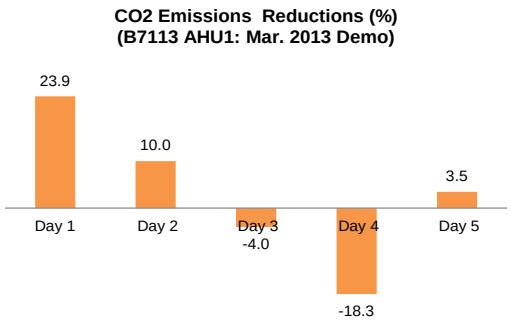

(a) Nov. & Dec. 2012 Demo (b) Mar. 2013 Demo

Figure C.2.17 CO2 emission consumption reductions (Building 7113 AHU1)

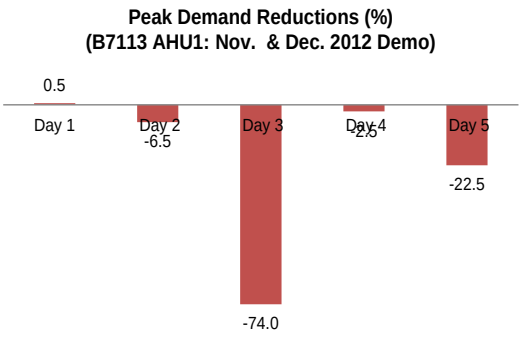

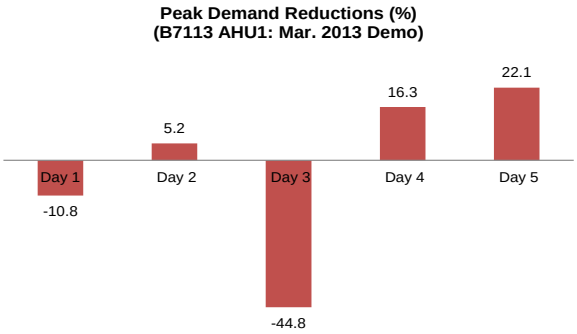

(a) Nov. & Dec. 2012 Demo (b) Mar. 2013 Demo

Figure C.2.18 Peak demand reductions (Building 7113 AHU1)

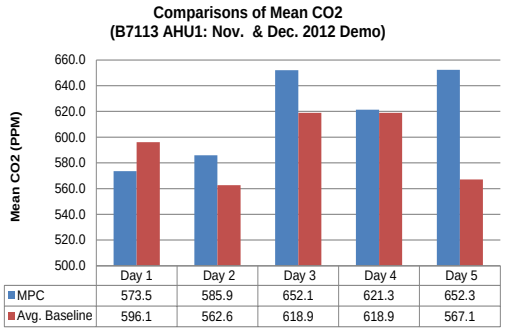

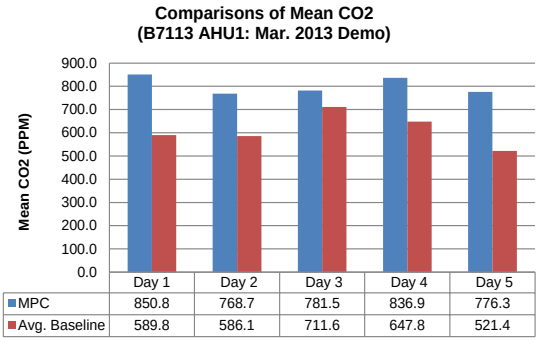

(a) Nov. & Dec. 2012 Demo (b) Mar. 2013 Demo

Figure C.2.19 Mean CO2 in zones (Building 7113 AHU1)

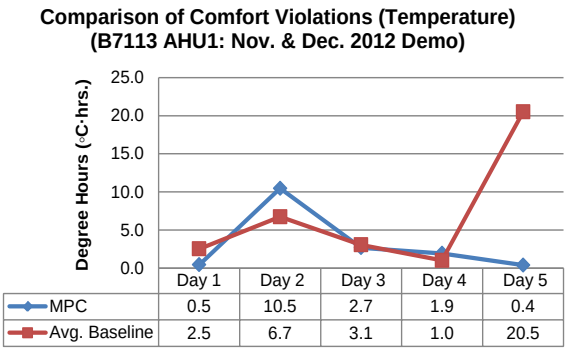

(a) Nov. & Dec. 2012 Demo

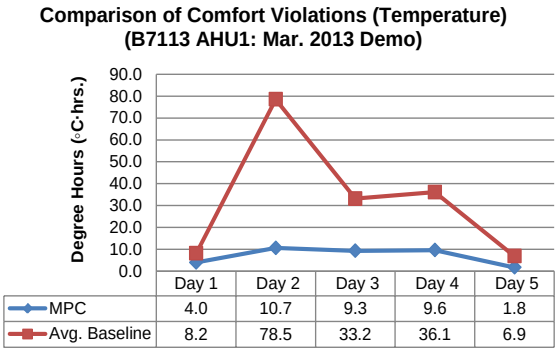

(b) Mar. 2013 Demo

Figure C.2.20 Comparison of comfort violations – zone temperature (Building 7113 AHU1)

C.3 PERFORMANC ESTIMATION FOR FAULT-ACCOMMODATING MODEL PREDICTIVE CONTROL

The integrated EPMO system, comprising of Fault Detection and Diagnostics and Optimal Control algorithms, was demonstrated in Feb. 2013 for AHU1 in Building 7114. The main fault that was identified to have the largest impact on the HVAC system energy consumption was outdoor-air damper actuator. To evaluate the impact of this fault and the effectiveness of fault-tolerant MPC algorithm employed in this study, two tests were conducted as summarized in Tables C.3.1 and C.3.2.

Table C.3.1 Test scenarios for Fault-Accommodating Control technology

Scenarios	**System**
Healthy MPC	Building 7114 AHU2
Fault-Tolerant MPC	Building 7114 AHU1
Baseline w. Fault Injection	Building 7113 AHU1

Table C.3.2 Demonstration conditions for the Fault-Accommodating Control

Demo Days	**Fault Injection**	**Demo Time Period**	**Mean Outdoor Air Temperature (◦F)**
Day 1	Outdoor air damper stuck at 70%	02/12/2013 9am - 15pm	27.2
Day 2	Outdoor air damper stuck at 100%	02/14/2013 8:30am - 17pm	37.4

Case 1: Fault-Tolerant MPC (Building 7114 AHU1) vs. "Healthy" MPC (Building 7114 AHU2)
Figures C.3.1 (a)-(f) present the performance of nominal MPC algorithm (with no injected faults) relative to the fault-accommodating MPC algorithm (with injected faults). The performance variables are: total energy consumptions, peak demand, CO_2 emissions, and thermal comfort. As expected, the fault-accommodating MPC algorithm requires larger energy consumption values because it has to heat a larger amount of outdoor air flow that enters the building, as a direct consequence of the larger outdoor-air damper positions, in order to meet the thermal comfort (which is similar as for the nominal MPC).

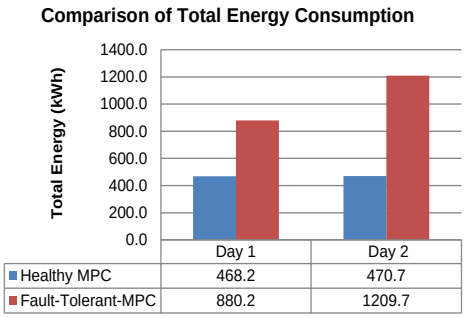

(a) Comparisons of total energy consumption

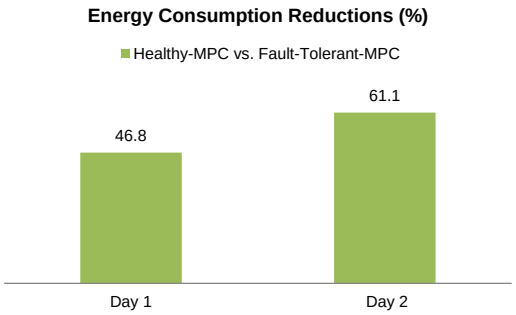

(b) Energy Consumption Reductions

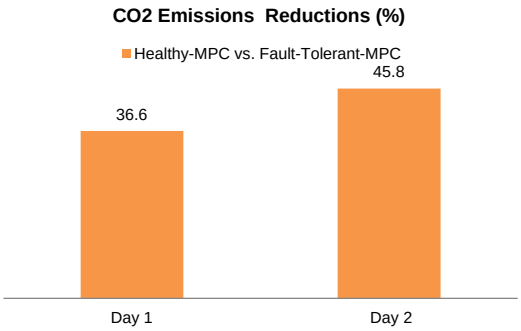

(c) CO2 emission reductions

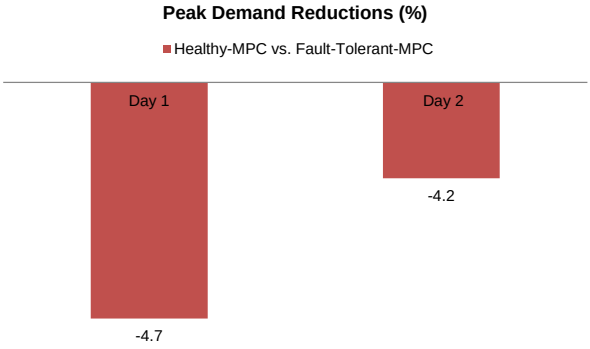

(d) Peak demand reductions

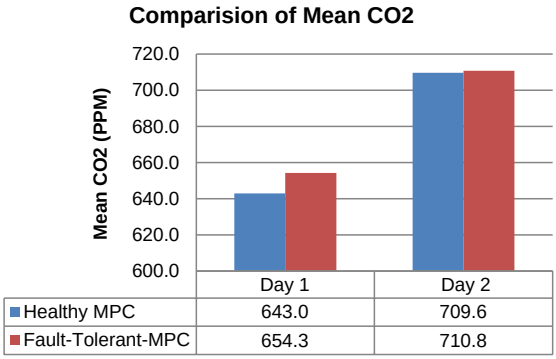

(d) Mean CO2 in zones

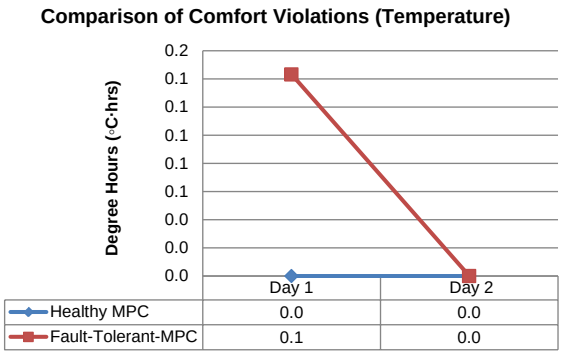

(f) Comparison of comfort violations

Figure C.3.1 Fault-Tolerant MPC control case study 1 (Healthy-MPC vs. Fault-Tolerant MPC)

Case 2: Fault-Accommodating MPC (Building 7114 AHU1) vs. Baseline with Injected Faults (Building 7113 AHU1)

Figures C.3.2 (a)-(f) present the performance of nominal MPC algorithm (with no injected faults) relative to the fault-accommodating MPC algorithm (with injected faults). The performance variables are: total energy consumptions, peak demand, CO_2 emissions, and thermal comfort. It is observed that the fault-accommodating MPC algorithm consumes less energy while meeting the thermal comfort constraints (whereas the baseline schedules exceeds the constraints by a significant value).

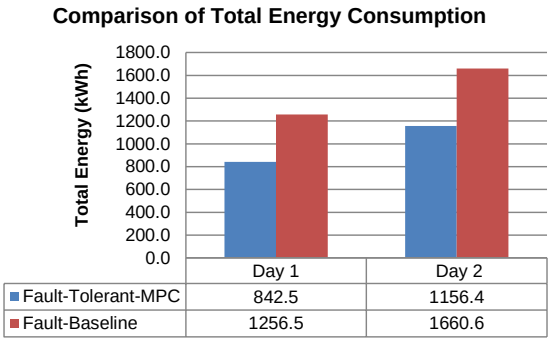

(a) Comparisons of total energy consumption

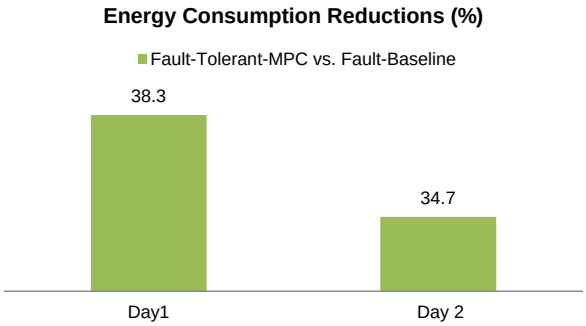

(b) Energy Consumption Reductions

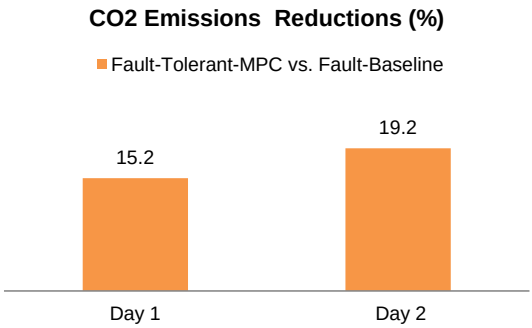

(c) CO2 emission reductions

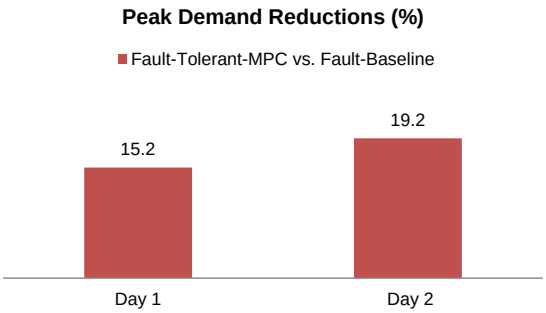

(d) Peak demand reductions

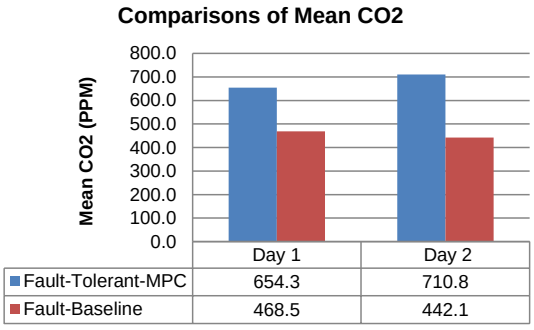

(e) Mean CO2 in zones

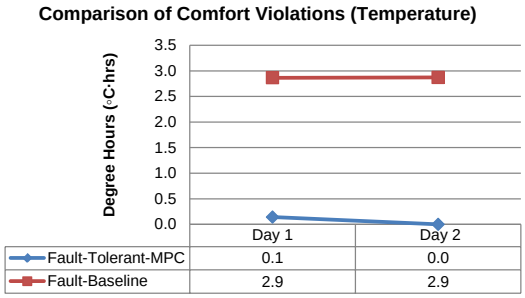

(f) Comparison of comfort violation

Figure C.3.2 Fault-Tolerant MPC control case study 2 (Fault-Tolerant MPC vs. Fault-Baseline)

C.4 BUILDING LIFE-CYCLE COST RESULTS

This section duplicates the output of the NIST BLLC 5.3-11 software tool used to generate the Simple Payback and Savings-to-Investment Ratio values as reported in Table 5.1.

NIST BLCC 5.3-11: ECIP Report
Consistent with Federal Life Cycle Cost Methodology and Procedures, 10 CFR, Part 436, Subpart A. The LCC calculations are based on the FEMP discount rates and energy price escalation rates updated on April 1, 2011.

Location:	Illinois	Discount Rate:	3%
Project Title:	BLDG7114	Analyst:	
Base Date:	April 1, 2011	Preparation Date:	Tue Sep 24 15:22:54 EDT 2013
BOD:	April 1, 2012	Economic Life:	10 years 0 months
File Name:	EPMO_PaybackCalculation_v2.xml		

1. Investment

Construction Cost	$72,850
SIOH	$0
Design Cost	$50,000
Total Cost	$122,850
Salvage Value of Existing Equipment	$0
Public Utility Company	$0
Total Investment	$122,850

2. Energy and Water Savings (+) or Cost (-)

Base Date Savings, unit costs, & discounted savings

Item	Unit Cost	Usage Savings	Annual Savings	Discount Factor	Discounted Savings
Electricity	$8.83319	4,152.7 MBtu	$36,682	7.377	$270,616
Energy Subtotal		4,152.7 MBtu	$36,682		$270,616
Water Subtotal		0.0 Mgal	$0		$0
Total			$36,682		$270,616

3. Non-Energy Savings (+) or Cost (-)

Item	Savings/Cost	Occurrence	Discount Factor	Discounted Savings/Cost
Annually Recurring	-$2,000	Annual	7.672	-$15,343
Non-Annually Recurring				
Training and Software	-$6,000	0 years 0 months	0.971	-$5,825
Non-Annually Recurring Subtotal	-$6,000			-$5,825
Total	-$8,000			-$21,168

4. First year savings	$34,082	
5. Simple Payback Period (in years)	3.60	(total investment/first-year savings)
6. Total Discounted Operational Savings	$249,448	
7. Savings to Investment Ratio (SIR)	2.03	(total discounted operational savings/total investment)
8. Adjusted Internal Rate of Return (AIRR)	10.56%	(1+d)*SIR^(1/n)-1; d=discount rate, n=years in study period

APPENDIX D: MANAGEMENT AND STAFFING

Dr. Trevor Bailey provided overall management for this project. Drs. Veronica Adetola, Sorin Bengea, Keunmo Kang, Pengfei Li, Abhishek Srivastava, and Soumik Sarwar focused on the tasks of modeling, estimation, control, energy diagnostics and optimal control implementation, and implementation for the Energy Performance Monitoring and Optimization System. Professor Francesco Borrelli and the graduate students Anthony Kelman and Sergey Vichik developed the software tool for generated an automated problem formulation based on the high level, user-friendly, specifications.

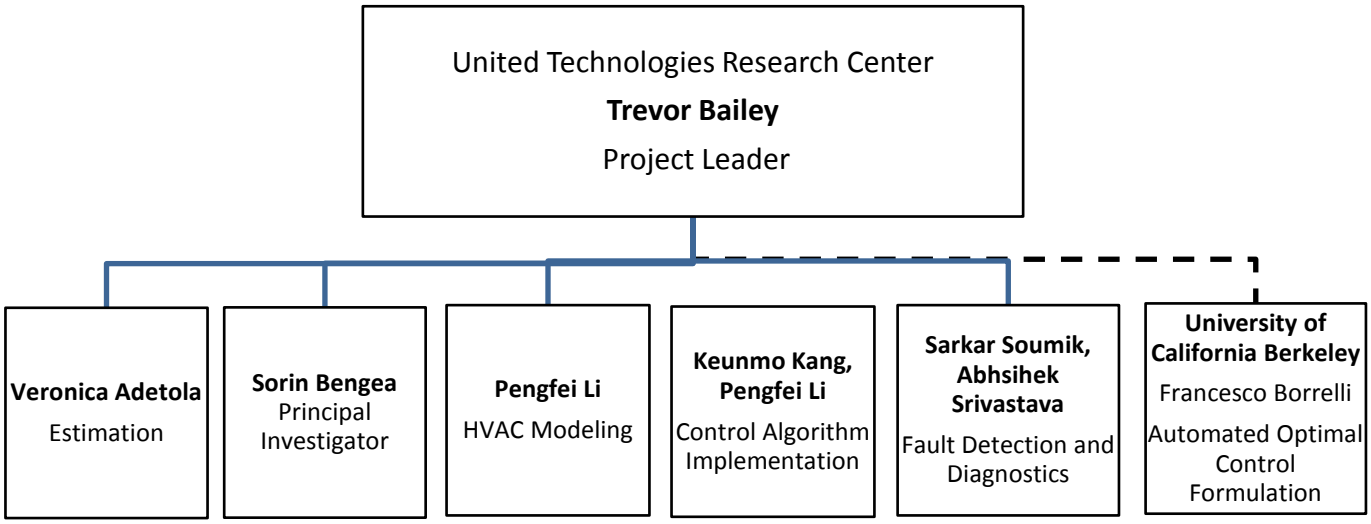

Figure D.1. Organization chart